DOT/FAA/TC-17/52

Federal Aviation Administration
William J. Hughes Technical Center
Aviation Research Division
Atlantic City International Airport
New Jersey 08405

Study of Transport Aircraft Water Mishap Kinematics and Regional Jet Mishap Kinematics

October 2017

Final Report

U.S. Department of Transportation
Federal Aviation Administration

NOTICE

Technical Report Documentation Page

1. Report No.	2. Government Accession No.	3. Recipient's Catalog No.
DOT/FAA/TC-17/52		

4. Title and Subtitle	5. Report Date
STUDY OF TRANSPORT AIRCRAFT WATER MISHAP KINEMATICS AND REGIONAL JET MISHAP KINEMATICS	October 2017
	6. Performing Organization Code
7. Author(s)	8. Performing Organization Report No.
Lance C. Labun John (Jack) P. Cress	
9. Performing Organization Name and Address	10. Work Unit No. (TRAIS)
Labun LLC 1342 E. Louis Way, Tempe, AZ 85284 Vortechs Helicopter Analytics, 19275 Reavis Way, Prunedale, CA 93907	11. Contract or Grant No.
12. Sponsoring Agency Name and Address	13. Type of Report and Period Covered
U.S. Department of Transportation Federal Aviation Administration Orlando CMO-29 5950 Hazeltine National Dr Citadel International Bldg Orlando, FL 32822	Final Report 01/10/2016 to 06/30/2017
	14. Sponsoring Agency Code AIR-600

15. Supplementary Notes

The FAA William J. Hughes Technical Center Aviation Research Division COR was Allan Abramowitz.

16. Abstract

This report presents the analysis and conclusions of two distinct studies into transport aircraft crashes. One study focuses on crash events with the transport category aircraft coming to rest in water. This study includes ditchings with and without full preparation and controllability, unintentional landings in the water, and runway overruns terminating in a body of water. The second study focuses on a particular class of aircraft known as regional jets. It endeavors to characterize the kinematics of crashes in which these aircraft are involved and the occupant outcomes for those crashes. Ultimately, these studies are part of a much larger effort by the FAA and other agencies to make air travel safer by understanding how occupants are injured in crashes and attempting to provide guidance to build aircraft that offer occupants an improved chance of survival.

17. Key Words	18. Distribution Statement
Aircraft crashes, Aircraft ditching, Aircraft kinematics, Aircraft water impacts, Transport aircraft water mishap kinematics, Regional jet mishap kinematics.	This document is available to the U.S. public through the National Technical Information Service (NTIS), Springfield, Virginia 22161. This document is also available from the Federal Aviation Administration William J. Hughes Technical Center at actlibrary.tc.faa.gov.

19. Security Classif. (of this report)	20. Security Classif. (of this page)	21. No. of Pages	22. Price
Unclassified	Unclassified	131	

Form DOT F 1700.7 (8-72) Reproduction of completed page authorized

TABLE OF CONTENTS

APPENDICES

LIST OF FIGURES

LIST OF TABLES

LIST OF ACRONYMS

ASN	Aviation Safety Network
BLM	Binary Logistic Model
CI	Confidence Interval
CSTRG	Cabin Safety Technical Research Group
ft/s	feet per second
ICAO	International Civil Aviation Organization
Prop.	Proportions
RJ	Regional Jet

EXECUTIVE SUMMARY

This report presents the analysis and conclusions of two distinct studies into transport aircraft crashes. One study focuses on mishaps with the aircraft coming to rest in water. This study includes ditchings with and without full preparation and control, unplanned landings in the water, and runway overruns terminating in a body of water. The second study focuses on a particular class of aircraft known as regional jets (RJs). It endeavors to characterize the types of crashes in which these aircraft are involved and the occupant outcomes for those crashes.

These studies are part of a much larger effort by the FAA and other agencies to make air travel safer by understanding injury mechanisms in crashes to provide a basis for development of regulatory requirements and design guidance. The water mishap study has arisen from a realization that the basis for the design guidance regarding aircraft ditching may no longer reflect the characteristics of ditching events. Indeed, this view was confirmed in the study. Two aspects of the design guidance that was observed to be false were the assumption that the aircraft be under power full control and that the crew have time to prepare for water entry. Of 15 survivable mishaps in which the aircraft landed in the water from flight, only three occurred with the aircraft having thrust, and one of these was an engine failure immediately after takeoff. Therefore, only two crews had time to fully prepare for a ditching with engine power. In five events, the aircraft unintentionally landed short in the water; therefore, the crew and passengers were completely unprepared for water entry. In seven events, the aircraft entered the water without thrust; consequently, the pilot's ability to place the aircraft in the prescribed ditching flight conditions was compromised. The relative frequency of the different types of events was confirmed in a larger population of less well-documented mishaps.

The ditching-without-power mishaps were found to cause more damage to the aircraft and more serious and fatal injuries to the occupants than ditching with power. Current ditching procedures need to reflect events in which the pilots do not have the benefit of thrust. In addition, the design conditions should also consider the kinematics of aircraft without thrust rather than just with thrust. The results show that aircraft runway overruns entered the water with very low speed and, consequently, generated little damage and very few injuries.

The population of RJs in the study is quite homogeneous in configuration; of the 24 aircraft in the data set, all but four have engines on the tail, and all but three of those four aircraft were of the high-wing configuration. All the severe crashes with heavy damage and high fractions of fatal and serious injuries occurred in mishaps in which the aircraft landed short of the airport or the aircraft lost control on takeoff, especially with ice/snow-contaminated wings.

Many of these crashes were characterized as nonsurvivable or partially survivable at best. The remainder of the crashes in the study did not experience severe impacts. Only one runway overrun ended in a severe impact and had fatalities and serious injuries.

The attempt to create predictive models for injury fraction using the kinematics data from the crashes was not as beneficial as anticipated. For the RJ mishaps, most of the fatalities and serious injuries were concentrated in the mishaps described by two scenarios. Even so, the broad range of values in the kinematic parameters meant that the single regressor (i.e., single kinematic parameter) models did not result in predictive models, which would be useful in establishing

impact conditions for design purposes. The multi-regressor models were more successful, and they do have potential for use in establishing impact conditions for design purposes. The outcome of the statistical analysis was similar for the water study.

1. INTRODUCTION

The following report describes and presents the analysis and conclusions of two distinct studies into transport aircraft crashes. One study focuses on crash events with the transport category aircraft coming to rest in water. This study includes ditchings with and without full preparation/controllability, unintentional landings in the water, and runway overruns terminating in a body of water. The second study focuses on a particular class of aircraft known as regional jets (RJs) and endeavors to characterize the types of crashes in which these aircraft are involved and the occupant outcomes for those crashes. Ultimately, this study is part of a much larger effort by the FAA and other agencies to make air travel safer by understanding how occupants are injured in crashes and by attempting to provide guidance to build aircraft that offer occupants an improved chance of survival.

The water mishap study has arisen out of a realization that the basis for the design guidance associated with aircraft ditching may no longer reflect the most common characteristics of ditching events. Ditching was envisioned as being executed in a planned and controlled manner with time to prepare the aircraft and the occupants for touch down, and having the power and control to land within a tightly defined window of parameters. However, it has become apparent that pilots are often faced with ditching without power and, consequently, with significantly reduced capability to fly the aircraft onto the water within that tightly defined window for successful ditching. Approximately twice as many ditchings occur without power as with power. In addition to these events in which the pilots know that they will be landing in water, another group of events consists of the aircraft being flown onto the water short of the runway. These events have happened with roughly the same frequency as the ditching without thrust. The outcomes for the prepared ditchings with power are reasonably benign as one would hope because these are the events to which the design guidance applies. The outcomes for landing short of the runway are not so benign, and the occupant outcomes for ditchings without power are worse than those for landing short.

The RJs represent a new class of transport aircraft, characterized by being smaller in cross-section than the transports traditionally referred to as narrow bodies and by being powered by turbojet engines rather than the turbo-props that are typically used for short-haul regional flights. For the purposes of the study, the aircraft weight was limited to 100,000 lb and the passenger seating capacity to just more than 100 lb. However, there is no formal definition for this aircraft type. These aircraft have grown in capacity over the years so that they now overlap the lower end of the narrow-body mid-range jets. The crash survival aspects of this relatively new class of aircraft have not been characterized, and this study seeks to gather that information to provide a basis for development of regulatory requirements and design guidance.

Each study is treated separately in this report. The basis for selecting the mishaps for inclusion in the study is described in each section. When common to both studies, detailed explanations of certain analytical procedures are described in section 2 of this report, following the two study reports. The objective of both studies necessitated acquiring detailed information about each mishap; therefore, to be included, a mishap had to have been investigated in depth and reported thoroughly in a publicly available document. Unfortunately, this requirement effectively eliminated many mishaps. Both studies started with a review of the FAA-sponsored Cabin Safety Technical Research Group database. Although the database contains hundreds of mishaps from

around the world, the reality is that most of the events with sufficient information for analysis in this study occurred in North America or in Europe, with a few recent events in Southeast Asia.

The two studies collected information about the aircraft, the number of crew and passengers, the kinematics of the flight and impact, the damage resulting from the impact, and the injuries experienced by all of the occupants, including the crews. These data were analyzed to extract information relating the aircraft design and kinematics to the occupant outcomes. The small number of mishaps in each study combined with relatively large variations in occupant outcomes limits the statistical tools and the robustness of the conclusions that could be drawn from the studies. A substantial effort was made to be as inclusive as possible in selecting mishaps. The RJ study includes mishaps that were both charter jet and regularly scheduled operations.

2. METHODS

This study consists of two distinctly different studies using similar methods. It is anticipated that many readers may be interested in one, but not both, studies. Consequently, the description of the study methods is presented separately so that the reader of either study can access the section as needed. Methods that are unique to one study or the other will be described in the appropriate section of the study. The method of selecting mishaps for each study is specific to that study and, consequently, described in that section.

2.1 ORGANIZING THE DATA

After selecting the final list of mishaps, the detailed data for these mishaps were extracted from the Cabin Safety Technical Research Group (CSTRG) database. The data for each study were stored in a Microsoft® Excel® workbook for that study consisting of four tabs: Mishap Data, Kinematics, Damage Data, and Injury Data. The list of mishap IDs was saved as a text list and imported to the CSTRG database as a custom list. The custom list, together with the Export Wizard, were used to export the data for each worksheet. The fields for each data query are provided in appendix A for the water study and in appendix B for the RJ study. For consistency and efficiency, the data queries for the two studies were kept as similar as practical. Each field became a column, and each mishap was a row.

After importing the data from the CSTRG, fields were added to the worksheets for additional data and in anticipation of the analysis. Lists of the data fields can be found in appendix A for the water study and in appendix B for the RJ study.

The data for each mishap were reviewed for completeness and supplemented with any additional information available from the investigation report. The report file was opened and the missing data, where available, were extracted and inserted into the database. The kinematics data, when available, were extracted from the report. The mishaps with incomplete kinematics data were identified as candidates for reconstruction. The reconstructions were done by Mr. Jack Cress [1]; all reconstructions were jointly reviewed and agreed upon between Mr. Cress and the author.

As noted above, information on the damage to the aircraft floor, seats and restraints, and interior appointments was often minimally described in the reports. Consequently, it was necessary to infer the interior damage from the descriptions of the evacuation and from photos of the exterior damage. Likewise, information on the functionality and use of doors and exits was often found in

several topics throughout the report, including the sections on survivability, evacuation, damage, and injury.

2.2 KINEMATICS RECONSTRUCTION TECHNIQUES

The reconstruction was initiated by thoroughly reading the published accident investigation reports and searching for other data sources, including contemporaneous news reports and photographs, and professional journals and websites for supplemental information. The information sought to support the reconstruction included:

- Aircraft gross weight.
- Atmospheric characteristics.
- Wind conditions.
- True airspeed.
- Ground speed (calculated).
- Velocity reference (Vref).
- Control positions (primarily flaps).
- Landing gear position.
- Aircraft damage (location, deformation).
- Design guidance and regulatory requirements for structure.
- Sea state and wave direction (for water mishaps).
- Sea bottom gradient (when pertinent to damage).
- Ground topography and obstacle interaction (when pertinent).
- Sequence of impacts (when multiple impacts of significant magnitude occurred).
- Ultimate aircraft configuration and wreckage distribution (accounting for sequence and loss of major components).

The acquired information was analyzed to estimate (when unreported) and resolve the primary impact parameters, velocity, and attitude into the aircraft's reference frame. This reference frame is a right-hand coordinate system with the *x*-axis as the longitudinal (roll) axis (+ forward), *y*-axis as the lateral (pitch) axis (+ right), and *z* axis as the vertical (yaw) axis (+ downward). In the final presentation, *z* was reported as positive downward. The conversions from earth reference frame to aircraft reference frame used the guidance from Dynamics of Flight [2] by Bernard Etkin.

After establishing the component velocities and attitude angles in aircraft reference frame, the peak deceleration forces (G-loads) were determined for each axis. The methods used were those described in Summary of Equations of Motion for Several Pulse Shapes [3]. For water impacts, geometric data for each aircraft (length and fuselage diameter) were combined with the three axes velocities and the aircraft attitude at impact. The velocities allowed the determination of the kinetic energy along each axis and then the volume of water displaced. The volume of water displaced longitudinally in rollout and the lateral water displacement were determined when applicable. The water movement information was then used with the Turnbow equations and judgement as to the pulse shape to determine the respective axial deceleration forces.

For terrain impacts, the reconstructions used engineering judgement for the pulse shape and the applicable Turnbow equations to convert the velocity change into a peak deceleration.

2.3 POTENTIALLY SURVIVABLE CRASHES

In the field of crashworthiness, the concept of a potentially survivable crash has evolved. A survivable crash is defined to be a crash in which: 1) the occupied volumes of the aircraft are maintained (i.e., not crushed or even briefly compromised), and 2) the decelerations along all three primary axes are below the human tolerance for injury for each direction for a restrained occupant. Crashes in which a part of the occupied volume is compromised and a part remains preserved, or in which a part of the aircraft experiences decelerations beyond human tolerance, are considered to be partially survivable. In the water impact study, only one event experienced a deceleration along the vertical axis that would exceed human tolerance for injury. Therefore, survivability for this group of mishaps was essentially determined by loss of occupied volume. One might argue that in a water-impact event wherein fuselage breakage occurs, the force of water into the occupied volume could be considered as injurious or debilitating as the fuselage structure intruding into the occupant volume. However, without the ability to know the nature of the water entry into the cabin, this study did not consider water in-rush as a loss of occupied volume. This definition for survivability does not consider the actual injuries experienced in the crash. The usefulness of this concept lies in determining design requirements for occupant protection based on structural and kinematic parameters.

The approach taken to estimate survivable crash limits in this study consisted of several steps. The first step was to eliminate the overrun accidents from this crash survivability analysis. The damage data—primarily the loss of occupant volume—were reviewed, and each crash was assigned a rating of survivable, partially survivable (some occupied volume was lost), or non-survivable (all occupied volume was lost).

2.4 CUMULATIVE SURVIVABILITY PLOTS FOR KINEMATIC PARAMETERS

One method of setting design requirements for survivability is to use the kinematic data from survivable mishaps and present them as a cumulative percentile. The plot is created by ordering the values for the particular parameter (e.g., airspeed) in ascending order. The percentage of all mishaps that fall at a value less than the value for each mishap is then determined. This percentile is simply the sequential number of each mishap divided by the number of mishaps. The percentile for each mishap is then plotted as the *y* value for each value of the x value parameter. Connecting the points with a curve provides a continuous estimate of the percentile for any value of the parameter.

The resulting plot is typically used to determine the value for the kinematic parameter of interest. Therefore, to know the airspeed corresponding to the 90th percentile survivable crash, one merely finds where the curve crosses the 90th percentile and reads the corresponding airspeed from the *x*-axis.

This method has been applied to vertical velocity, airspeed, flight-path angle, the three attitude angles, and the peak deceleration along each of three aircraft axes.

2.5 CREATION OF THE DAMAGE METRIC

The general damage to the mishap aircraft is reported in each investigation report. However, at the detail level of interest for survivability, less information is provided than would be desired. Two

important considerations for survivability are the integrity of the occupant restraint chain (belt-seat-floor-structure) and the sustainment of a survivable volume for each occupant. Several reports made specific reference to the disruption of the floor and the integrity of the seats as observed after the crash. Both of these observations are critical to the integrity of the restraint chain. For the occupant to be restrained through the duration of the crash, the seat must remain attached to the floor, and the floor must remain structurally sound. Severe disruption of the floor will also interfere with evacuation.

In reviewing the report for each mishap, several descriptors for damage were recorded into the data worksheet. Damage information was recorded by segment of the fuselage. The five segments used are the cockpit, the forward cabin, the overwing cabin, the aft cabin, and the tail. These segments were selected based on the observation that when aircraft break up, they often break at manufacturing joints or at structural discontinuities. The segment labeled “cockpit” breaks away from the forward end of the uniform cross section, which is labeled “forward cabin.” The flight attendant seat is usually in the cockpit segment along with the galley, but not always. The forward cabin in turn often breaks away from the segment labeled “overwing cabin.” The limits of the overwing section are taken to be the limits of the wing fairings. The rear cabin is defined as the segment from the end of the wing fairings back to the tail, where the tail begins at the point at which the underbelly begins to slope upward rather than remain level. Each of the four joints had a cell in the datasheet, and a Y (for “yes”) was recorded for each joint where a break was reported or could be inferred to have occurred. Where a break did not occur, an N (for “no”) was recorded. The seat rows were assigned to each section on the basis of seat maps. If available, the seat map in the report was used; in the absence of a map in the report, the most relevant seat map that could be located on the Internet was used to assign seat rows to each segment. Very few aircraft had passenger seating in the tail, but some had flight-attendant seating there. Consequently, a few injuries were recorded in the tail segment.

In addition to the fuselage breaks, the other damage descriptors were: underside skin and structural damage, floor disruption, seat failure, and loss of occupant volume. Considered the least direct threat to the occupants, damage to the underside skin of the aircraft was determined from photographs and descriptions in the investigation reports. The information in the investigation reports was supplemented by performing Internet searches for images of the wreckage. The damage severity for each aircraft segment was recorded as widespread (W), localized (L), or none (N). In a similar fashion, the floor disruption was recorded as W, L, or N, based on photographs and descriptions in the reports. However, it should be noted that very few of the reports or Web sources contained photographs of the aircraft interiors after the crash; therefore, most of the information on interior conditions came from the report text. Likewise, for seat failures, the reports commented when there were seat failures and, in some cases, actually stated that seat failures had not occurred. In certain mishaps, the integrity of the seats could be inferred from the descriptions of the evacuation. Last, the loss of occupied volume was recorded as W, L, or N, based on external photos and information in the text of the reports.

The lack of correlation between injuries and the fuselage breaks led to the idea of combining the damage descriptors into a more encompassing damage indicator. For this approach to the analysis, the different damage severities and types were weighted based on the likelihood of that damage increasing the number of injuries. Therefore, severity was weighted by assigning a multiplier of 2 for each segment containing the type of damage rated “Widespread,” a multiplier of 1 for each

segment rated “Local,” and 0 for each cell rated “None.” The underside skin-damage values were weighted by a factor of 1; the floor disruption values were multiplied by 2; and the seat failure was weighted by a factor of 3. Each fuselage break was multiplied by 3 and the score assigned to the segment behind the break. The score for each segment where loss of occupied volume occurred was multiplied by 4. The five terms were added up for each fuselage segment to create a “Damage Metric.” Therefore, the damage to each segment of an aircraft could be identified with a single value, and by adding the values for each segment together; a single value for the aircraft was obtained.

In some cases, quite a few cells were missing information, as indicated by NI for “no information” (counted as zero in the damage factor). By counting up the number of NI cells in each mishap, those mishaps whose damage metrics may be significantly affected by the absence of information could be identified. The effect of the missing cell is to reduce the value of the damage metric because NI is assigned a zero value. Several means for working around these missing data were considered, but none were deemed satisfactory. For the benefit of the reader, the number of NI cells is given in table 17. The total damage metric for these mishaps may be lower than would have been recorded had all the information been available.

2.6 BINARY LOGISTIC REGRESSION ANALYSIS

The binary logistic approach interprets the injury data as having just one of two outcomes for each occupant: severe[1] injury (fatal/serious) or minor/no injury. In this view, the expectation is that for each parameter, the fraction of severe injuries will be low (near zero) for low values of the parameter, and the severe-injury fraction will increase to the limit value of one as the value of the parameter increases. For example, it is expected that the fraction of severe injuries will increase as the impact velocity increases. The equation that the regression fits assumes that the dependence on the parameter is a linear function. Therefore, the logistic equation being fitted is an exponential with a linear form to the exponent (referred to as the linear predictor). The output variable p is the estimated probability that an occupant is severely injured. The total number of occupants on a mishap aircraft meeting the model parameters can be multiplied by the estimated probability of an occupant being severely injured to provide an estimated number of fatally and seriously injured occupants. For an n-parameter (i.e., n-regressor) model, the equation contains one constant and n coefficients.

[1] The term “serious injury” generally refers to injuries that required hospitalization. Most investigation reports list these separately from fatalities. For this analysis, fatalities have been grouped with serious injuries, and the combined numbers are referred to as ‘‘severe injuries” for convenience.

The linear form of equation 1 is:

$$p = \frac{1}{1 + e^{-(x'\beta)}} \tag{1}$$

Therefore, the linear form of the single parameter (i.e., single regressor) of equation 2 is:

$$p = \frac{1}{1 + e^{-(\beta_0 + \beta_1 x)}} \tag{2}$$

The response variable for all modeling was fatal/serious injury events. Several kinematic variables were evaluated as candidate regressor variables. These include airspeed (ft/s), vertical velocity (ft/s), flight-path angle (degrees), pitch angle (degrees), vertical peak deceleration (G_z), and longitudinal peak deceleration (G_x). In the regional jet analysis, additional parameters were considered, including lateral peak deceleration (G_y), yaw angle (absolute value degrees), and roll angle (absolute value degrees). Each of these kinematic variables was modeled individually and as part of larger binary logistic regression model fitting analyses, using multiple regressor variables in an attempt to identify a best-fitting-model case.

The software used to accomplish these binary logistic regression analyses is Minitab® Version 16. All statistical analyses and modeling were performed using a level of significance (α) of 0.10. Therefore, the confidence intervals (CIs) presented in the analysis are all 90%. The interpretation of these 90% CIs is that, in repeated aircraft crash instances that meet the general parameters and conditions for the cases analyzed (e.g., fixed-wing aircraft type and water impacts), 90% will, in the long run, result in an estimated probability of fatal/serious injuries to occupants that falls within the indicated CI. The regression analysis includes a hypothesis to determine if the constant and the regressor coefficient(s) have non-zero values. The software calculates a *p*-value, and if this *p*-value is <0.100, then the constant or the coefficient is likely non-zero. The software then calculates three "goodness-of-fit" statistics: Pearson, Deviance, and Hosmer-Lemeshow. These test statistics have resultant *p*-values, and *p*-values <0.100 indicate the resultant model is a poor fit. The Summary Measures of Association consist of three metrics that quantify the model's ability to accurately predict the fatal-serious injury probability for new crash events that can be categorized in the same manner as those used to develop the model. The three metrics are: the Somers' D, Goodman-Kruskal Gamma, and Kendall's Tau-a. These three metrics vary in value from 0–1, with higher values indicating greater predictive capability. One additional evaluation of the binary logistic model (BLM) is made with regard to its prediction. This subjective evaluation by the author is whether the model predicts a trend, which is consistent with an intuitive expectation. Therefore, if a model predicts a decreasing fraction of severe injuries with increasing impact velocity, that model would be labeled "counter intuitive."

3. TASK 1 – WATER IMPACT STUDY

3.1 SELECTING MISHAPS FOR WATER STUDY

The CSTRG database was queried to identify suitable mishaps using the following fields and field values:

OPERATION = PASSENGER

DITCHING = D (unknown whether planned or unplanned)

This query returned 164 mishaps. A slightly different query was used to obtain an additional 10 mishap candidates. The CSTRG database was then used to determine the information available for each of the mishaps by reviewing the "resume" or summary text, and the mishap "home page" information, with specific attention to the availability and source of any report on the accident.

The availability of a report is important to this effort because detailed information on the kinematics of the impact, the damage to the aircraft, and the distribution of injuries within the wreckage are essential to understanding the survivability of these mishaps.

In addition to the CSTRG, the Aviation Safety Network (ASN) database [4] (a service of the Flight Safety Foundation) was used to acquire information about report sources and aircraft seating layouts. In many cases, the ASN database contained a direct link to the investigation report.

Mishaps were selected for inclusion in the study based on several criteria, including:

- Reference to an existing report.
- Primary impact (has to be with a body of water, not terrain or buildings).
- Aircraft's final position (i.e., in water).
- Potential for survivability.

Mishaps involving float-equipped planes and mishaps at high velocities and severe angles (i.e., non-survivable) were not considered.

The list of selected mishaps was then investigated in greater depth, and the title or source of the report was identified. Copies of the reports were downloaded from the Internet when available. Several mishaps were identified as being documented in various International Civil Aviation Organization (ICAO) documents. None of these documents could be located directly on the Internet, and a list of these mishaps was compiled and emailed to multiple people at the ICAO. The library at Embry Riddle University was also contacted to determine if it had a collection of ICAO documents. None of the ICAO-referenced reports were obtained. Foreign language reports were read with the assistance of Google Translate™ (French and Portuguese) to translate table of contents, figure captions, figure labels, tables, and selected segments of text. This method enabled two additional mishaps to be included in the analysis, although some difficulty was encountered if terms had technical meanings different from conversational meanings.

Three accidents were added to the list as a consequence of communication with an Aviation Rulemaking Advisory Committee on Crashworthiness and Ditching member. Several other accidents were suggested by this same source, but they did not meet the criterion of completeness of information.

Based on these two levels of review, 22 mishaps were selected for inclusion in the study. However, even for these mishaps, the datasets were not as complete as desired, especially the locations within the aircraft of injured and uninjured occupants, and the damage severity within the aircraft. The

damage description as it pertains to floor dislocation and seat disruption was particularly sparse, and, in many cases, the damage had to be inferred. For the more recent events (year 2000 and onwards), photographs of the damaged aircraft beyond those in the report were obtained using Google searches based on the date, date location, or date-airplane type/tail number. Photos were also found by seeking print publications local to the accident site and searching their databases. The list of water-impact mishaps is provided in appendix C and table 2.

3.2 ANALYSIS

3.2.1 Aircraft Population—Water

Although a diverse population of aircraft was sought, the population available ultimately consists of those airplanes that have crashed, those that crashed in countries where thorough investigations were conducted, and those that were in mishaps suitable for analysis. The aircraft in the dataset are characterized by such design features as number of engines, engine types, engine locations, wing position, weight class, and seats per row. Table 1–8 enumerate the aircraft-in-the-water dataset in terms of design characteristics.

Table 1. Number of engines—Water

Number of Engines	Number of Aircraft in the Dataset
2	16
3	3
4	3

Table 2. Engine configuration—Water

Engine Configuration	Number of Aircraft With Configuration
Engines on wing	15
Engines on tail	4
Engines on tail & in tail fin	1
Engines on wing & in fin	2

Table 3. Engine type—Water

Engine Type	Number of Aircraft With Type
Turboprop	7*
Turbojet	14
Reciprocating engine propeller	1

*All turboprop aircraft except one had the High-wing configuration.

Table 4. Wing configuration—Water

Wing Configuration	Number of Aircraft With Wing Configuration
Low-wing	16
High-wing	6 *

*All High-wing aircraft were turboprops.

Table 5. Aircraft weights—Water

Weight Category	Number of Aircraft in Each Category
A = less than 12,500 lb	0
B = 12,500–100,000 lb	10
C = 100,000–250,000 lb	7
D = 250,000–400,000 lb	2
E = greater than 400,000 lb	3

Table 6. Seats per row—Water

Total Seats per Row (Maximum) *	Number of Aircraft
0	1*
2	1
4	7
5	3
6	6
7	1
8	2

*Differs from definition in the CSRTG database, which is maximum number of seats without an aisle.
*One aircraft, a Shorts SD3-60, was configured for cargo at the time of the mishap.

Table 7. Total seats on aircraft—Water

	Total Passenger Seats
Average Number of Seats	96.3
Greatest Number of Seats	354
Least Number of Seats	0*
No. Aircraft With No Information	3

*One cargo configured airplane was included in the dataset.

Table 8. Mishap aircraft—Water

ATR72	BAC1-11	DC10-30CF
A320-214	CARAVELLE III	DORNIER 228
A310	CV880M	F27-500C
B727-235	DC3	HS748-1 -105
B737-8GP	DC8-62	IAI 1124A
B737-300	DC9-33F	NORD 262
B747-409B	DC10-30	SD3-60 (2)

The mishaps are also diverse in terms of both severity and scenario. The dataset exhibits a wide range in the phase of flight (see table 9), number of people injured, and the severity of damage to the aircraft. More relevant mishaps occurred during descent, approach, and landing than during takeoff and climb (see table 9). In mishaps ending with the aircraft in sea water, the aircraft was rarely salvaged. Four aircraft were considered “severely” damaged, and 18 were considered “destroyed.” The extent and the nature of the damage will be considered in greater detail in subsequent sections. In 19 of the 22 mishaps, the fuselage was considered to be “ruptured” as a result of impact. In 10 of the 22 mishaps, pre-ditching preparations were made; therefore, in 12 cases, there were no preparations. Eight of the 12 mishaps occurred during takeoff, aborted takeoff, or climb. Consequently, in four of the mishaps in which flight had been achieved, there was no preparation for ditching. The distance of the mishap from the shore ranged from right on the water line to 30 miles, with an average of 3.3 miles and a median of 0.4 miles (see table 10). The relationship of the median and average indicate that the majority of mishaps occurred very near shore, and the two mishaps farther off shore raised the average.

Table 9. Phase of flight and overrun—Water

Phase of Flight	Number of Mishaps
TAKEOFF	2
ABORTED	3
CLIMB	3
FLIGHT	1
DESCENT	1
APPROACH	7
LANDING	5
Characterized as "overrun," including both takeoff and landing (counted above).	6

Table 10. Distance from shore—Water

Distance of Impact From the Shore	Distance (miles)
Average	3.3
Median	0.4
Greatest	30.0
Least	0.0 (shoreline)

For the purpose of this study, injuries caused by the impact are of primary interest. Those injuries, which were clearly identified in the report as unrelated to the impact, are excluded from the injury count. Only one mishap in the dataset was completely free of injuries (see table 11). Lap infants are excluded from the passenger counts and injury counts in this study. In many investigation reports, minor injury counts are combined with no-injury counts; consequently, these two counts are combined throughout the analysis for consistency. The median value being lower than the average value in some categories indicates that the average was raised by one or more mishaps with large numbers. The distribution of injuries will be discussed in section 3.2.

Table 11. Severity of injuries—Water dataset

	Total Fatalities	Total Severe Injuries	Total Minor/No Injury
Average	14.1	5.9	63.1
Median	2	4	29
Maximum	169	17	285
Minimum	0	0	0

3.2.2 Mishap Scenarios—Water

The original/current basis for ditching design requirements is posited on an intentional landing in water, which occurs with enough advanced warning to prepare the aircraft for that landing. This concept for ditching assumes that the pilot still has some thrust (i.e., engine power) and, therefore, has sufficient control of the aircraft to manage the landing within the manufacturer's recommended parameters. In particular, the pilot has the ability to control aircraft pitch, roll, and yaw. The pilot also has the ability to optimize the vertical and horizontal velocities. The presence of thrust may also enable the pilot to maneuver the aircraft around to land parallel to the peaks and troughs of the waves or to attempt to land in the same direction as the wave motion rather than counter to the direction of the waves. Conversely, the lack of thrust forces the pilot to maneuver the aircraft within the constraints of the aircraft's existing airspeed and altitude (which can be viewed as kinetic energy and potential energy). Lack of thrust limits the pilot's ability to maneuver the aircraft and results in the use of pitch as the principle means for changing the airspeed and descent rate.

The 22 mishaps were classified into scenarios, and all but one fell cleanly into one of five scenarios. The classic planned landing on water (scenario A) described only three mishaps (see table 12.). In one of these, the pilot took the plane a few feet above the water and waited for the engines to flame-out. The third mishap in this scenario was an overweight aircraft that lost one of two engines just after takeoff, could not sustain climb, and, therefore, was ditched with reduced thrust. Entering the water without power is more common (seven events included) than the classic ditching with power (three events). The no-thrust events (scenario B) include loss of both engines because of ingestion (i.e., birds, ice, and water), loss of one engine followed by the inadvertent shutdown of the good engine, and running out of fuel (i.e., erroneous indication and leakage). In this dataset, the second-most-common scenario for transitioning from airborne into water is landing short, wherein the pilots lose situational awareness and land in the water short of the intended runway. Five instances of landing short in the water were suitable for inclusion. The remaining mishap involved flying into the water during the climb out. This case occurred when a stall warning caused the pilots to overcorrect and fly the plane into the sea. This latter event was treated as a separate scenario because the thrust was maintained at climb settings with the intent to continue flying, not ditch. However, the aircraft remained nearly level, impacting the water at low flight path and pitch angles but at high airspeed.

Briefly, the scenarios are designated:

- Scenario A – Ditching with some thrust (three instances).
- Scenario B – Ditching without thrust (seven instances).
- Scenario C – Landing on water short of the runway (five instances).
- Scenario D – Impact water during climb out (one instance).
- Scenario E – Runway overrun (landing or takeoff) (six instances).

Table 12. Water entry scenarios

CSTRG ID	Short Name	Aircraft Type	Scenario
20091118	NORFOLK ISLAND IAI 1124A	IAI 1124A	A
19940424A	BOTANY BAY DC3	DC3	A
19700502A	ST CROIX DC9	DC9-33F	A
20090115A	HUDSON RIVER A320	A320-214	B
20050806A	PALERMO ATR72	ATR72	B
20020116A	BENGAWAN SOLO RIVER	B737-300	B
20010227A	SCOTLAND SD360 DITCH	SD360	B
20000113A	LIBYA SD360	SD360	B
19910418A	NUKU HIVA DO228	DORNIER 228	B
19790310A	MARINA DEL REY N262	NORD 262	B
20130413A	NGURAH RAI B737	B737-8GP	C
19790217A	NEW ZEALAND F27	F27-500C	C
19780508A	PENSACOLA B727	B727-235	C
19690113A	SANTA MONICA BAY DC8	DC8-62	C
19670630A	CARAVELLE HONG KONG	CARAVELLE III	C
20000130A	ABIDJAN A310	A310	D
19931104A	HONG KONG B747-400	B747-409B	E
19840228A	JFK DC10	DC10-30	E
19820123A	BOSTON DC10	DC10-30CF	E
19790731A	SHETLAND 748	HS748-1 -105	E
19720719A	CORFU BAC1-11	BAC1-11	E
19671105A	HONG KONG, CV880M	CV880M	E

Based on the sample in this study, landing on the water without thrust is actually a more common scenario than landing with thrust. The reasons vary from bird, water, or ice ingestion (three instances); to loss of one engine after rotation followed by the shutting down of the good engine (two instances); to running out of fuel while still at flight altitude (two instances). Landing short of the runway in the water is also indicated as a common scenario. The number of mishaps (total

of 164) from the original query was revisited to determine how many of the accidents in the larger sample fit into one of the five scenarios. There were accidents that were outside the interest of this study, but 80 mishaps were found with sufficient information to assign them to one of the five scenarios (see table 13). The study sample overstates the frequency of ditching without power and understates the frequency of landing short in the water. Nevertheless, 20% of the potentially survivable landings on water in the larger mishap set were ditchings with no power. Ditchings in which there was some power available from at least one engine were considered "planned ditch with power," scenario A. The fraction of events that are of this type is confirmed by the larger set of mishaps. The percentages are rounded to the nearest full percent, and therefore may not add up to exactly 100%.

Table 13. Scenario frequencies—Water

	22 Mishaps Studied in Detail (percent)	80 Mishaps From Query With Assignable Scenario (percent)
Planned Ditch With Power (A)	14	15
Planned Ditch Without Power (B)	32	21
Landing Short in Water (C)	23	30
Level Flight into Water After Takeoff (D)	5	5
Runway Overrun (E)	27	29

Another water landing scenario occurs when the pilot unintentionally lands short of the runway. Five of the mishaps in the dataset are events of this type. The pilot has power, although it may be throttled down and is flying an approach profile, but because of circumstances, collides with the water rather than landing on the runway. Here, the impact kinematics are determined by the approach profile, or an approximation of the approach profile, and the pilot is in control but flying a landing approach, not a ditching profile.

The last scenario consists of overrunning the end of the runway (includes one instance of going into the sea off the side of the runway) and entering the water as the primary impact. This mishap scenario happens in one of two ways: either the landing touchdown allows insufficient stopping distance, or a takeoff is aborted with insufficient stopping distance. In either case, lack of runway friction or improper operation of the braking system may contribute to the failure to stop within the runway length. In these cases, the pilot has no control over the horizontal (longitudinal) velocity or the pitch angle; however, the pilot often yaws the aircraft to avoid the structures off the end of the runway. In cases for which the primary impact was into or onto such a structure, the mishap was not included because the damage was different in nature from the damage caused by water.

3.2.3 Mishap Scenarios and Buoyancy

The emergency provision for ditching [5] states that if the system provides for jettisoning fuel, "the jettisonable volume of fuel may be considered as buoyancy." In the 15 events analyzed in this report (see table 14) for which the aircraft entered the water from the air, the reference to jettisoning

fuel appears to be irrelevant. Four aircraft entered the water during takeoff or climb and would not have had time to jettison fuel. Eleven aircraft entered the water during descent, approach, or landing phases. Three of these had no fuel or minimal fuel, and that was the reason for ditching. The remainder of aircraft presumably had the normal reserve or more. Seven events were ditchings without power. In many cases, fuel was on board, but there was little time available to jettison it because the crew would be busy either trying to restart the engines or understanding the nature of the problem. Based on the mishaps in this study, the guideline would be applicable more frequently if the fuel load considered for buoyancy purposes becomes the one planned for reserve in normal operation. However, this guideline would have overestimated the buoyancy in the four mishaps that entered the water during or shortly after takeoff, when the fuel load would be greatest. The Abidjan mishap is discounted from consideration because the severe breakup of the aircraft flotation was not a consideration.

Table 14. Fuel loads for mishaps, scenarios A–D

ID	Mishap Name	Phase	Scenario	Fuel Status (assumed unless noted)
20091118	NORFOLK ISLAND IAI 1124A	LANDING	A	Near empty (report)
19940424A	BOTANY BAY DC3	CLIMB	A	Fuel for mission
19700502A	ST CROIX DC9	APPROACH	A	Empty (report)
20090115A	HUDSON RIVER A320	CLIMB	B	Fuel for mission
20050806A	PALERMO ATR72	FLIGHT	B	Empty (report)
20020116A	BENGAWAN SOLO RIVER B737	APPROACH	B	Normal reserve end of flight
20010227A	SCOTLAND SD360 DITCH	CLIMB	B	Fuel for mission
20000113A	LIBYA SD360	DESCENT	B	Normal reserve end of flight
19910418A	NUKU HIVA DO228	LANDING	B	Normal reserve for mission; because of island destination, may have been fueled for return flight
19790310A	MARINA DEL REY N262	TAKEOFF	B	Fuel for mission
20130413A	NGURAH RAI B737	APPROACH	C	Normal reserve end of flight
19790217A	NEW ZEALAND F27	APPROACH	C	Normal reserve end of flight
19780508A	PENSACOLA B727	APPROACH	C	Normal reserve end of flight
19690113A	SANTA MONICA BAY DC8	APPROACH	C	Normal reserve end of flight
19670630A	CARAVELLE HONG KONG	APPROACH	C	Normal reserve end of flight
20000130A	ABIDJAN A310	TAKEOFF	D	Fuel for mission, but flotation not an issue because of break-up.

3.2.4 Kinematics of Impact—Water

Before delving into the differences between the individual scenarios, it is worthwhile to look at the larger dataset. Using the larger set of data for the purpose of setting design guidelines and test conditions may be desirable. In this analysis, the data for scenarios A–C are grouped together. These scenarios have the common attribute that the impact with water occurs from the air (i.e., the aircraft is airborne prior to impact, and the pilots are in the process of landing). The one mishap (scenario D) in which the aircraft was still at takeoff power is excluded from this group. Being airborne causes at least two factors to be different compared to the overrun scenario: The velocity

is higher, and the attitude has an additional degree of freedom. The overrun scenario is analyzed in section 3.2.4.3, in which each scenario is reviewed separately.

In characterizing kinematics of these impacts, histograms were created to show the number of mishaps that occurred within ranges or "bins" of each parameter. The cumulative percentile is also presented on each chart. The kinematic parameters analyzed are: vertical velocity, airspeed, flight-path angle, pitch angle, roll angle, yaw angle, peak vertical deceleration, peak longitudinal deceleration, and peak lateral acceleration. These plots of the data indicate the most frequent values with which crashes occur for each kinematic parameter.

The vertical velocity (absolute value) histogram (see figure 1)[2] reveals an approximately normal-shaped distribution (i.e., the most common velocity is near the middle of the range of all velocities). For the vertical velocity, the average value of 18.9 ft/s is similar to the mean value 17.1 ft/s.

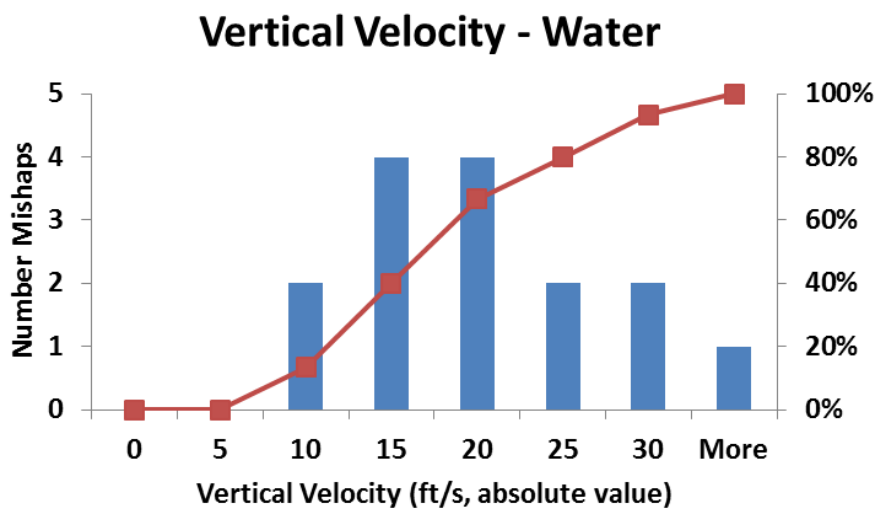

Figure 1. Vertical velocity scenarios A-C – Water

For the airspeed, the average value of 194 ft/s is similar to the median of 200 ft/s. Either value is representative of the central tendency for this parameter, and the fact that the two are approximately equal is a confirmation that the two values are good representations of the sample set. The range of airspeed (see figure 2) is from 123–272 ft/s for individual mishaps. Approximately half of the mishaps occurred with speeds below 200 ft/s.

[2] The histogram charts created in Excel are read using the number under the column as the upper limit of that bin. The bin width is the difference between two bins. In the diagram, there was no mishap with a velocity of -5–0; likewise, 0–+5; two mishaps in the range 5-10 ft/s, and four mishaps between 10 and 15; likewise, 15 to 20.

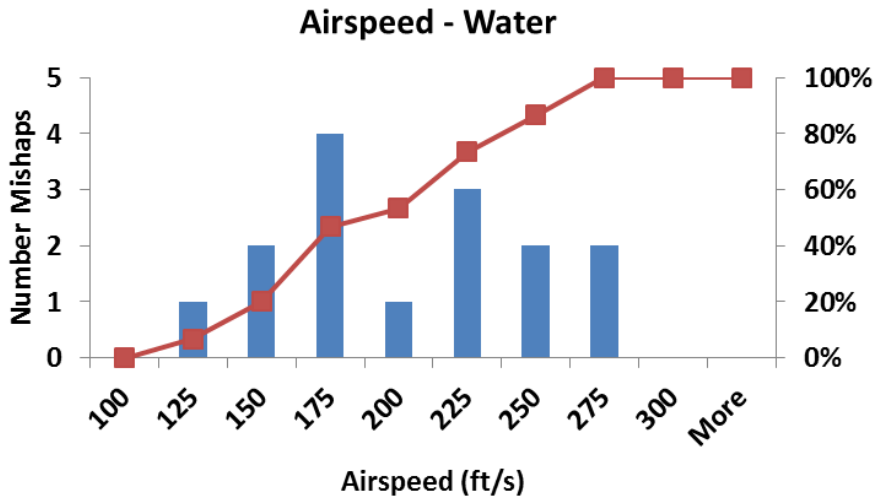

Figure 2. Airspeed – Water scenarios A–C

The flight-path angle is the angle between the path of the aircraft center of gravity and the horizon (see figure 3). Flight-path angles were entered in the analysis as negative angles indicating downward but are displayed (see figure 4) as positive values. The flight-path angles are clustered within the range of 0–8º, with just one extreme value greater than 16º (see figure 4). In the extreme flight-path-angle case, a double-engine flame-out occurred shortly after rotation. The pilot did not have much airspeed but elected to reduce the forward speed by pulling up the nose, resulting in a higher vertical descent rate.

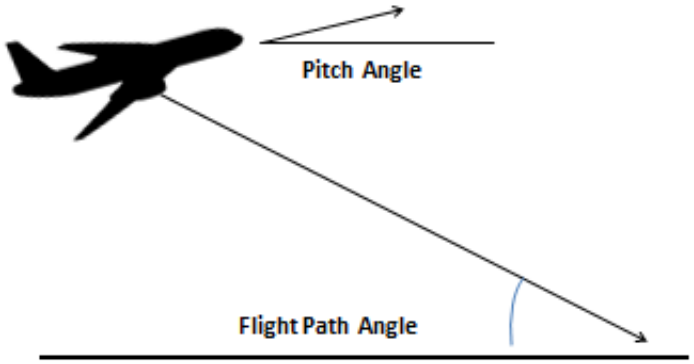

Figure 3. Flight path—pitch angle relationship

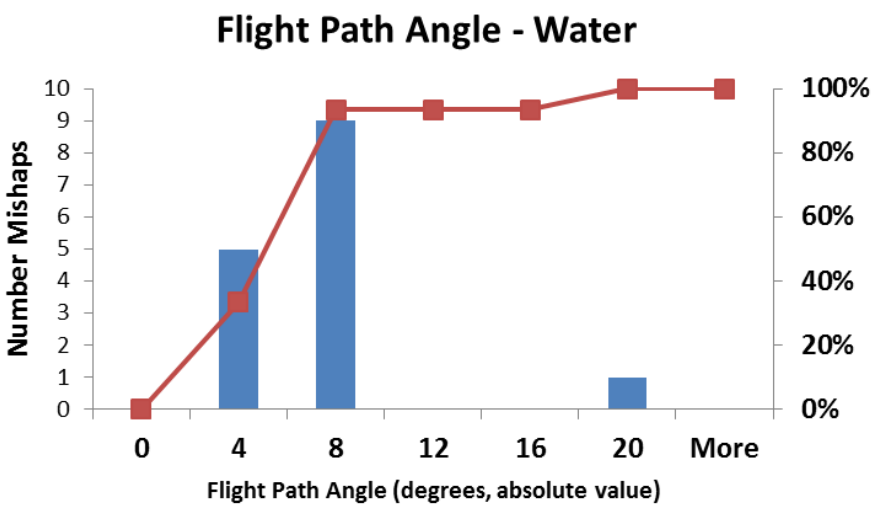

Figure 4. Flight-path angles in scenarios A–C—Water

The pitch angle is the angle between the longitudinal axis of the aircraft and the horizon (see figure 3); nose up is positive pitch angle. The pitch angle histogram (see figure 5) revealed that, out of the 14 mishaps with known pitch angles, only two impacted with the nose down, and those were less than 5º below the horizontal. The most common attitude was within the range of +5 and +10º.

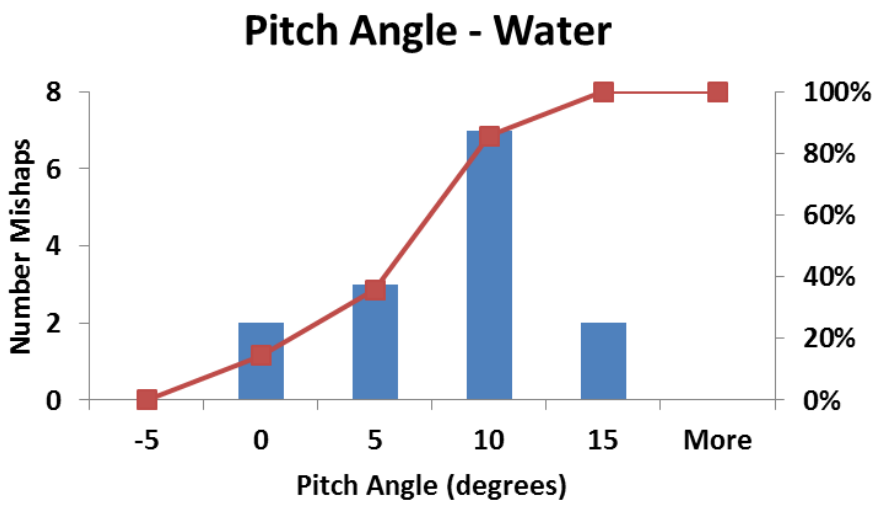

Figure 5. Pitch angle in scenarios A–C—Water

Considering that the aircraft involved in scenarios A–C were generally under control, the roll (see figure 6) and yaw (see figure 7) angles were limited to a narrow range around the nominal flight condition of 0 roll and 0 yaw.

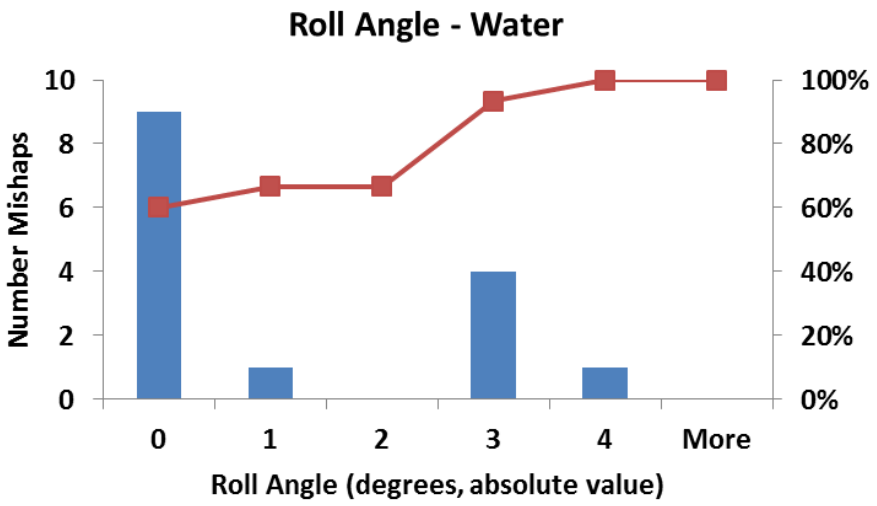

Figure 6. Roll angle in scenarios A–C—Water

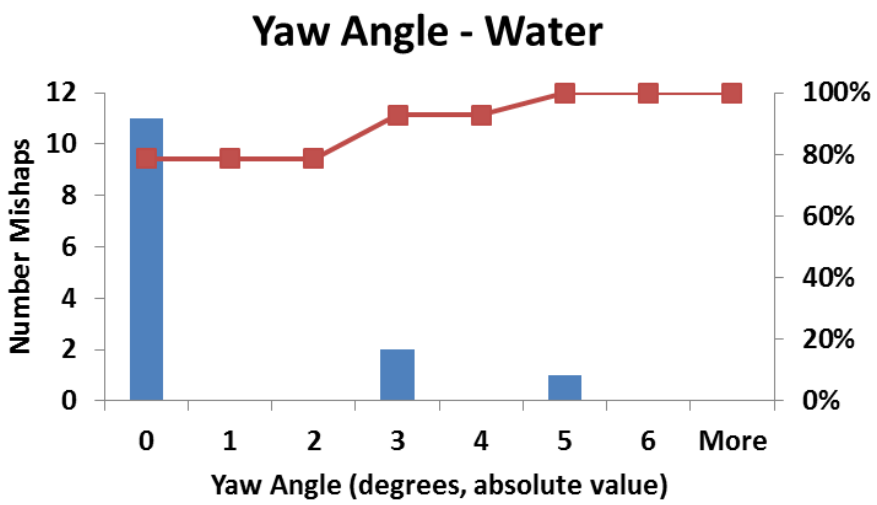

Figure 7. Yaw angle scenarios A–C—Water

Because only a few of the aircraft involved had flight data recorders (FDR) equipped with sensors to measure vertical (also referred to as "Normal") acceleration, most of these data values are estimated by reconstruction. None of the aircraft was equipped to record longitudinal acceleration; consequently, all data in this plot are reconstruction estimates. As can be seen in figure 8, the longitudinal deceleration was less than 4 G in 40% of the mishaps and less than 16 G in the remainder. These values represent the peak deceleration in the event. Survivors in several reports were quoted as saying that the impact was no worse than a hard landing. In the longitudinal direction, the reason for the low peak values, in spite of the high airspeeds, is likely the distance over which the deceleration occurred. With low flight-path angles, the aircraft would likely decelerate slowly as the fuselage skipped over the crests or slowly settled into the water tail first. More than one report stated that multiple contacts were felt by the survivors. The vertical deceleration is an even tighter distribution with 10 of the 13 mishaps experiencing a vertical deceleration between 0 and 5 G (see figure 9). The case of the highest vertical acceleration was an

event in which the aircraft unexpectedly ran out of fuel at cruise altitude, and the pilots spent time unsuccessfully trying to restart the engines (not realizing that the fuel had been exhausted) and then trying to reach an alternate airport. When they finally planned to ditch, there was insufficient time to complete the ditching check list. Additionally, the pilots attempted to turn shortly before water contact, losing airspeed and increasing sink rate.

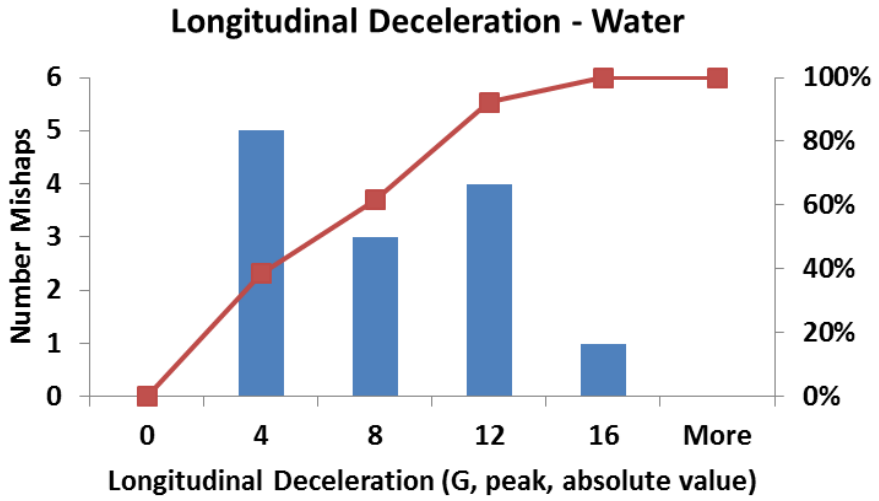

Figure 8. Peak longitudinal deceleration in scenarios A–C—Water

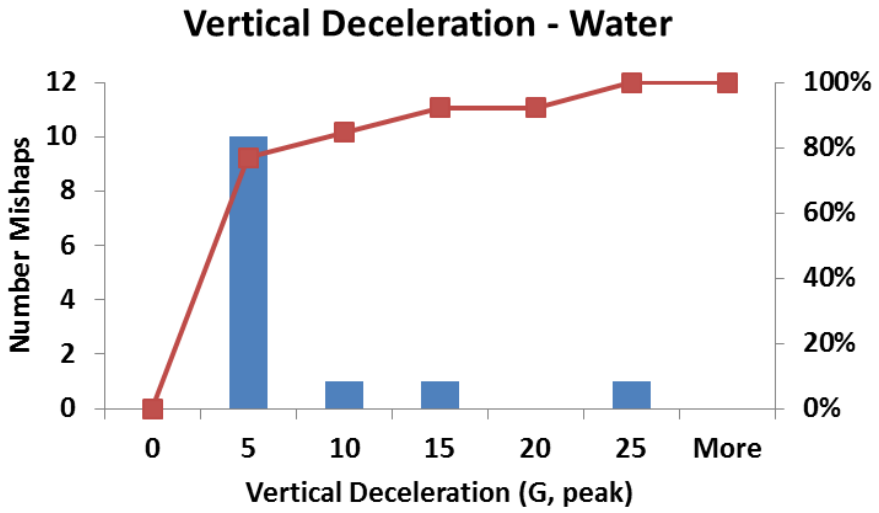

Figure 9. Peak vertical deceleration in scenarios A–C—Water

Considering the small number of mishaps and the even smaller numbers associated with each scenario, statistical considerations indicate that median values may be more representative of the sample than average values. Consequently, in the remainder of this discussion, both average and median values will be presented. When the two values agree, it can be inferred that the population of values is reasonably symmetric as opposed to being positively or negatively skewed.

3.2.4.1 Sea state information—water

The investigation reports provided information on the sea state for only 7 of the 16 crashes (scenarios A–D) from the air (see table 15). Specific sea states were reported in only two cases. This lack of information was unfortunate for two reasons. The first is that only the aircraft kinematics can be used to describe the impact—with no information of the wave action or relative direction of impact to the sea. Even though, in several cases, the survivors reported feeling multiple impacts, without knowing the sea state, it is insufficient to infer whether these contacts were with wave crests or the aircraft skipped over a flat surface. The second negative aspect is that no information is available to use for choosing limits on the sea state that is to be considered for setting ditching requirements. The fact that many mishaps occurred near shore (two occurred in rivers) implies that setting ditching conditions based on an average of worldwide sea states is unduly severe.

Table 15. Sea state data—Water

Mishap	Scenario	Wind (degrees/kts)	Sea Description
20091118A	A	110/10	No sea information.
19940424A	A	Calm	No sea information.
19700502A	A	110/10	No sea information.
20090115A	B	No information	Calm (report) river current 1.4 kts with flight dir.
20050806A	B	330/77	Wave direction SE sea state NW 3 to 4 Douglas scale.
20020116A	B	Thunderstorm—No detail near impact.	Narrow river, rain storm. Post-mishap photo shows flat surface.
20010227A	B	030/16	Sea state 5, sea swell 2. Tide ~ high.
20000113A	B	120/15	No sea information.
19910418A	B	060/18–24	Perpendicular to the swell, touched down on a swell front.
19790310A	B	250/8	No sea information.
20130413A	C	90/7	Landed in direction of surf. Photo indicates very low surf.
19790217A	C	360/15	No sea information.
19780508A	C	190/7	Wind, wave, and current action minimal.
19690113A	C	060/10	No sea information.
19670630A	C	250/10	No sea information.
20000130A	D	250/4	No sea information.

3.2.4.2 Kinematics of each mishap scenario—water

The first three scenarios are similar in that they are all events for which the aircraft is descending with the intent to land. They differ in the degree of control of the pilots and the expectation of where the landing will occur. Both the vertical and longitudinal velocities (see table 16) are higher for the ditchings without thrust than for the ditchings with thrust. The relative difference is much larger for the vertical velocity; therefore, the flight-path angle for the ditching without thrust is steeper. Without thrust, the pilot's control of the vertical velocity is limited. From the pitch angle (see table 16), it is evident that pilots, who are aware of imminent landing (A and B), are bringing the nose up in anticipation of contact with the water. In contrast, when the pilots are not yet anticipating actual touchdown, the aircraft attitude is on average level (min. to max. = -3.1 to +3.0, whereas in both of the ditching scenarios, all mishaps are positive pitch). The impact with the water could also be characterized by the angle between the axis of the aircraft and the flight path that the airplane is traveling. The aircraft angle of attack (see table 16, far right column) is approximated by pitch angle minus flight-path angle. This calculated angle highlights a large difference between a ditching without thrust and either ditching with thrust or landing short. The higher value of this aircraft angle of attack suggests that aircraft ditching without thrust will strike the water tail first; the consequences of the tail-first contact will be investigated in the damage and injury discussions. The trends discussed in this paragraph are also reflected in the median values (see table 16) of the same parameters, therefore indicating that the trends are not drastically affected by one or more extreme values in each parameter.

Table 16. Kinematics of ditching scenarios—Averages—Water

Scenario {# of events in average}	Med./Avg. Vert. Vel. (ft/s)	Med./Avg. Airspeed (ft/s)	Med./Avg. Flight-Path Angle (deg.)	Med./Avg. Pitch Angle (deg.)	Avg. Aircraft Angle of Attack (deg.)
A: Ditch w/thrust {2}	-9.4/-10.7	148/161	-3.6/-3.8	6.0/6.0	9.8
B: Ditch w/o thrust {7}	-19.5/-15.6	187/170	-7.0/-5.0	8.1/6.8	15.1
C: Landing short {5}	-23.8/-24.2	232/233	-5.4/-6.2	0.1/0.2	5.5
D: Climb out to water {1}	-10.9/-10.9	354/354	-1.8/-1.8	0/0	1.8
E: Runway overrun {6}	-6.3/-10.0	68.0/80.2			

The scenario identified as "loss of control on climb-out" (D) covers one mishap that did not fit into any of the other scenarios. In response to a stall warning shortly after takeoff, the aircraft was leveled-off and actually was pitched nose down at very low altitude. The accident occurred at night from a runway that ended over the water with little to no visual reference. As a consequence, the aircraft entered the water at a high airspeed and a low descent rate. The engines remained at takeoff (or climb) thrust, but due to darkness and lack of landmarks, the pilots lost awareness of their altitude and flew into the water. The aircraft was torn apart by impact forces.

3.2.4.3 Kinematics of runway overruns – water

The scenario identified as "runway overrun into water" consists of two manifestations: 1) either aborted takeoff with insufficient stopping distance, or 2) a poorly executed landing (too much speed or "landing long" with insufficient stopping distance). In all but one of these mishaps, the aircraft had thrust available (in some cases, reverse thrust was being applied) and was under braking. In the one different scenario, the aircraft could not rotate due to a locked elevator and went off the end of the runway at near takeoff speed with thrust applied. In the mishaps covered by this scenario, the primary impacts are considered to be the nose impacting the water and the flight path to be the slope of the shore into the water. In a few cases, the nose can have a downward vertical component to its velocity as it drops from a precipitous seawall, but this velocity is localized at the nose. In some cases, the plane may have a significant pitch angle—if the nose wheel drops off a seawall—while the main gear remains on the runway for some period of time. The events in this scenario are characterized by low longitudinal impact velocities (average longitudinal velocity = 80 fps, the median = 68 ft/s), compared with the three ditching scenarios. These all had average longitudinal velocities exceeding 148 ft/s. For this scenario, mishaps were not selected if the aircraft collided with a structure prior to entering the water or ended on structure over the water.

3.2.5 Quantifying Damage – Water

An attempt was made to correlate the fuselage breaks with the various kinematic parameters and with injuries, but none of the break locations showed a good correlation to the kinematics or to the injuries. There were only 20 breaks recorded out of 88 locations[3] (22 aircraft multiplied by four locations in each aircraft). As described in the method section, the damage metric was created to provide a quantitative descriptor of the damage in each segment of the aircraft. By adding up the damage metric for each segment, a damage descriptor for the entire fuselage of the aircraft is created.

The damage modes include underside fuselage damage, floor disruption, seat failure, and loss of occupied volume. The damage mode in each fuselage segment (i.e., cockpit, forward cabin, overwing cabin, rear cabin, and tail) is assigned one of three levels: none, localized, or widespread. When a break occurs, it is assigned to the rearward of the two segments that have separated. The values for the water dataset are presented below (see table 17). With a maximum of 24 fields describing aircraft damage, the mishap with the least information was the DC-9 ditching near St. Croix (19700502A), which sank in deep water shortly after impacting the water. The effect of any missing cell is to reduce the value of the damage metric because NI is assigned a zero value. Several means for working around this missing data were considered, but none was deemed satisfactory. As a consequence of the large number of missing data, the St. Croix mishap (19700502A) was eliminated from the damage analysis. The column on the right of table 17 lists the number of cells containing NI; the total damage metric for these mishaps may be lower than would have been recorded had all of the information been available.

[3] Common break locations are: between cockpit and forward cabin, between forward cabin and overwing cabin, between overwing cabin and rear cabin, and between rear cabin and tail.

Table 17. Mishap damage metrics – Water

Reference # ID	Scenario (A–E)	Cockpit Damage Metric	Fwd Cabin Damage Metric	OW Cabin Damage Metric	Rr Cabin Damage Metric	Tail Damage Metric	Total Damage Metric	# of NI
20091118	A	0	0	9	2	0	11	3
19940424A	A	0	0	3	0	0	3	0
19700502A	A	0	0	0	0	0	0	15
20090115A	B	1	1	2	4	4	12	0
20050806A	B	20	20	15	13	5	73	0
20020116A	B	8	4	2	6	10	30	3
20010227A	B	20	2	2	2	5	31	8
20000113A	B	14	11	8	8	13	54	5
19910418A	B	10	10	5	0	0	25	10
19790310A	B	4	5	0	0	0	9	6
20130413A	C	1	1	1	10	1	14	0
19790217A	C	6	15	12	12	0	45	1
19780508A	C	1	2	2	7	12	24	0
19690113A	C	16	12	9	23	20	80	0
19670630A	C	4	6	4	8	14	36	6
20000130A	D	20	23	23	23	23	112	0
19931104A	E	8	3	0	0	0	11	3
19840228A	E	10	4	0	0	0	14	3
19820123A	E	13	14	0	0	0	27	0
19790731A	E	8	10	11	1	1	31	5
19720719A	E	1	0	0	0	0	1	0
19671105A	E	13	14	7	0	0	34	0

The frequency with which the different damage modes occurred within each segment are presented in table 18. An overall trend is for damage to occur less frequently for the segments farther to the rear. Although floor disruption occurred in roughly half of the mishaps, seat failure occurs significantly less often. The cockpit was the segment most often experiencing loss of volume. Breaks occurred more often on either end of the forward fuselage than on either end of the rear fuselage. Looking at the distribution of breaks over the various scenarios (see table 19) reveals that the ditchings with thrust averaged only one-third of the rate of fuselage breaks as the ditchings without thrust. Ditchings without thrust experienced more frequent breaks than landing short. Acknowledging that scenario A is a small sample of just three mishaps, the question of causation for this difference should be considered.

Table 18. Damage modes assigned to segments – Water

All Mishaps (22 Mishaps)	Cockpit (# of Mishaps)	Forward Cabin (# of Mishaps)	Over-wing Cabin (# of Mishaps)	Rear Cabin (# of Mishaps)	Tail (# of Mishaps)
Underside skin damage	16	16	13	13	16
Floor disruption	13	15	9	11	8
Seat failure	7	7	5	5	5
Loss of occupant volume	13	7	4	5	6
Fuselage breaks	NA	6	6	4	4

Table 19. Fuselage break frequency – Water

	Number of Fuselage Breaks	Number of Fuselage Breaks per Mishap
Scenario A: Ditching with Thrust (3 mishaps)	1	0.33
Scenario B: Ditching Without Thrust (7 mishaps)	7	1.00
Scenario C: Landing Short (5 mishaps)	4	0.80
Scenario D: Flight into Water (1 mishap)	4	4.00
Scenario E: Runway Overrun (6 mishaps)	4	0.67

To understand the larger number of breaks occurring in ditchings without thrust, the difference in kinematic parameters are isolated from table 19 and presented in table 20. In each case, the kinematic value for scenario B, ditching without thrust, is in the direction expected to lead to more damage. In particular, the vertical velocity at impact for scenario B is nearly double the value for scenario A. The flight-path angle must be higher because the median vertical velocities are very different between the two scenarios, whereas the airspeeds are more similar. The pitch angles are not widely different, but when combined with the flight-path angle, lead to a parameter with a large difference. This parameter may be indicative of how severe the slap-down may be on impact. The term “slap-down” is used to describe the rotation of the aircraft about the initial point of contact between the tail and the water. In the three ditching with power mishaps, only one fuselage break occurred between the forward cabin and the wing box. Whereas in the seven ditchings without power, there were two breaks at each potential break location, except the forward cabin to overwing cabin, where there was just one break.

Table 20. Kinematic comparison between scenarios A and B – Water

	Scenario A Ditching with Thrust (3)	Scenario B Ditching without Thrust (7)
Median Vertical Velocity (ft/s, - is downward)	-9.4	-19.5
Median Airspeed (ft/s)	148	187
Flight-Path Angle (degrees, - is downward)	-3.6	-7.0
Pitch Angle (degrees, + is nose up)	6.0	8.1
Pitch Angle—Flight-Path Angle (degrees, + is nose up)	9.8	15.1

The damage metric values obtained for each mishap range from 0–120 (see table 17). Recalling that scenario A is the water entry with power (conventional ditching), it is evident that the damage metric in this scenario was generally low and indeed, the average value is 7 and median is 7 (this scenario was a sample of only two usable mishaps).

The indicated damage was far greater for scenario B (seven events), water entry without power, for which the average value is 33 (median 30). For the landing short in water, scenario C (five events), the average was 40 (median 36). The runway overrun scenario E had a lower average damage metric (average 20.5, median 19.7) than the average for the water landing scenarios (A–C). The lower value of the damage metric (see table 21) was consistent with the damage being generally limited to the cockpit and forward cabin, and the generally lower velocity of the impact.

The number of mishaps in each scenario was limited. Consequently, the group of scenarios (A–C) in which the impact was from the air was analyzed first to look for trends in the damage that will support design guidelines.

Using the damage metric, the median and average amount of damage occurring in all ditchings can be compared to the median and average damage for overrun mishaps (see table 21). Both the medians and the averages indicate that the damage was greater for the mishaps where the aircraft impacted the water from the air compared with those impacting the water as a result of a runway overrun. In the case of scenario E, the median and the average being close to each other in value served to confirm that each was representative of the sample and that the population values were reasonably symmetric about these central tendency values.

Table 21. Damage metric air and overrun – Water impacts

	Impacts from the Air (Scenarios A–C)	Impacts due to Overruns (Scenario E)
Median Damage Metric (unitless)	25.0	20.5
Average Damage Metric (unitless)	31.5	19.7

3.2.5.1 Damage related to kinematics from the air (A–D) – water

Having developed a means to quantify the damage in a single value, a correlation between the damage incurred and the various kinematic parameters can now be sought. The correlation between velocity and damage metric (see figures 10–11) is not strong for either the airspeed (velocity along the flight path) or for vertical velocity. There was no good means to consistently characterize the state of the water that the aircraft impacted, and the variability of the water surface impacted may contribute to the overall variability in the damage data, as may differences in aircraft configuration (to be investigated in section 3.2.7). Looking for correlation between the damage and either the flight-path angle or the pitch angle (see figures 12–13) also proved unproductive. An angle, which might be described as an "angle of attack" was created by subtracting the flight-path angle from the pitch angle (see figure 3), resulting in the angle between the axis of the aircraft and the velocity vector of the aircraft. This angle had an even poorer correlation with damage than either the pitch or the flight-path angle.

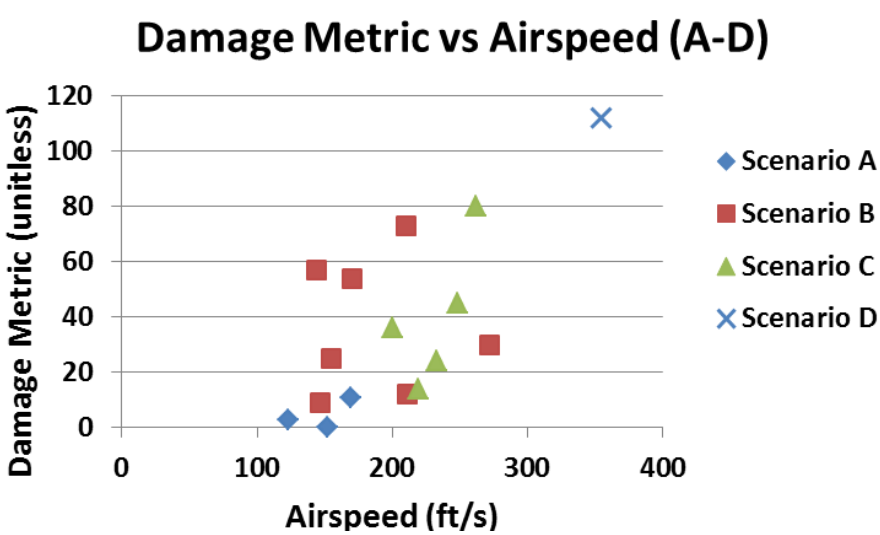

Figure 10. Damage correlation to airspeed—Water

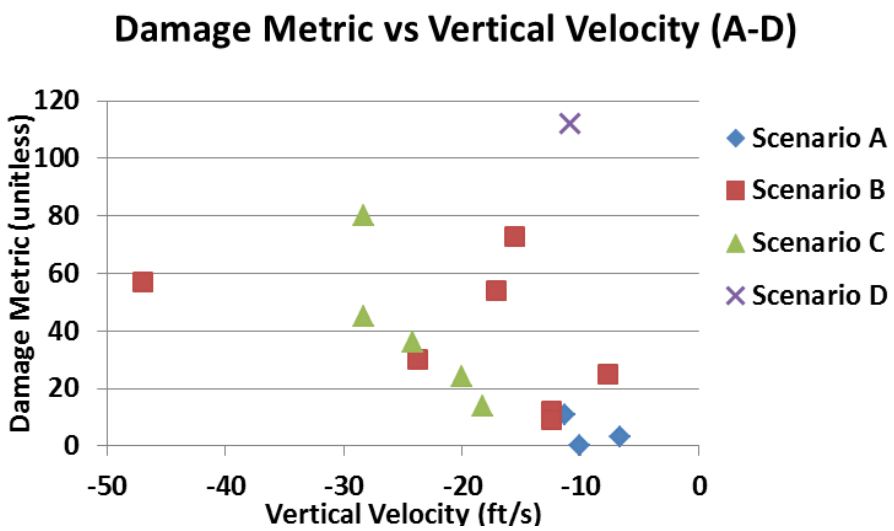

Figure 11. Damage correlation to vertical velocity—Water

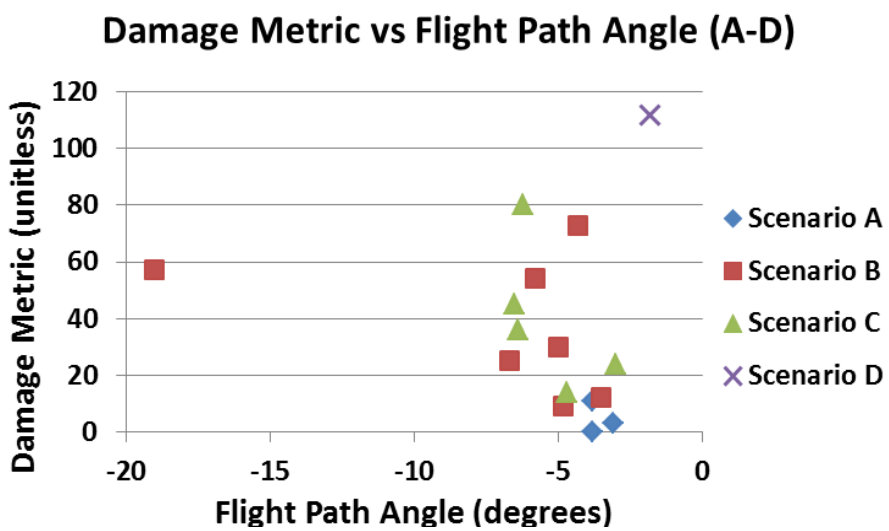

Figure 12. Damage correlation to flight-path angle—Water

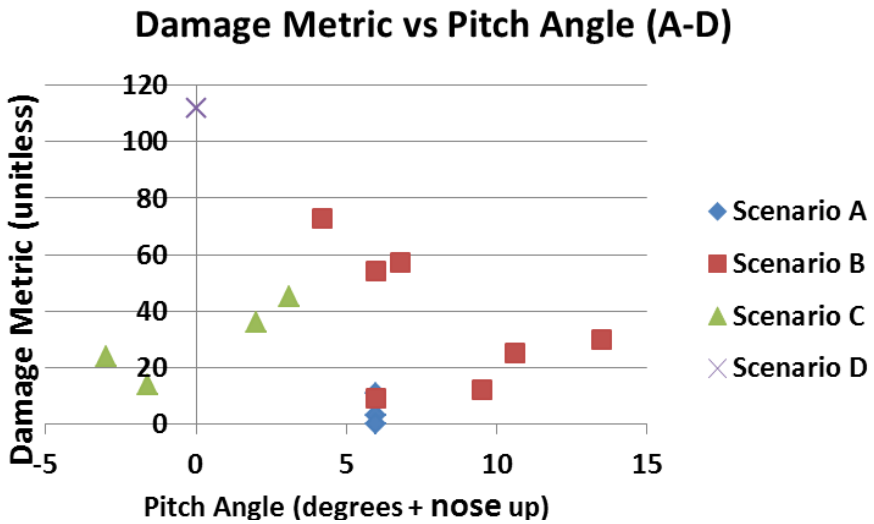

Figure 13. Damage correlation to pitch angle—Water

3.2.5.2 Segment damage by scenario – water

The damage metric is built up segment by segment. Consequently, the trends between segments within a scenario and between scenarios within a segment can be viewed (see table 22). Comparing the damage between scenarios, it is evident that the ditching without power leads to greater damage on average than ditching with power. The one exception is the overwing segment where average damage is roughly equal for the two scenarios. Recalling the differences in kinematics between these two scenarios (see table 16), the most significant differences were in vertical velocity and the flight path and pitch angle. The larger impact angles may contribute to the greater damage, particularly at both ends of the aircraft. This inference is supported by the trend in damage for aircraft that landed short (scenario C), which has a median flight-path angle intermediate to scenarios A and B, but a nearly flat pitch angle. The damage metrics for scenario C are generally intermediate to scenarios A and B but slightly higher to the rear of the aircraft. The overruns demonstrate a clear bias for damage in the two forward segments.

Table 22. Segment damage by scenario—Water

	Cockpit (Total Damage Metric/ #Mishaps)	Forward Cabin (Total Damage Metric/ #Mishaps)	Overwing Cabin (Total Damage Metric/#Mishaps)	Rear Cabin (Total Damage Metric/ #Mishaps)	Tail (Total Damage Metric/ #Mishaps)
Scenario A	0	0	6	1	0
Scenario B	11	9	5	5	7
Scenario C	6	7	6	12	9
Scenario D	20	23	23	23	23
Scenario E	9	8	3	0	0
Scenarios A–C	8	7	5	7	7

3.2.6 Damage Dependence on Design Characteristics – Water

The dependence of damage on design factors for water impacts from the air (scenarios A–C) was analyzed using the Damage Metric. Of the 15 mishaps in these three scenarios, nine were low-wing aircraft and six were high-wing aircraft (see table 23). As noted earlier, all of the high-wing aircraft were turboprops. The median damage metric for the high-wing aircraft is substantially higher than the median damage metric for the low-wing aircraft. The difference in the average damage metrics is not as great as the difference between the median damage metrics. The low-wing sample has a very wide range of values. Looking at the vertical velocities, the similarity in median values suggests that there is not a large difference in vertical velocity between the two aircraft types. The high-wing sample contains one mishap with an unusually high descent rate (47 ft/s), which raises the average. As can be anticipated, the low-wing aircraft, which are all turbojets except for one, have a higher median airspeed, and this large difference is confirmed by the averages. Looking at the entire group of water impacts, they exhibited only a very weak trend of increased damage as airspeed increased (see figure 10). Therefore, based on airspeed only, the low-wing aircraft would be anticipated to experience the higher damage metrics as a consequence of the higher impact speeds. The difference in median airspeeds implies that the low-wing aircraft impact with 67% more kinetic energy than the high-wing aircraft. However, it is the high-wing aircraft that experience the higher damage metrics; therefore, it is reasonable to conclude that the high-wing configuration does in some way contribute to the greater damage experienced by these aircraft.

Table 23. Damage dependence on wing configuration

Scenarios A–C	Low-Wing Aircraft	High-Wing Aircraft
Damage metric median	14.0	49.5
Damage metric average	23.3	43.8
Vertical velocity median (ft/s)	-18.3	-16.4
Vertical velocity average (ft/s)	-16.2	-21.4
Airspeed median (ft/s)	211	163
Airspeed average (ft/s)	205	179
Number of mishaps (#)	9	6

Another design factor recorded in the study was the number of seats in a row in each aircraft. This parameter was altered from the parameter defined in the CSTRG database. The database records the largest number of seats without the interruption of an aisle. However, for structural response purposes, the diameter of the fuselage was deemed to be of greater interest. Consequently, the value reported here is the total number of seats across the airplane, which is effectively a parameter related to fuselage cross-section and related bending and torsional strength. This analysis was also limited to the impacts from the air (scenarios A–C, with a total of 15 events). Two row sizes proved to be the most common: four and six seats. The two configurations showed little difference in the damage caused in the mishaps (see table 24). If, in fact, the severity of damage depends on fuselage cross-section, the values of fuselage cross-section for these two samples are too close together for the trend to reveal itself. The range in seats per row for the entire sample is two to nine seats.

Table 24. Damage dependence on seats per row

	Aircraft with 4 Seats per Row	Aircraft with 6 Seats per Row
Median Damage Metric	28	24
Average Damage Metric	32.5	32
Number of Events	6	5

One feature of this relationship that is worth noting is that the runway overrun mishaps are disproportionately populated by large cross-section aircraft. Out of six aircraft in scenario E, the number of seats per row are nine, eight, seven, six, five, and four. In the whole population of 22 aircraft, only four had seven or more seats per row, and three of those four were in the runway overrun scenario.

For both the ditching with power and the ditching without power scenarios, all the aircraft involved were equipped with two engines. However, it should be noted that these ditchings were not all due to engine failure, as at least two were due to insufficient fuel, which would have brought the aircraft down regardless of the number of engines. Of the five aircraft that landed short, one had three engines, and another had four. The loss of control on climb-out (scenario D) was a two-engine aircraft. Only two of the aircraft in the runway overrun scenario were equipped with two engines (these two were in the lightest weight category), but this is not surprising considering that of the six mishap aircraft, three aircraft were in the heaviest weight category.

3.2.7 Damage and Engine Configuration

The engine configuration shows a strong effect on the damage outcome (see table 25). Of the 15 aircraft ditching, 11 had all engines on the wing, and only three had engines on the tail. One of these three was a tail/fin configuration; the remainder engines were the tail configuration. Both the mean and the median values have far higher damage metric values for the aircraft with wing-mounted engines. To eliminate causes other than the engine configuration, the vertical velocities and airspeeds were compared for these two sample sets (see table 26). The two groups, wing-mounted engines and tail-mounted engines, had similar vertical velocities, as indicated by both the median and average values for the sample. Likewise, the airspeeds for both samples are very similar, as expressed by the median and average of each sample. The similarity in velocity indicates that the difference in damage experienced by the two different configurations is not due to a difference in their impact velocities. Having eliminated velocity as the possible cause, the other kinematic parameters—pitch angle and flight-path angle—are reviewed. For both of the angles, the median values and the average values are similar; consequently, only the median values will be reported (see table 27). Neither of the angles demonstrates a large difference in value between the wing-mounted engine group and the tail-mounted engine group. Given that there is a large difference in damage between the two datasets, one might expect to see the large difference in damage reflected as a large difference between either peak vertical deceleration or peak longitudinal deceleration. For example, hypothetically, the low hanging wing-mounted engines would present more surface area to the water on impact in either the vertical or longitudinal direction and, consequently, would have higher peak deceleration. However, the median values indicate that the tail-mounted engine configuration experiences higher decelerations along both axes. Therefore, there appears to be no kinematic explanation for why the wing-mounted engine configuration experiences higher levels of damage than the tail-mounted configuration. Recalling that the damage metric only quantifies fuselage damage modes, it is not obvious why the damage should be so different between these two sub-groups.

Table 25. Damage dependence on engine placement – Water

	Wing-mounted Engines	Tail or Tail/ Fin-mounted Engines
Median Damage Metric (unitless)	37.5	17.5
Average Damage Metric (unitless)	42.8	17.8
Number of Events	12	4

Table 26. Velocities for engine configuration samples – Water

	Wing-mounted Engines	Tail or Tail/ Fin-mounted Engines
Median Vertical Velocity (ft/s)	-17.1	-15.7
Average Vertical Velocity (ft/s)	-19.8	-16.4
Median Airspeed (ft/s)	210	185
Average Airspeed (ft/s)	197	189

Table 27. Engine configuration kinematic parameters – Water

	Wing-mounted Engines	Tail or Tail/ Fin-mounted Engines
Median Pitch Angle (deg.)	6.0	4.0
Median Flight-Path Angle (deg.)	-5.0	-3.8
Median Peak Vertical Deceleration (G)	2.3	3.5
Median Peak Longitudinal Deceleration (G)	-4.2	-6.1
Number of Events	11	4

3.2.8 Evacuation Routes

The database contains information regarding the availability of exits and their use. This information was supplemented by the narrative of the accidents and the evacuation description provided in the investigation reports. However, the use and functionality of all doors and exits were incompletely reported. For the purposes of this discussion, doors are openings that are full human height and extend to the floor; all other openings intended for escape are referred to as exits. Exits specifically for the cockpit are not discussed. A door or exit is deemed "functional," if it is mechanically operational post-crash. A door or an exit is deemed "usable" if it is both functional AND able to be used for egress. Therefore, a door that was below water level, blocked by debris, or not readily accessible from inside the aircraft is considered not usable. Likewise, a door blocked on the outside by terrain, debris, or flames is unusable. In one case, a raft was inadvertently inflated inside the aircraft and effectively blocked both forward doors. In another case, the floor collapsed below the right forward door, therefore preventing people from using the door while also hindering the flight attendant in facilitating passengers' exit through the left door. It is noted that sometimes a door or exit was inappropriately activated.

The 22 aircraft in the study had 85 doors and 55 exits (see table 28); of these, the condition of approximately two-thirds was reported. Therefore, the overall average for the complete dataset was 1.94 usable doors per aircraft and 2.2 usable exits.

Table 28. Doors and exits all mishaps – Water

(22 Aircraft)	Doors (No.)	Exits (No.)
Installed on mishap aircraft	85	55
Condition reported	57	39
Reported as functional	41	34
Reported as useable	35	33

The numbers provided in table 28 are the number of doors whose functionality and usability are known. The average number for each scenario (see table 29) is the average number of doors for all mishaps in that scenario. The minimum number gives the lowest number of doors available in all mishaps within the scenario. Although none of these mishaps experienced post-crash fire, some aircraft did sink and so the availability of escape would have been critical to survival. The exits were accounted for in the same manner (see table 30). Although there were mishaps in which no doors were usable (minimum= 0.00), and there were mishaps in which no exits were usable (see table 30), there was only one mishap in which no doors AND no exits were rated usable. This mishap was the ATR 72, which ditched near Palermo (20050806A). The aircraft broke up, and all who escaped exited through openings in the structure. The high-wing aircraft floated with the wings in the water and, therefore, the remains of the cabin were submerged. In another specific instance, a service door (door 1B) was usable and in fact used by one person, but a floor panel was dislodged by the impact and consequently, the door was effectively unusable, and most people exited through door 1A.

Table 29. Post-crash door availability – Water

	Doors on Aircraft (Average #/ Minimum #)	Functional Doors (Average #/ Minimum #)	Usable Doors (Average #/ Minimum #)
Scenario A	1.67/1.00	0.67/0.00	0.33/0.00
Scenario B	2.71/1.00	1.75/1.00	0.80/0.00
Scenario C	4.20/1.00	2.00/1.00	2.20/1.00
Scenario A–C	3.00/1.00	1.58/0.00	1.23/0.00
Scenario E	6.00/3.00	4.40/0.00	3.80/0.00

Table 30. Post-crash exit availability—Water

	Exits on Aircraft (Average # / Minimum #)	Functional Exits (Average # / Minimum #)	Usable Exits (Average # / Minimum #)
Scenario A	2.67/2.00	2.50/2.00	2.50/2.00
Scenario B	2.43/0.00	2.00/1.00	1.60/0.00
Scenario C	4.00/1.00	3.00/1.00	2.80/1.00
Scenario A–C	3.00/0.00	2.55/1.00	2.25/0.00
Scenario E	1.33/0.00	2.00/2.00	2.00/2.00

Across the different scenarios, the lowest average number of usable doors was in the ditching with power scenario A (see table 29). This result is something of an artifact because this scenario contains the IAI1124 aircraft, which has only one door (unusable after the ditching), a DC-3 with only two doors (one usable), and a DC-9 with two doors (neither usable). Generally, the lack of usable doors was offset by usable exits. scenario E (overruns) includes one 747 and two DC-10s (all doors and no exits)—therefore, the large number of usable doors and relatively low number of usable exits. In some cases, exits were the preferred escape route because they led onto the wings rather than into the water. In many cases, these evacuations were orderly because the impact had been modest. Further, many of the evacuations in these cases were accomplished through one or two doors; consequently, the functionality of the other doors was not discussed in the report.

One mishap in which the usability of doors and exits may have been a factor in survivability was St. Croix DC-9 (19700502A). The aircraft was successfully ditched (fuel starvation) without fuselage breakup; however, it sank within 10 minutes with 23 of 65 occupants lost. Little is known about the damage to the aircraft beyond the statement in the report that it did not break up. The aircraft was not recovered, so damage was not determined by investigators, and there was no map or record of where survivors or fatalities were seated or where they were when the aircraft sank. Of the 23 lost, only one was a crew member. Two crew and 35 passengers were listed as having non-fatal injuries. The cabin was not well prepared for the ditching; crew who were helping passengers and some passengers were unbelted at impact. The forward-loading door was jammed. An emergency raft was inadvertently deployed inside the aircraft, rendering both forward doors blocked for access from the cabin, although the doors were functional. One person escaped prior to the raft inflating. Most survivors escaped through overwing exits. Consequently, injuries could have contributed to the inability to egress, but these determinations cannot be made without autopsies. It was not specifically reported, but it can be inferred that the lost crewmember was one of the three cabin attendants.

3.2.9 Survivable Crashes

The rationale for identifying the crashes as survivable, partially survivable, or non-survivable was discussed previously in section 2 of this report. The method for determining survivability is the same for both the water mishaps and the RJ mishaps. The runway overrun crashes are excluded from this analysis because there is generally just the longitudinal velocity, and the nature of the impacts are different from the impacts in which the aircraft has been airborne.

After identifying the list of survivable crashes, the cumulative percentile for the airspeed and the vertical velocity of each mishap is determined independently of the other velocity. The mishap with highest vertical velocity was rated as partially survivable and had a vertical velocity of 47 ft/s (see figure 14). It is apparent from the plot that this one mishap lays significantly above the next closest mishap. Using this velocity as a design guide, the amount of energy that structure would need to absorb is substantially greater than that of the next higher mishap. For reference purposes, the 90th percentile level is -28.3 ft/s (see figure 14). The result of the same process for the airspeed (see figure 15) reveals a more uniform increase. The 90th percentile value for airspeed is 255 ft/s (see figure 15). The 90th percentile is selected for the reference line merely out of convention. There is no formal requirement that 90th percentile be used as any sort of reference or design guidance.

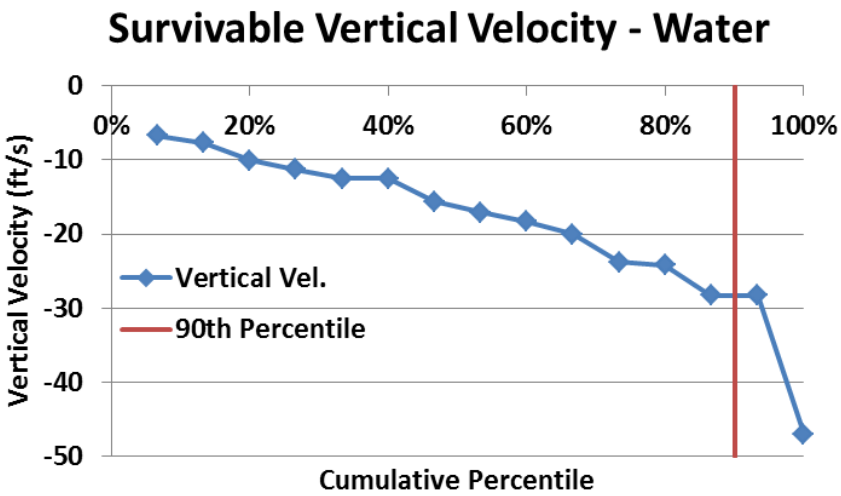

Figure 14. Survivable vertical velocity (A–D)—Water

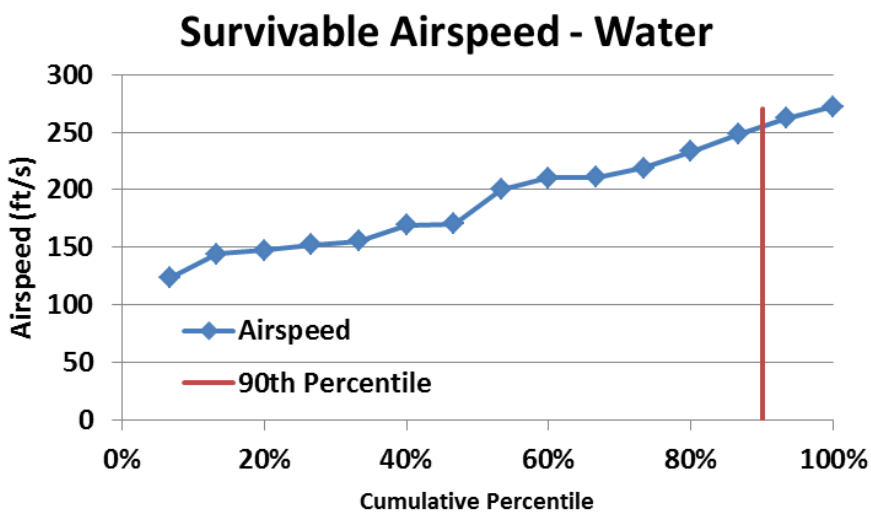

Figure 15. Survivable airspeed (A–D)—Water

The 90th percentile values for the two axes can be combined using the equation for an ellipse to create an estimate for the resultant 90th percentile velocity (see figure 16). In the figure, more points than might be expected appear outside the ellipse. However, the 90th percentile was determined only along each axis; a careful look at the position of these points relative to the *x*- and *y*-axis intercepts revealed that there are just two points beyond the *x*-axis intercept and two beyond the *y*-axis intercept, as seen in the two single-axis plots (see figures 14–15). The one non-survivable crash excluded from the survivable velocity determination has been added to the plot for the reader's information.

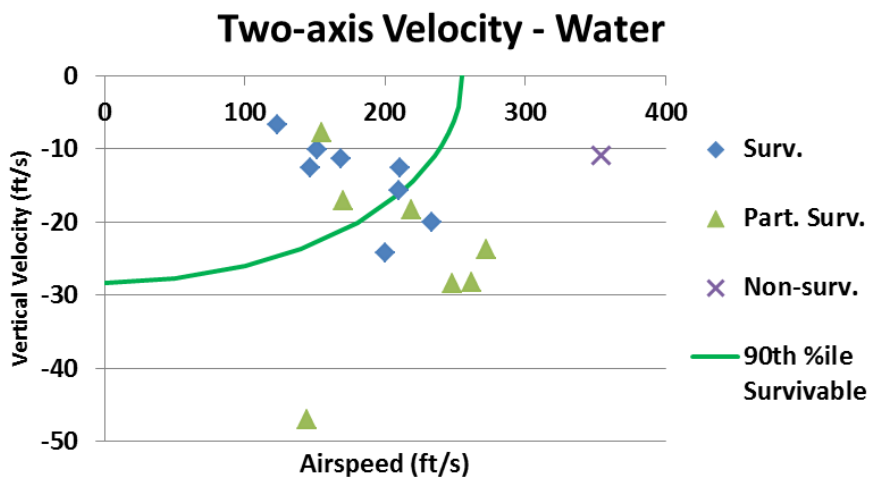

Figure 16. Two-axis velocity (A–D)—Water

3.2.10 Injury Analysis

In analyzing the injuries resulting from the mishaps in this study, the distribution of injuries among the different types of mishaps (i.e., water landing versus overrun) will be viewed. The injuries will be correlated with the kinematics and aircraft characteristics. The injuries for the entire aircraft will be viewed first, and then the injury frequency will be determined by aircraft segment.

In many of the reports, minor injuries are treated in one category with non-injuries. In other reports, two separate counts are provided for minor and no injury. In as much as the numbers from the combined reports cannot be separated again, minor injuries and non-injuries are reported together for all mishaps. In the entire water impact study, there were 1829 occupants, of whom 310 were fatally injured, including drowning, and 135 received serious injuries. Therefore, 1384 received minor or no injuries.

In most of this analysis, serious injuries are treated together with fatalities. Serious injuries potentially can hinder egress, and that hindrance can lead to failure to escape. In the case of the water mishaps, there were no post-crash fires, but there were aircraft that sank. Just as post-crash fire makes the timing of escape critical, so does the potential for sinking. As the data were extracted from the database and placed in the Excel workbooks, accommodation in the spreadsheets was made to record the number of people at risk for drowning because of serious injuries. However, this part of the analysis was not developed. In only a few cases, autopsies were performed to determine whether the fatalities were the result of trauma or drowning.

Beginning at the top level, the injuries (e.g., fatalities, serious injuries, and minor-no injury) are reviewed for the ditching scenarios (scenarios A–C) and for the overruns (scenario E). The sum of the average percent values within a column (see table 31) should add up to approximately 100%, but the sum of the median values need not. In this initial comparison, the overrun mishaps produced far smaller fractions of fatal and serious injuries than did the mishaps involving the aircraft landing on the water from the air. The fatalities included people who were drowned with or without severe trauma. Few of the overruns ended in water sufficiently deep to submerge the fuselage. The median/average number of occupants (crew plus passengers) is provided to give some idea of the number of people involved. Scenario E has far larger occupant numbers because the overrun scenario contains several large, high-capacity aircraft.

Table 31. Injury frequency—Air vs. overrun—Water impact

	Scenarios A–C Impact From Air (Median % / Average %)	Scenario E Overrun Impacts (Median % / Average %)
Fatal Injury (percent of all occupants)	33/29	0/6
Serious Injury (percent of all occupants)	18/16	2/3
Minor/No injury (percent of all occupants)	57/55	98/91
Total Occupants (#)	41/48	152/156

3.2.10.1 Injury fraction dependence on velocity—water

The two-axis velocity plot can also be used to visualize the dependence of injuries on impact speeds (see figure 17). The plot displays all the mishaps in scenarios A–C. All these mishaps had at least one serious injury. The fractions of serious plus fatal injuries ([number of fatal + number of serious]/ number of occupants) for these mishaps fell in three clusters, as indicated in the figure legend. Although two of the three events with the lowest severe injury (severe injury = fatal or serious) fraction fall within the 90th percentile curve, one does not. For the second cluster, with up to half of the occupants severely injured, more mishaps fall beyond the 90th percentile curve than within it. Only two of the five highest injury fraction mishaps fall on or outside the velocity curve. Therefore, there is no clear correlation between the two velocities and the fraction of serious plus fatal injuries.

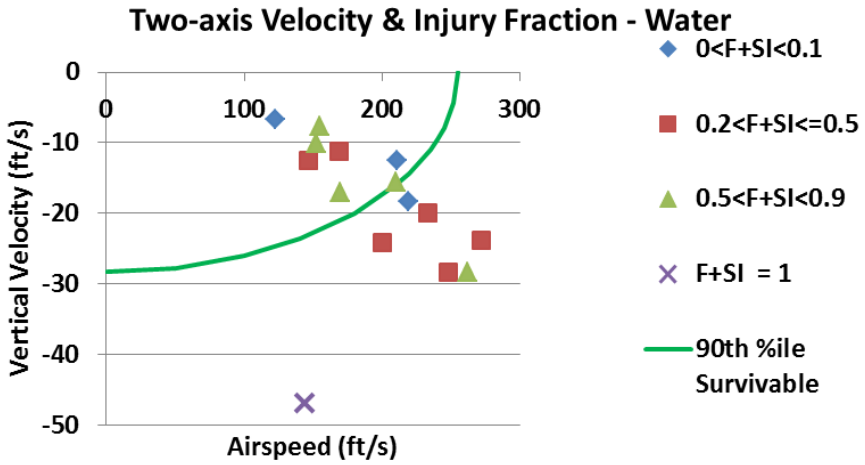

Figure 17. Serious + fatal injury fraction (A–C) on two-axis velocity plot

3.2.10.2 Injuries in each scenario and segment—water

Ditching without power resulted in a higher rate of fatalities than ditching with power (see table 32). Landing short had a higher severe injury rate than ditching with power, but less than ditching without power. The single climb-out event resulted in total destruction of the aircraft, and the severe injuries were correspondingly high. As seen previously (see table 31), the rate of serious and fatal injuries was low for the runway overruns.

Table 32. Severe injuries by scenario and aircraft segment—Water

	Cockpit (% Fatal + Serious Injury)	Forward Cabin (% Fatal + Serious Injury)	Overwing Cabin (% Fatal + Serious Injury)	Rear Cabin (% Fatal + Serious Injury)	Tail (% Fatal + Serious Injury)
Scenario A	10%	0%	5%	No occupants	100%
Scenario B	60%	40%	20%	14%	88%
Scenario C	14%	0%	50%	41%	71%
Scenario D	100%	100%	100%	98%	100%
Scenario E	27%	Insufficient data	Insufficient data	Insufficient data	0%
Scenarios A–C	34%	28%	26%	21%	81%

Looking at the injuries by segment requires knowledge of not only the distribution of injuries but also knowledge of the locations of all the passengers. To take into account the varying sizes of aircraft in the study, the study looks at the fraction of occupants injured in each segment rather than the numbers of occupants. Ideally for this study, each report contains an injury map that shows the location of all the passengers and the severity of their injuries. With mishaps in which there are few severe injuries (i.e., fatalities or serious injuries), these maps are seldom provided. In cases for which no seat map was provided, but the load factor (number of occupants/number of seats) was high (arbitrarily >75%), the empty seats were assumed to be uniformly distributed, and so correspondingly, the occupants could be assumed to be uniformly distributed. When a fractional

occupant arose in these calculations, a whole occupant was assigned forward of the two segments (based on personal observation that a majority of people tend to sit forward). The sample size for each mishap scenario is already small; therefore, missing injury data by segment would limit the conclusions that could be drawn. In the case of the overrun scenario, there are fatality data for just one mishap and no injury data by segment except for the cockpit. The cockpit data are inferred from details usually provided relating to the pilots and cabin crew (whose locations are also often provided).

The fraction of fatalities did show a pattern among scenarios (see figure 18). The fractions on the right side of the legend indicated the number of mishaps within the group that had data. There were no fatalities in the ditchings with power (A). However, for the ditchings without power (B), the fraction of fatalities was rather evenly distributed through the various segments and was in the range of 20%–30% in each segment. The landing-short scenario (C) revealed a pattern of greater fatalities toward the rear of the aircraft. The crash during climb-out (D) was a single catastrophic case in which only a few people survived. In the overrun scenario (E), the few fatalities that did occur were in the forward cabin segment. Grouping the impacts that occurred from the air together (A–C) revealed a different pattern from the individual scenarios, wherein the median percent of fatalities was higher in the rear segments.

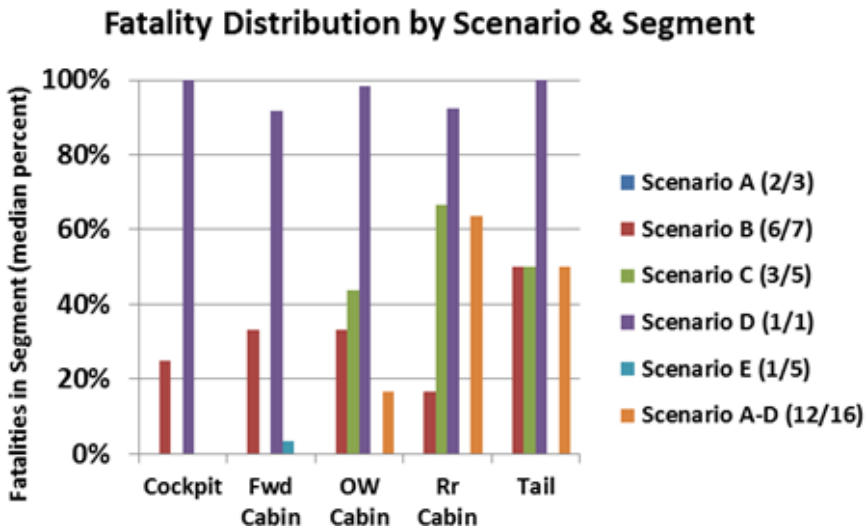

Figure 18. Fatality distribution by segment—Water

The pattern of the serious injuries is less clear than the pattern of the fatalities (see figure 19), partially because there were fewer serious injuries to analyze, and there was less information on the locations of the serious injuries. The overrun mishaps could only be analyzed for the cockpit because the distributions of passengers in the other segments and the distribution of the serious injuries were not available. Likewise, in many of the other mishaps, data are missing for the forward, overwing, and rear cabins.

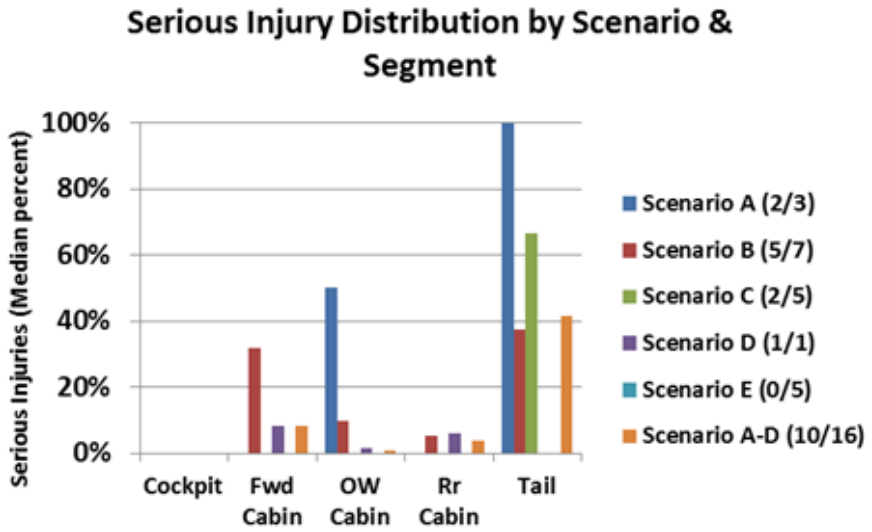

Note: Scenario E mishaps were not well-documented for the location of passengers or the injured occupants; consequently, the only segment with useful data was the cockpit, which did have serious injuries in just two mishaps.

Figure 19. Serious injury distribution by segment—Water

3.2.10.3 Injuries related to kinematics – water

The severe-injury fractions (fatal injuries + serious injuries/number of occupants) has been plotted against four of the major kinematic parameters (i.e., airspeed, vertical velocity, flight-path angle, and pitch angle). The plotted points are coded through the legend to identify the scenario; therefore, the overall trends, and trends within each scenario, are visible.

In the plot of severe-injury fraction against the airspeed (see figure 20), the overall trend is higher injury fractions as the airspeed increases. The runway overruns generally occurred at low speeds and consequently had low-injury fractions. The highest airspeed event (scenario D) has a nearly 100% severe-injury fraction. Scenario C, landing short, shows a consistent upward trend, whereas the ditchings without power (B) reveal almost a countertrend, suggesting that there is another more important factor influencing the outcome of these mishaps. The limited number of ditchings with power suggest a steep dependence on airspeed.

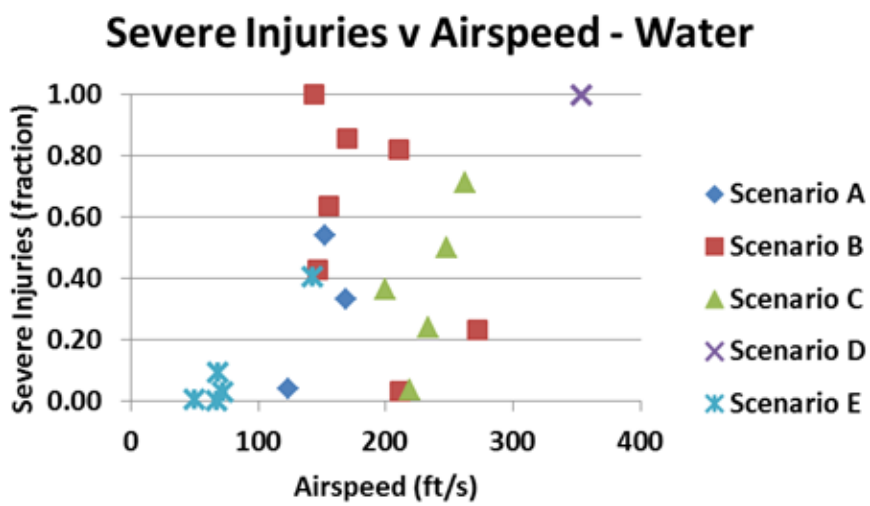

Figure 20. Severe injuries vs. airspeed—Water

For the parameter vertical velocity (see figure 21), the ditching without power (scenario B) does not show a clear trend, whereas the severe-injury fraction might be expected to increase as the vertical velocity increases. The scenario B mishap with the greatest vertical velocity did result in 100% severe injuries. With the exception of two low-injury-fraction events, the fraction of severe injuries in this scenario is generally high compared with that of the ditching with power mishaps (A). The landing-short mishaps (scenario C) exhibit the strongest correlation between the severe-injury fraction and the vertical velocity. The vertical velocity recorded for the runway overrun mishaps (scenario E) is limited to the nose of the aircraft (i.e., it only occurs in cases in which the nose goes downslope or drops off a seawall). Therefore, any injuries due to these velocities will be confined to the two forward segments of the aircraft.

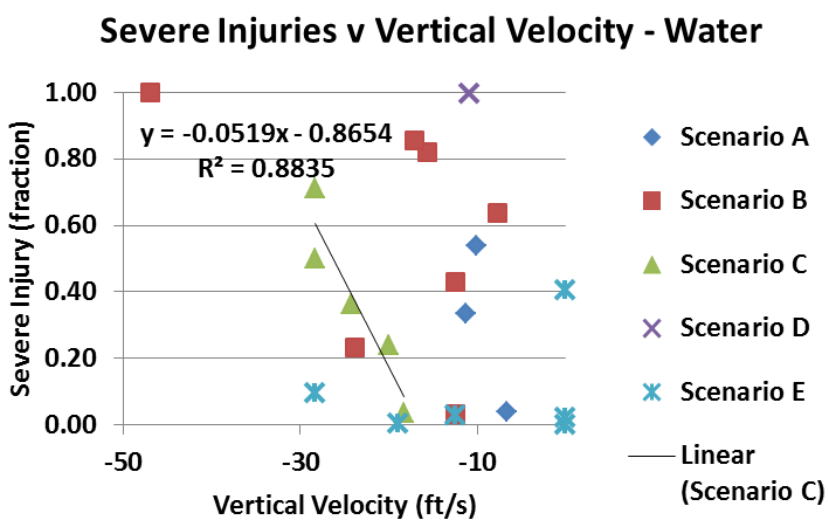

Figure 21. Severe injuries vs. vertical velocity—Water

The three scenarios of impact from the air, scenarios A–C, reveal a very steep dependence of injury fraction on flight-path angle (see figure 22). For the runway overrun, the negative flight-path

angles represent the nose dropping off a seawall. Therefore, the angles can be quite high without leading to serious injuries because the longitudinal velocity is low.

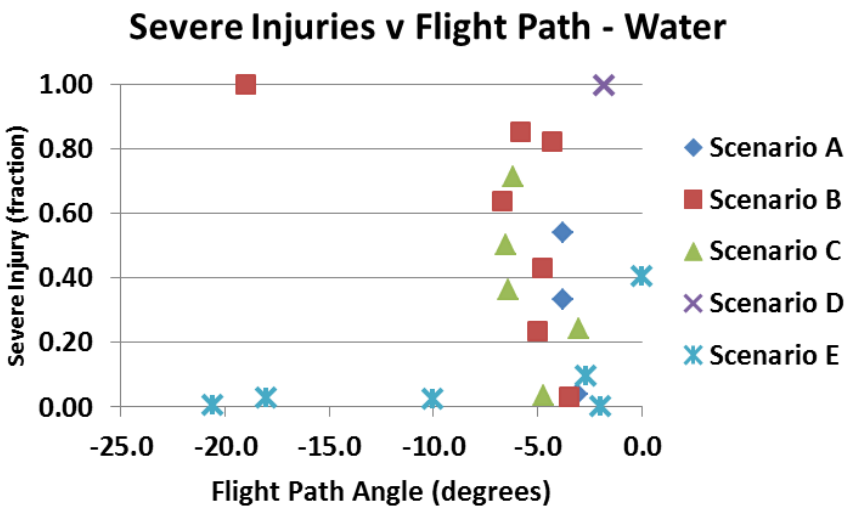

Figure 22. Severe injuries vs. flight path—Water

The trends in severe-injury fraction relative to the pitch angle (see figure 23) are less clear. Note that zero pitch angle (i.e., nose level) is in the middle of the *x*-axis. It could be argued intuitively that the injury fraction may increase on either side of zero. That is the least damaging and, therefore, the least injurious way for an aircraft to enter the water level. As the nose pitches increasingly downward, it would tend to plunge into the water and increase the deceleration rate of the aircraft. Conversely, as the nose is pitched higher, the tail will strike first, slowing the tail, while the nose continues at the same velocity, causing the aircraft to rotate about the contact point in the water and "slam" down onto the water's surface. The result could be a high vertical velocity for the forward end of the aircraft. Clearly, the optimum pitch may not be precisely zero, but there are insufficient data available in this study to determine the optimum angle. Depending on the relationship between vertical velocity and airspeed, several different responses of the aircraft following initial contact can be envisioned. All data for the ditching without power mishaps (B) are with the nose up; the data suggest that a higher nose angle may, in fact, reduce total severe injuries. An attempt was made to look at the injury fractions by segment for the scenario B mishaps to see a pattern in the segment injuries that would provide additional information, but there was inadequate detail in the segment injury breakdown for the individual mishaps.

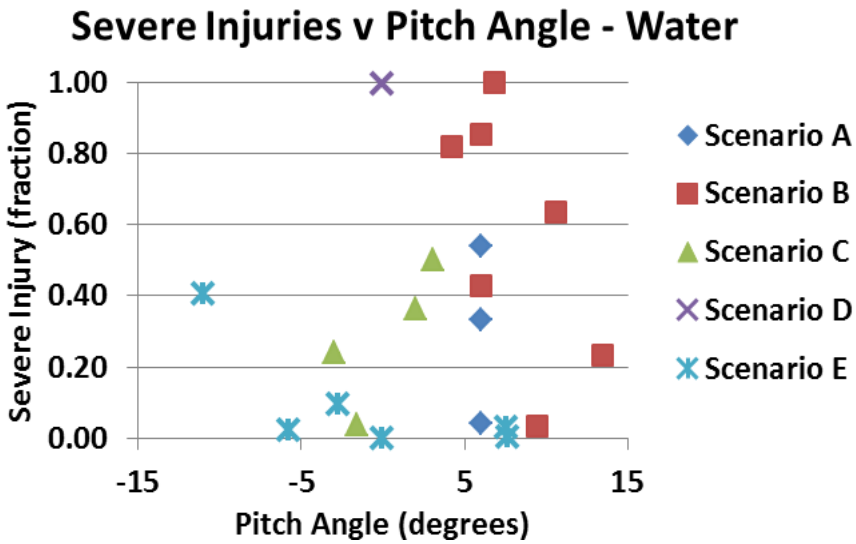

Figure 23. Severe injuries vs. pitch angle—Water

3.2.10.4 Correlation of injury to damage—water

The injury levels would be expected to correlate with the damage levels wherein the injury levels would be higher when there is greater damage. Specifically, higher fractions of fatal and serious injuries would be expected to occur with higher damage metric values (see figure 24). For the landing-from-air scenarios (A–C), the injury fractions show a consistent upward trend with increasing damage metric values. In scenario A, the point with a high injury fraction but a low damage metric is the St. Croix mishap in which the aircraft sank quickly, and damage information is missing from 15 of 24 cells (resulting in a low value). A trend line is shown for the landing short (scenario C) data, revealing a high correlation factor (R^2 = 0.93). It is evident that the ditching-without-thrust (scenario B) data will have a similar slope, but a higher intercept value, although the correlation factor will be less than that for scenario C. The overrun mishaps (scenario E) are characterized by damage concentrated in the nose and the forward part of the forward cabin, and by overall low damage metrics.

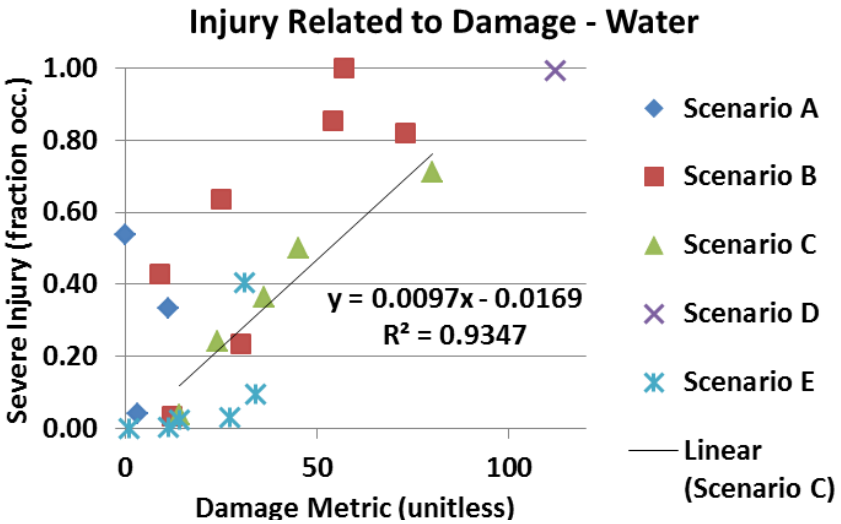

Figure 24. Injury fraction related to damage metric—Water

The data for damage and injuries were recorded by aircraft segment. The correlations of serious injuries and fatalities in the different segments for each scenario to the damage can be inferred by comparing the figures (injury: see figures 18 and 19; with damage: see figure 25). The pattern of fatalities was confirmed by the pattern of damage metric values for the crashes into water without power (scenario B) and the catastrophic accident (D), and, to a lesser extent, for the landing short scenario (C). The overrun scenario experienced fatalities only in the forward cabin; this is consistent with the damage being concentrated in the cockpit and forward cabin. Grouping the landing from air scenarios (A–C) develops a pattern of fatalities concentrated at the rear, but the damage is more uniformly distributed. This latter phenomenon may be due to the difficulty people in the rear cabin and tail have in escaping when there is a fuselage break forward of their position with consequent in-rushing water.

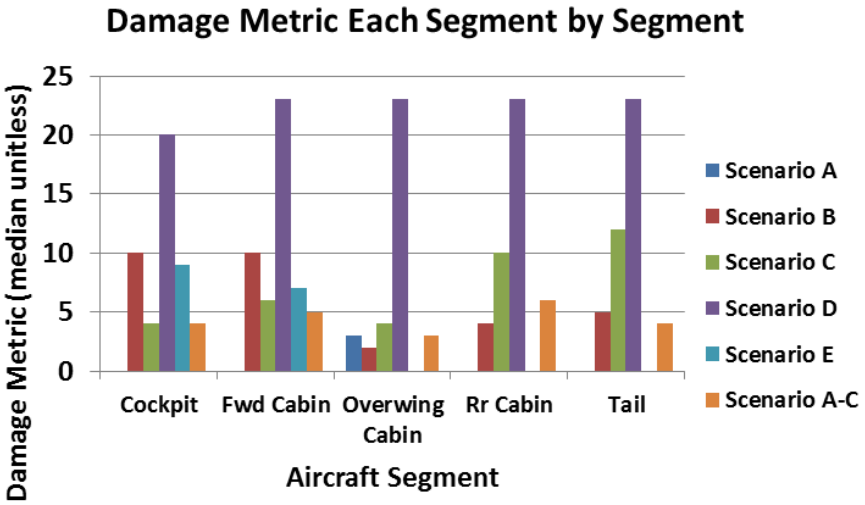

Figure 25. Damage metric segment breakout—Water

3.2.10.5 Injury related to aircraft design characteristics—water

The first characteristic investigated is the difference between high-wing and low-wing configurations in injury outcomes. The values that were compared (see table 33) were the median and average percent of fatalities and serious injuries for the entire aircraft in each mishap. The results are presented for scenarios A–C; the number of aircraft of each type is listed in the last row of the table. The high-wing aircraft demonstrated a significantly higher frequency of fatalities than the low-wing aircraft. However, this trend was not confirmed by comparing the serious injuries. The median values generally are consistent with the average values. All but one of the high-wing aircraft mishaps was a ditching without power. All three of the ditchings with power were low-wing aircraft, as were only two of the ditchings without power. The climb-out scenario was one catastrophic case involving a low-wing aircraft. All the overrun mishaps (E) were low-wing aircraft. The high-wing mishaps demonstrated greater median damage metric values than the low-wing aircraft, and this trend is reflected in the injury data.

Table 33. Injury dependence on wing configuration—Water impact

Scenarios A–C	High-Wing Fatalities	Low-Wing Fatalities	High-Wing Serious Injuries	Low-Wing Serious Injuries
Median % occupants injured	48	2	9	18
Average % occupants injured	55	12	15	12
# of aircraft configuration in scenario (#A / #B / #C)	0/5/1	3/2/4	0/5/1	3/2/4

As previously discussed, the damage metric for wing-mounted engines was higher than for the tail-mounted engine configuration (see table 25). The same trend is confirmed by fatalities correlated to the same aircraft characteristic (see table 34). The median and average fraction of fatalities is higher for the engines-on-wings configuration than for the engines-on-tail configuration. The rates for serious injuries do not confirm this trend. The difference in serious-injury rates between the two configurations shows no clear trend. Seven of the eleven engine-on-wing aircraft were in the ditching-without-power scenario, whereas none of the engine on tail mishaps fell in this scenario.

Table 34. Injury dependence on engine configuration—Water impact

Scenarios A–C	Engine on Wing Fatalities	Engine on Tail Fatalities	Engine on Wing Serious Injuries	Engine on Tail Serious Injuries
Median % occupants injured	41	18	4	19
Average % occupants injured	33	18	15	19
# of aircraft for each configuration in scenario (#A / #B / #C)	1/7/3	2/0/2	1/7/3	2/0/2

Based on the damage metric trend and the fatalities trend, the ditching without power scenario (B) appears to have more severe-injury consequences than the ditching with power scenario (A). However, as can be seen in looking at the engine configuration and wing configuration interactions, the aircraft design characteristics would appear to also affect the outcomes.

3.2.10.6 Binary logistic analysis of injuries—water

Binary logistic analysis treats the dependent variable as having two states with the probability of the variable being in one state or the other depending on one or more independent variables. For the purpose of this study, occupant injuries are assigned to one of two levels: fatal and serious injuries are considered to be in the severe state (1), and no injury or minor injury are considered to be in the mild state (0). Part of the rationale for assigning serious injury into the same category as fatality is that for water impact, a serious injury may compromise the occupant's ability to egress to the point of determining whether the occupant survives or drowns. The outcome of a successful model is a generally S-shaped curve showing a monotonically increasing probability of fatality/serious injury as the parameter increases in value. Normally, the probability would begin near 0 for a low value of the parameter and increase to 1 (probability = 1 or 100%) as the parameter increases. The details of the analysis are described in the methodology section of this report.

3.2.10.7 Binary logistic analysis of injuries using kinematic data—water

The analysis method is first applied to the grouped dataset for scenarios A–C or those mishaps in which the aircraft entered the water from the air either as a ditching or an attempted landing. The parameters tested as single parameters include:

- Airspeed
- Vertical velocity
- Flight-path angle
- Pitch angle
- Vertical peak deceleration
- Longitudinal peak deceleration

The BLM contains all of the injury data from 15 mishaps. In these 15 mishaps, 224 occupants (crew and passengers) received fatal or serious injuries, whereas 493 received no injury or only minor injuries (total 717). In certain models, selected mishaps were eliminated because of lack of data, but the number of mishaps and occupants is stated.

3.2.10.8 Scenarios A–C, single-parameter models

3.2.10.8.1 Airspeed

The model based on airspeed will be used to describe the output of the statistical software. The probability of an occupant sustaining serious or fatal injuries is predicted based on the independent parameter airspeed. Although the curve is S-shaped, the regression is essentially fitting to a straight-line dependence on airspeed (argument of the exponential is in straight-line form *mx+b*). Consequently, there are two values related to the model equation 3: the constant and the regressor coefficient (see table 35).

$$p = \frac{1}{1 + e^{-(\beta_0 + \beta_1 x)}} \tag{3}$$

Table 35. Scenarios A–C, single-parameter BLMs—Water

Parameter (Mishaps/ Occupants)	Constant Coefficient (*p*-value & coefficient value)	Regressor Coefficient (*p*-value & coefficient value))	Goodness-of-Fit (*p*-value)	Summary Measures of Assoc.	Trend: Intuitive or Counter-Intuitive	Predictive Capability
Airspeed (15/717)	p=0.163 0.634	p=0.002 -0.007	0.000 0.000 0.000	0.24 0.25 0.10	Counter-Intuitive	Not strong
Vertical velocity (15/717)	$p \leq 0.000$ -1.598	p=0.001 -0.046	0.000 0.000 0.000	0.10 0.11 0.04	Intuitive	Not strong
Flight path (15/717)	$p \leq 0.000$ non-zero	$p \leq 0.000$ non-zero	0.000 0.000 0.000	0.38 0.40 0.16	Intuitive	Moderately strong
Pitch (14/672)	$p \leq 0.000$ -0.971	p=0.523 0.011	0.000 0.000 0.000	-0.01 -0.01 -0.00	No trend	Not strong
Vertical peak deceleration (13/635)	$p \leq 0.000$ -1.294	$p \leq 0.000$ 0.097	0.000 0.000 0.000	0.44 0.46 0.19	Intuitive	Moderately strong
Longitudinal peak deceleration (13/635)	$p \leq 0.000$ -1.735	$p \leq 0.000$ -0.187	0.000 0.000 0.000	0.43 0.46 0.18	Intuitive	Moderately strong

In the airspeed model, the *p*-value for the constant coefficient is greater than 0.100 (i.e., the desired level of significance [α]), which means that the constant is likely 0. The goodness-of-fit metrics refers to three statistical metrics (Pearson, Deviance, and Hosmer-Lemeshow); in this case, all three measures are 0, indicating that the model does not fit the data well (see figure 26). The summary measures of association are three statistical metrics, which indicate the model's ability to accurately predict values with new data; these metrics are Somers' D, Goodman-Kruskal Gamma, and Kendall's Tau-a. For the airspeed model, the values for these three metrics are all low, and consequently, the model does not have strong predictive capability. The column labeled "Trend" is a subjective evaluation by the author of whether the model predicts the expected injury-fraction trend for that parameter. In this case, the term "intuitive" indicates that as the parameter becomes increasingly severe, the likelihood of severe injuries also increases. A counterintuitive model, such as Airspeed, predicts that the severe injury probability decreases with increasing airspeed at impact—not the trend most people would expect. The Predictive Capability column is the analyst's interpretation of the Summary Measures of Association Metrics for how well the model will work at accurately predicting the outcomes of other substantially similar mishaps.

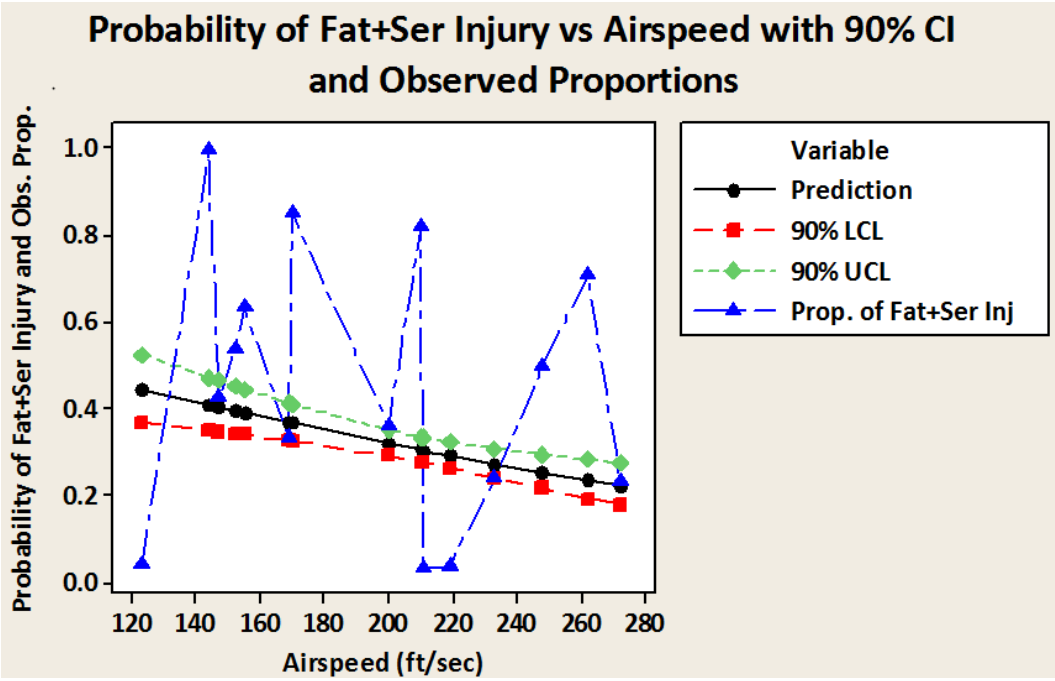

Prop. = Proportions

Figure 26. BLM for airspeed (A–C)—Water

Looking at the other models (see table 35), three models have moderately strong predictive capability (i.e., flight path, vertical peak deceleration, and longitudinal peak deceleration).

3.2.10.8.2 Flight path

The flight-path-angle model included data from all 15 mishaps. The coefficients for both the constant and the regressor are non-zero, and the trend is in the expected direction (see figure 27). The goodness-of-fit metrics are very low, as has been the case throughout this analysis. The predictive capability metrics are moderately strong and nearly equal to the same metrics for the two deceleration parameters described on the next page.

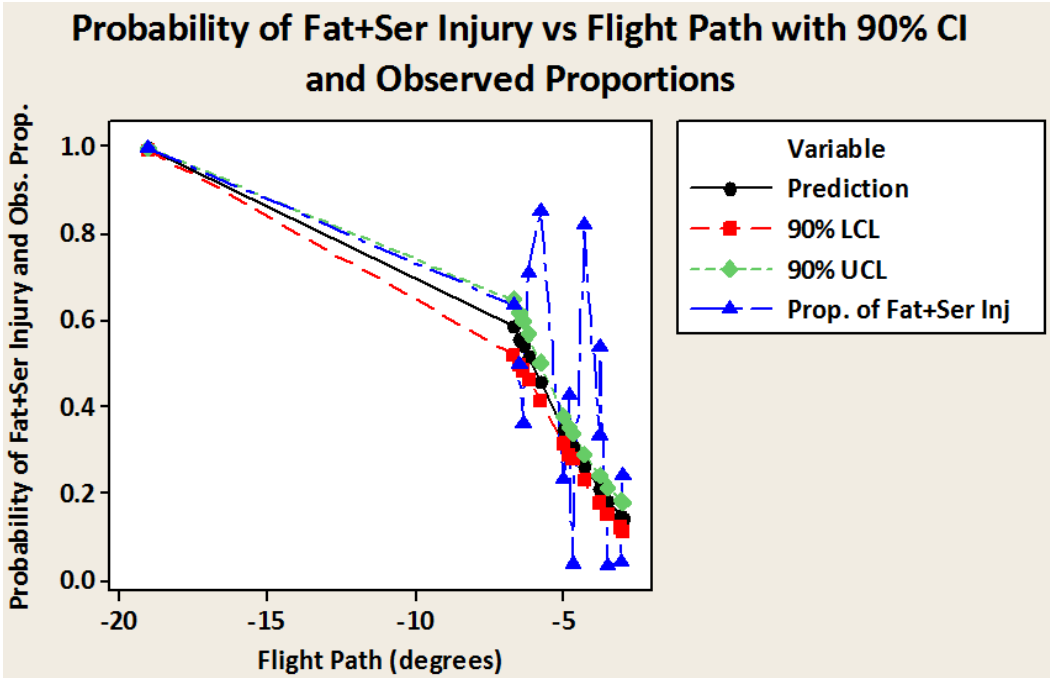

Figure 27. BLM for flight path (A–C)—Water

3.2.10.8.3 Peak vertical deceleration

Arguably more directly related to injury causation than the velocity or angles of the aircraft, the peak deceleration might be expected to exhibit a better correlation. Two mishaps were missing values for the peak vertical deceleration; consequently, the analysis is based on 192 occupants with serious or fatal injuries, and 442 occupants with minor or no injuries in 13 mishaps (see table 35). The *p*-values for both the constant coefficient and the regressor coefficient are equal to 0.000, which means that both coefficients are likely non-zero. Although a model was created, the *p*-values for all of the goodness-of-fit statistics are 0.000, less than the 0.100 needed to indicate a meaningful fit, as confirmed by the plot of the model and the data (see figure 28). The injury data are widely scattered on either side of the model curve. The summary measures of association are medium strength, which indicates the model will have moderate predictive capability. The trend of the model is as anticipated.

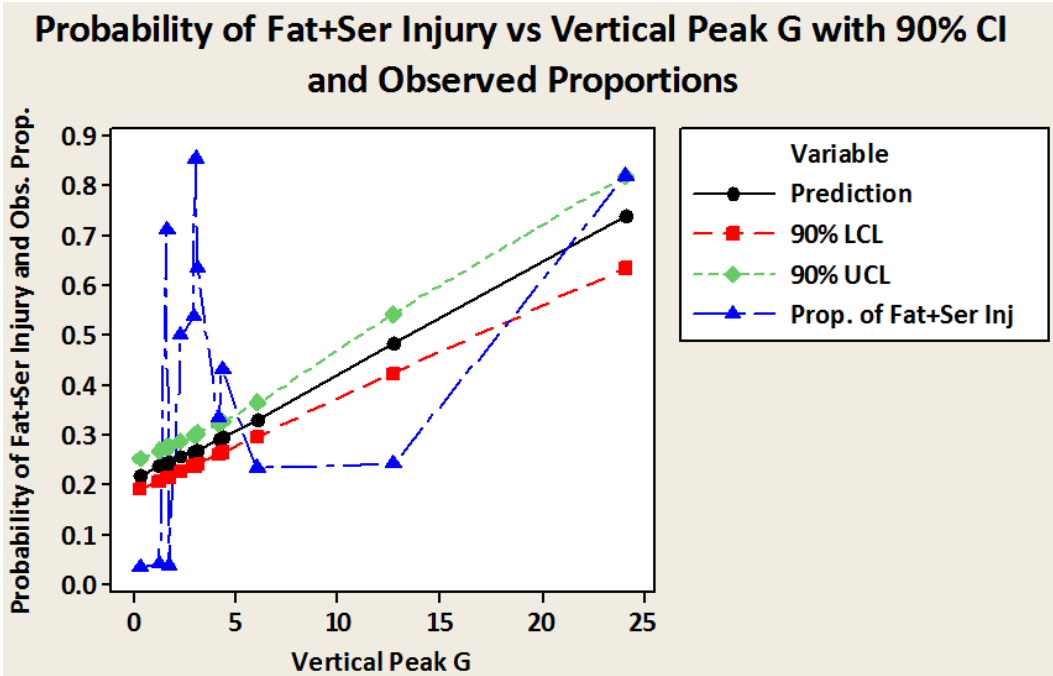

Figure 28. BLM for peak vertical deceleration (A–C)—Water

3.2.10.8.4 Peak longitudinal acceleration

Values of the peak longitudinal acceleration are missing for the same two mishaps with the missing peak vertical acceleration data. Consequently, the same mishaps and number of occupants are used in this analysis (see table 35). The *p*-values for the constant coefficient and for the regressor coefficient are less than or equal to 0.000; therefore, each coefficient is expected to be non-zero. Although a model can be created, once again the fit-to-the-data is poor, as evidenced in the plot (see figure 29), and by the fact that all three goodness-of-fit *p*-values are less than or equal to 0.000. However, the summary measures of association are of medium to high strength, and these values indicate a moderate predictive ability for the model.

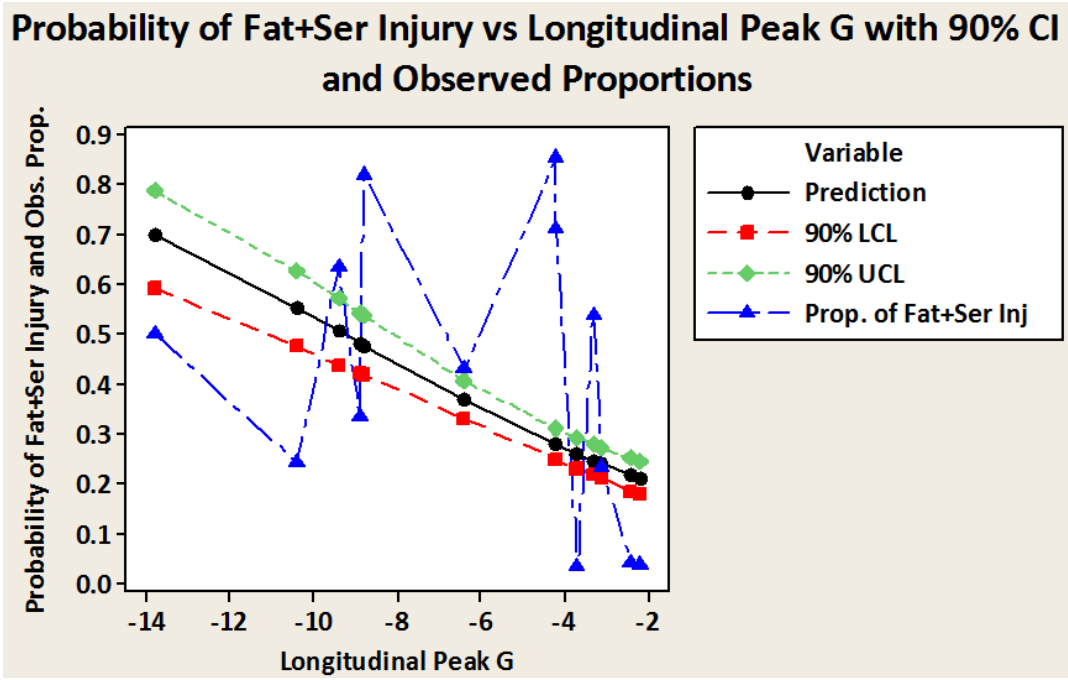

Figure 29. BLM for peak longitudinal acceleration—Water

3.2.10.8.5 Multi-parameter kinematic model for scenarios A–C

The multi-parameter model (see equation 4) attempts to incorporate all six parameters into a single model to predict the probability of occupants incurring severe injury for a given set of values. The six parameters are vertical velocity, airspeed, flight-path angle, pitch angle, peak vertical deceleration, and peak longitudinal deceleration. Three mishaps are missing one or more of the necessary values. Consequently, the model is based on 12 mishaps in which 161 occupants incurred serious or fatal injuries and 429 occupants incurred minor or no injury. Looking first at the *p*-values for the constant coefficient and the six regressor coefficients, the coefficient for the peak longitudinal deceleration has a *p*-value greater than 0.100, and, therefore, can be presumed to be zero. Consequently, the longitudinal deceleration data were dropped from the input and the model rerun using only the remaining five parameters. The *p*-values for constant coefficient and five regressor coefficients were all less than 0.100 (see table 36) and so are inferred to be non-zero. The model (see equation 4) is in five dimensions (see table 37) and consequently cannot readily be plotted.

$$\hat{p} = \frac{1}{1+e^{-(1.97980-0.0560635x_1-0.307668x_2-0.427534x_3+0.114833x_4+0.193623x_5)}} \qquad (4)$$

Where $\hat{p}$ is the estimated probability for the event (i.e., fatal/serious injury) given a specific airspeed (x_1), vertical velocity (x_2), flight path (x_3), pitch angle (x_4), and vertical peak G (x_5). The three goodness-of-fit indicators disagree; two indicate a poor fit to the data, whereas one suggests a good fit (see table 36). The three summary measures of association are all medium-to-large values, indicating good predictive capability. These metrics apply to the entire model rather than to each parameter, as in the single-parameter models. To visualize the predictive capability of the

model, the values of the parameters for each mishap have been used in the model to predict the severe-injury probability for that mishap. The calculated value (*y*-axis) has been combined with the actual value in the mishap (*x*-axis) to form an *x*-*y* pair and the result plotted (see figure 30). If the model accurately predicted the values for the serious plus fatal injury probability, then the *x* and *y* values would be equal, and all the points would lie on the line connecting (0,0) and (1,1). It is readily apparent that the model is not useful for predicting the outcome of future events. It can be inferred that the problem with the single-parameter models is not strong interaction between the parameters; otherwise, the multi-parameter model would be better than the single-parameter ones.

Table 36. Multi-parameter BLM metrics for scenarios (A–C)—Water

Parameter (# mishaps/# occupants)	Constant Coeff. (*p*-value)	Regressor Coeff. (*p*-value)	Goodness-of-Fit (*p*-value)	Summary Meas. of Assoc.	Predictive Capability
Airspeed (12/590)	$p = 0.025$ non-zero	$p = 0.000$ non-zero	0.000 0.000 0.355	0.74 0.79 0.30	Good
Vertical velocity		$p \leq 0.000$ non-zero	NA	NA	NA
Flight path		$p = 0.001$ non-zero	NA.	NA	NA
Pitch angle		$p \leq 0.000$	NA	NA	NA
Vertical peak deceleration		$p \leq 0.000$	NA	NA	NA

Table 37. Scenario A–C, BLM coefficients—Water

Parameter	Coefficient	Valid Input Range	Units
Constant	1.98	All	
Airspeed	-0.0561	123 to 272	Ft/s
Vertical velocity	-0.308	-6.70 to-28.3	Ft/s
Flight-path angle	-0.428	-3.0 to -6.7	Degrees
Pitch angle	+0.115	-3.0 to +13.5	Degrees
Vertical peak deceleration	+0.194	+0.30 to +24.1	G

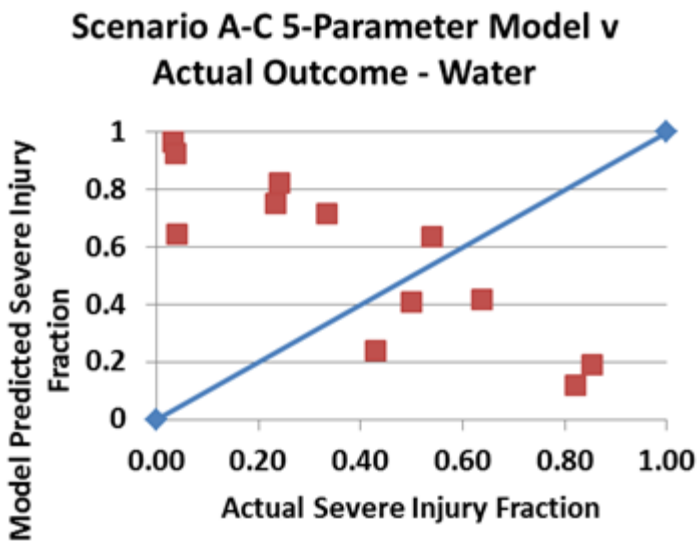

Figure 30. 5-parameter model prediction vs. severe injury data—Water

In summary, the approach of using a binary logistic regression to model the fraction of severe injuries using kinematic parameters as input has not been productive for the group of mishaps encompassing landing on the water from the air.

3.2.10.9 Binary logistic regression applied to single scenarios

The largest dataset was initially believed to have the best chance of delivering usable models; however, when that expectation was not fulfilled, datasets of three separated scenarios were analyzed. Three scenarios—ditching without thrust (B), landing short in the water (C), and runway overrun into the water (E)—have sufficient mishaps to perform regressions with a reasonable expectation of useful results. Although there are fewer samples in each of these regressions than in the analysis of scenarios (A–C), because the mishaps within each are of the same type, the data may have less scatter, leading to better fits and better prediction capabilities.

3.2.10.10 Scenario B—ditching without power

This scenario contains seven mishaps and covers a wide gamut of parameter values. Single-parameter regression was run on six of the kinematic parameters for scenario B (see table 38). These regression models also showed poor goodness-of-fit metrics, but most of them had medium strong or moderate predictive capability than did the scenario A–C dataset. Only one parameter (i.e., vertical velocity) was identified as “not strong.”

Table 38. Single-parameter BLMs for scenario B—Water

Parameter (Mishaps/ Occupants)	Constant Coefficient (*p*-value & coefficient value)	Regressor Coefficient (*p*-value & coefficient value)	Goodness-of-Fit (*p*-value)	Summary Measure of Assoc.	Trend: Intuitive or Counter	Predictive Capability
Airspeed (7/326)	p=0.000 4.18	p=0.000 -0.0238	0.000 0.000 0.000	0.60 0.66 0.26	Counter intuitive	Medium strong
Vertical velocity (7/326)	p=0.000 -1.62	p=0.013 -0.0562	0.000 0.000 0.000	0.32 0.35 0.14	Intuitive	Not strong
Flight path (7/326)	$p \leq 0.000$ -6.37	$p \leq 0.000$ -1.23	0.000 0.000 0.000	0.65 0.71 0.29	Intuitive	Moderate
Pitch angle (7/326)	$p \leq 0.000$ -2.80	$p \leq 0.000$ -0.410	0.000 0.000 0.000	0.46 0.51 0.20	Not applicable	Moderate
Vertical peak deceleration (6/324)	$p \leq 0.000$ -1.49	$p \leq 0.000$ +0.144	0.000 0.000 0.000	0.59 0.65 0.26	Intuitive	Moderate
Longitudinal peak deceleration (6/324)	$p \leq 0.000$ -3.13	$p \leq 0.000$ -0.485	0.000 0.000 0.000	0.60 0.66 0.26	Intuitive	Moderate

The airspeed model for scenario B contains a lot of scatter (see figure 31). The model predicts injury outcomes counter to the anticipated trend; one would expect the probability of severe injuries to increase as airspeed increases. The vertical velocity model (see figure 32) is an example of a model with a “not strong” predictive capability. Although the trend is as expected, the data have such large scatter that only one data point falls on the model. Flight path, pitch angle, vertical peak deceleration, and longitudinal peak deceleration all have metrics indicating moderate predictive capability; however, the plots of the data and the model show most data points outside the confidence limits of the model.

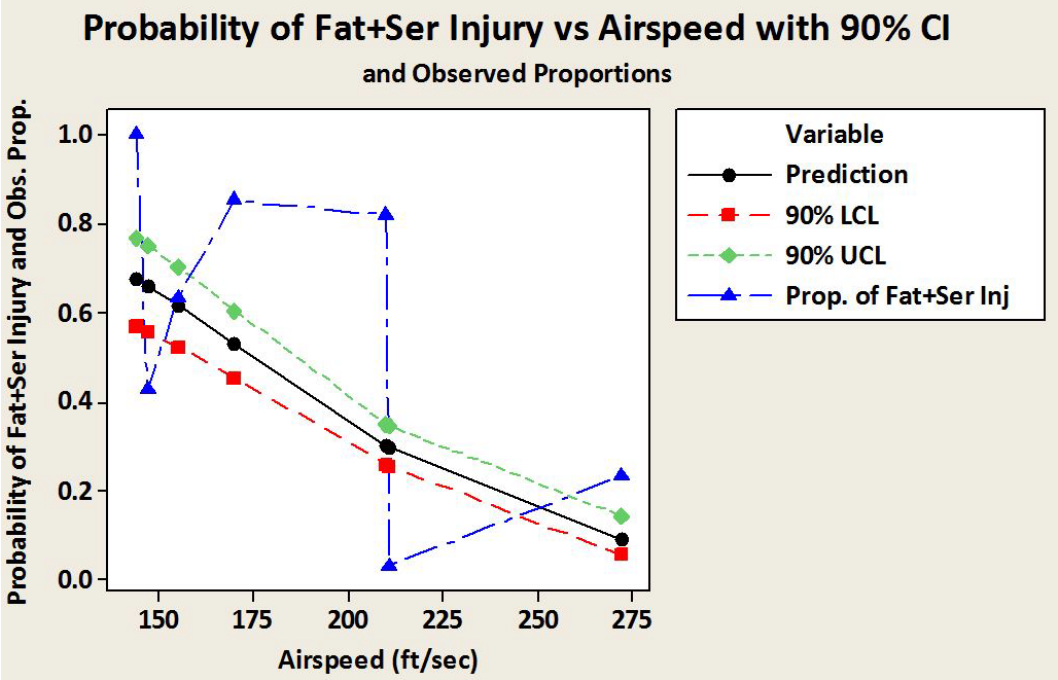

Figure 31. Injury fraction scenario B—Airspeed—Water

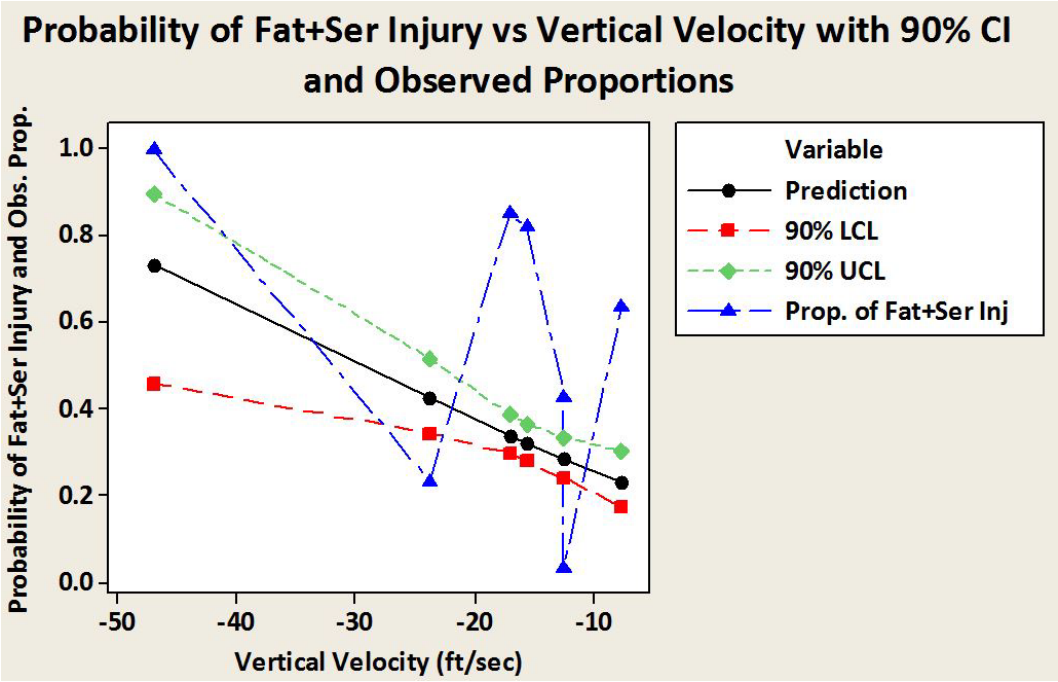

Figure 32. Injury fraction scenario B—Vertical velocity—Water

3.2.10.11 Multi-parameter model—scenario B

Two regressors (i.e., peak longitudinal acceleration followed by airspeed) were removed from the analysis because they were found to be non-significant. The multi-parameter model in equation 3 reflects these changes. The *p*-values for the coefficient of the constant and the coefficients of the four remaining parameters all indicated that these coefficients were non-zero (see table 39). The goodness-of-fit *p*-values indicate that the model could be viewed as fitting the data. The summary measures of association have moderate-to-large values indicating good prediction capability for the model. The model coefficients are displayed in equation 5 and in the coefficient table (see table 40), together with the usable limits for each parameter.

$$\hat{p} = \frac{1}{1 + e^{-(-6.42108 - 0.0946469x_1 - 1.44658x_2 - 0.345605x_3 + 0.0699445x_4)}} \tag{5}$$

Where $\hat{p}$ is the estimated probability for the event (i.e., fatal/serious injury) given a specific vertical velocity (x_1), flight path (x_2), pitch angle (x_3), and vertical peak G (x_4).

Table 39. 4-parameter BLM metrics scenario B – Water

Parameter (# Mishaps/# occupants)	Constant (*p*-value)	Regressor (*p*-value)	Goodness-of-Fit (*p*-value)	Summary Meas. of Assoc.	Predictive Capability
Vertical velocity (7/324)	$p \leq 0.000$	$p \leq 0.016$	$p=0.752$ $p=0.752$ $p=0.989$	0.81 0.89 0.35	Good
Flight path		$p \leq 0.000$	NA	NA	NA
Pitch angle		$p \leq 0.000$	NA	NA	NA
Vertical peak deceleration		$p \leq 0.015$	NA	NA	NA

Table 40. 4-parameter BLM coefficients scenario B—Water

Parameter	Coefficient	Valid Input Range	Units
Constant	-6.42	All	
Vertical velocity	-0.0946	-7.7 to -23.8	Ft/s
Flight-path angle	-1.45	-3.5 to -6.7	Degrees
Pitch angle	-0.346	+4.2 to +13.6	Degrees
Vertical peak deceleration	+0.0699	+0.3 to +24.1	G

The confidence limits apply only for input data within the range of input values for each parameter. Plotting the model predicted injury fraction against the observed injury fraction (see figure 33) indicates good prediction capability because the points fall along the equivalence line.

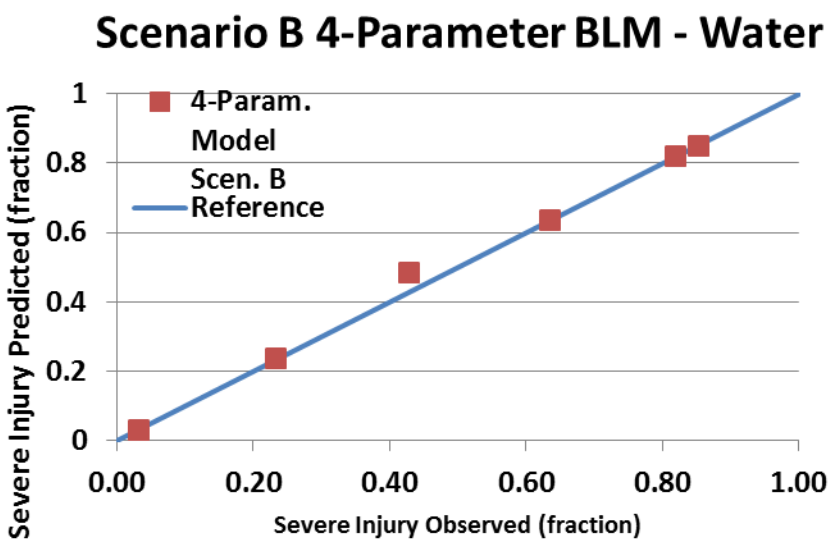

Figure 33. 4-parameter BLM scenario B model vs. observation—Water

3.2.10.12 Scenario C—landing short in the water

Although it seems surprising that there would be five of these events, it is the third most common mishap among the five scenarios. As with scenario B, the single-parameter models were attempted first, followed by a multi-parameter model. Only three of the six single-parameter models produced metrics with moderate or moderately strong predictive capability. The model coefficients are provided so that these models can be recreated (see table 41).

Table 41. Single-parameter BLM for scenario C—Water

Parameter (Mishaps/ Occupants)	Constant (*p*-value & coefficient)	Regressor (*p*-value & coefficient)	Goodness -of-Fit (*p*-value)	Summary Measures of Assoc.	Trend: Intuitive or Counter	Predictive Capability
Airspeed (5/295)	$p \leq 0.000$ -7.52	$p \leq 0.000$ +0.0290	0.000 0.000 0.000	0.23 0.28 0.09	Intuitive	Not strong
Vertical velocity (5/295)	$p \leq 0.000$ -8.44	$p \leq 0.000$ -0.328	0.022 0.027 0.022	0.62 0.74 0.25	Intuitive	Not strong
Flight-path angle (5/295)	$p \leq 0.000$ -4.01	$p \leq 0.000$ -0.574	0.000 0.000 0.000	0.32 0.39 0.13	Intuitive	Moderate
Pitch angle (4/250)	$p \leq 0.000$ -1.31	$p \leq 0.000$ +0.300	0.000 0.000 0.000	0.24 0.33 0.08	Not Applicable	Not strong
Vertical peak deceleration (4/215)	$p \leq 0.000$ -1.13	$p = 0.953$ -0.002	0.000 0.000 0.000	0.00 0.00 0.00	No trend	Moderately strong
Longitudinal peak deceleration (4/215)	$p \leq 0.000$ -1.66	$p \leq 0.020$ -0.0970	0.000 0.000 0.000	0.42 0.57 0.15	Intuitive	Moderate

The multi-parameter model, equation (6) for scenario C, has only three usable parameters: airspeed, vertical velocity and flight-path angle (see table 42). The coefficients for the model (see table 43) can be used to create predictions using this model. The model equation is:

$$\hat{p} = \frac{1}{1 + e^{-(-6.28883 - 0.0202448 x_1 - 0.610864 x_2 + 0.784998 x_3)}} \tag{6}$$

As can be seen on the plot (see figure 34), the model predicts four of the five severe-injury fractions very well.

Table 42. 3-parameter BLM metrics for scenario C—Water

Parameter (# Mishaps/# occupants)	Constant (*p*-value)	Regressor (*p*-value)	Goodness-of-Fit (*p*-value)	Summary Measures of Assoc.	Predictive Capability
Airspeed (5/295)	*p*=0.001	*p*=0.100	0.340 0.362 0.832	0.62 0.74 0.25	Good
Vertical velocity		*p*=0.000	NA	NA	NA
Flight-path angle		*p*=0.009	NA	NA	NA

Table 43. 3-parameter BLM coefficients for scenario C – Water

Parameter	Coefficient	Valid Input Range	Units
Constant	-6.29	All	
Airspeed	-0.0202	200 to 262	Ft/s
Vertical velocity	-0.611	-18.3 to -28.3	Ft/s
Flight-path angle	+0.785	-3.06 to -6.5	Degrees

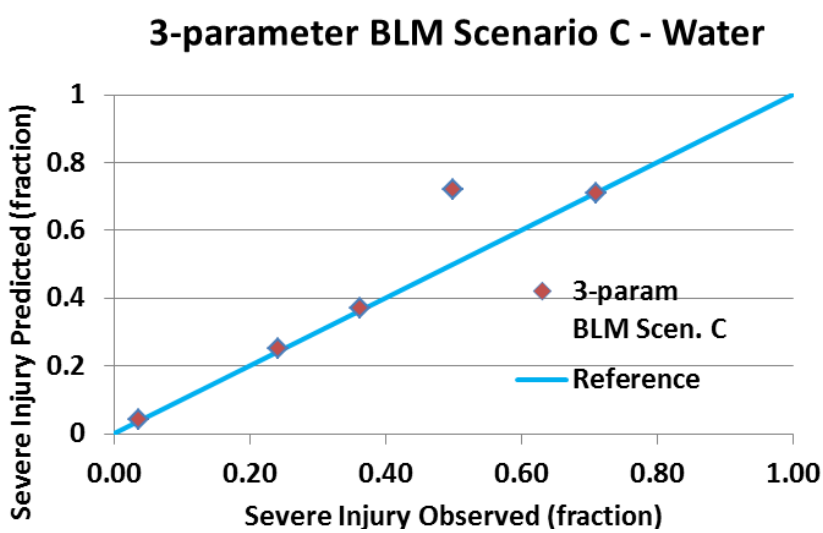

Figure 34. 3-parameter BLM for scenario C—Water

3.2.10.13 Scenario E—runway overruns into water

For the runway overrun scenario, only two of the single-parameter models have even moderate predictive capability (see table 44). These two are the flight-path angle and the pitch angle. The two models, based on peak decelerations, had only two data points available on which to base each model, and neither gives the anticipated trend.

Table 44. Single-parameter BLM for scenario E—Water

Parameter (Mishaps/ Occupants)	Constant (*p*-value & coefficient)	Regressor (*p*-value & coefficient)	Goodness-of-Fit (*p*-value)	Summary Measures of Assoc.	Trend: Intuitive or Counter	Predictive Capability
Airspeed (5/756)	$p \leq 0.000$ -6.30	$p \leq 0.000$ +0.0418	0.000 0.000 0.000	0.62 0.71 0.06	Intuitive	Low to moderate
Vertical velocity (5/756)	$p \leq 0.000$ -2.79	p=0.145 0.023	0.000 0.000 0.000	0.13 0.18 0.01	No trend	Not strong
Flight path (6/933)	$p \leq 0.000$ -1.66	$p \leq 0.000$ +0.161	0.000 0.000 0.035	0.61 0.68 0.05	Counter intuitive	Moderate
Pitch (6/933)	$p \leq 0.000$ -3.36	$p \leq 0.000$ -0.197	0.000 0.000 0.000	0.55 0.66 0.05	Not applicable	Moderate
Vertical peak deceleration (2/339)	p=0.004 -1.53	p=0.013 -0.250	Not applicable, only 2 pts.	0.31 0.56 0.03	Counter intuitive	Low to moderate
Longitudinal peak deceleration (2/339)	p=0.000 -2.26	p=0.013 0.220	Not applicable, only 2 pts.	0.31 0.56 0.03	Counter intuitive	Low to moderate

The multi-parameter model has only two usable parameters: the vertical velocity and the pitch angle. The presence of vertical velocity and pitch angle may seem surprising for the runway overrun scenario. Several of these events resulted in the nose of the aircraft abruptly dropping off the end of the runway into the water. Therefore, a pitch angle and a vertical velocity could be determined, although these angles were small. The metrics (see table 45) and the coefficients (see table 46) for these models are provided below. The models do predict generally low values for severe-injury fraction in this type of mishap (see figure 35).

Table 45. 2-parameter BLM metrics for scenario E—Water

Parameter (# Mishaps/# occupants)	Constant Coeff. (*p*-value)	Regressor Coeff. (*p*-value)	Goodness-of-Fit	Summary Meas. of Assoc.	Predictive Capability
Vertical velocity (6/933)	$p \leq 0.000$	$p=0.005$	0.000 0.000 0.000	0.60 0.67 0.05	Moderate
Pitch angle		$p \leq 0.000$	NA	NA	NA

Table 46. 2-parameter coefficients for scenario E – Water

Parameter	Coefficient	Valid Input Range	Units
Constant	-3.969	All	
Vertical velocity	-0.042	0 to -28.3	Ft/s
Pitch angle	-0.250	-11 to +7.7	Degrees

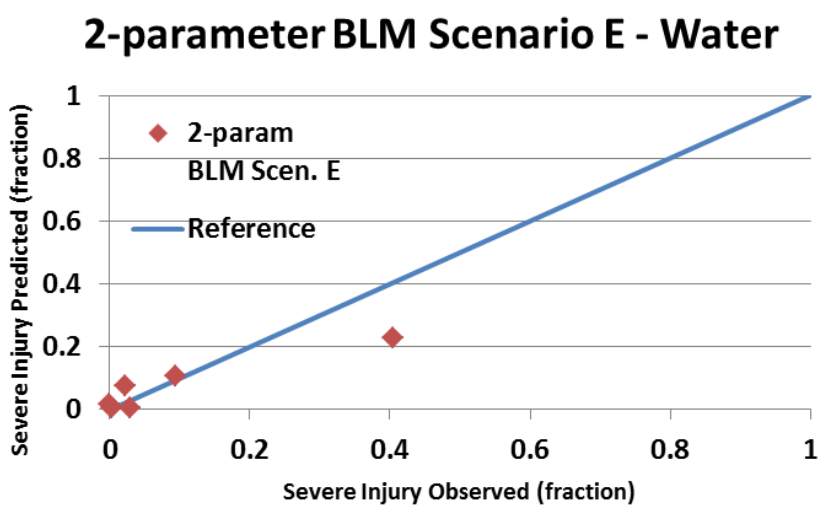

Figure 35. 2-parameter BLM for scenario E—Water

3.2.10.13.1 Logistic regression summary—water

The experiment to fit binary regression models to the water mishap data has not produced any strongly predictive single-parameter relationships with models that fit the data well. Ideally, the transition from mishaps with low-injury fractions to mishaps with high-injury fractions would occur over a narrow range in values for some if not all kinematic parameters. When a narrow transition occurs, one is justified in selecting a value near that range for design guidance. The expectation in creating these models was to understand the dependence of injury on the various kinematic parameters and, therefore, be able to use the models to assist in selecting impact conditions for crashworthiness testing or to select values for requirements. However, the single-parameter models are generally not predictive. The group of ditching scenarios (A–C) had a dataset characterized by a great deal of scatter; therefore, the single-parameter models saw observations

fall well outside the predicted model. These models confirm qualitatively that the flight path, the peak vertical deceleration, and the peak longitudinal deceleration are important parameters in determining injury outcome, but those dependences are well known in the field of crashworthiness. Likewise, the scenario B single-parameter models had only moderate predictive capability at best. Airspeed, flight path, pitch angle, vertical-peak deceleration, and longitudinal-peak deceleration were confirmed as being qualitatively important to injury outcome, but the quantitative predictive capability is not of practical use. In the scenario C dataset, only flight path and the vertical and longitudinal peak decelerations exhibited moderate predictive capability. The correlations qualitatively confirm once again that these impact parameters are instrumental in determining the injury outcome, but the relationships extracted are not sufficiently quantitative to be useful in making decisions in selecting test parameters or setting design guidance. The overrun scenario (E) produced the least useful models. The only strongly predictive variables were flight path and pitch angle—two parameters that are rather unexpected for these mishaps. These two parameters only have non-zero values when the aircraft drops off a seawall or dike after leaving the runway.

Some of the multi-parameter models appear to be predictive. These models were evaluated by using the input data to calculate a predicted serious and fatal injury probability and then comparing the prediction to the observed fraction. The multi-parameter model for the group scenarios A–C was not a successful predictor by this measure. In fact, the points (see figure 30) fall in an oval-shaped cluster with its long axis across the equivalence line rather than along it. This model is not useful even qualitatively. The multi-parameter model for ditching without thrust mishaps (scenario B) could be useful in selecting test conditions to simulate ditching without thrust (see figure 33). The input parameters are vertical velocity, flight path, pitch, and vertical peak deceleration. Using flight path combined with vertical velocity will provide airspeed or groundspeed, and these parameters together will define the key conditions for a drop test. However, in a water test, the peak deceleration is determined by the interaction with the water and, therefore, may not be a controllable variable. Likewise, the multi-parameter models for the landing short of the runway mishaps (scenario C) are predictive, as indicated by the predicted versus observed plot. This model uses airspeed, vertical velocity, and flight path as input parameters, which comprise a useful, but not quite complete, set of parameters. In as much as flight path can be determined from the two velocities, knowing the pitch angle would be more helpful in defining a test. In the overrun scenario, groundspeed would be expected to be the key parameter in predicting the fraction of occupants severely injured. However, it does not appear in the model; only vertical velocity and pitch appear. These two parameters only appear when an aircraft drops off a seawall or a dike as it enters the water. The fact that they are the only parameters to appear in the model may suggest that these parameters, or at least their presence, are more important in determining the injury outcome than groundspeed at impact with the water.

3.3 TASK 1 – SUMMARY CONCLUSIONS

What may be described as the reasons for aircraft ending in the water were not entirely as expected. The planned landing of the aircraft on water because of imminent fuel exhaustion characterized only 14% of the mishaps in the study and 15% of the mishaps in a larger population of mishaps. The aircraft landing on the water without the benefit of engine thrust is the largest group of mishaps in the study, comprising 32% of the mishaps (21% in the larger population). Twenty-three percent landed in the water short of the intended landing runway; 27% overran the runway into water.

The dataset consists of 22 mishaps, which have been categorized into five scenarios to better study the diverse range of mishaps. Twenty-two is not a large sample size for developing good statistics, and because the number of mishaps in each scenario varies from a low of one to a high of seven, confidence in statistical conclusions is limited.

Differences in the damage and injury outcomes for aircraft with high wings compared with those with low wings were found in this study. The high-wing aircraft exhibited greater damage and a higher fraction of severe injuries than did the low-wing aircraft. Because most of the high-wing mishaps are concentrated in the ditching without thrust scenario, the facts are inconclusive regarding one-wing configuration being more injurious than the other. Likewise, it appears that ditching without thrust is more injurious than ditching with power. However, there are only three aircraft in the ditching with power scenario.

The distribution of damage along the fuselage was found to have certain patterns. Generally, damage is less severe and less widely distributed in the afterward segments. Despite floor disruption occurring in roughly half of the mishaps, seat failure occurs significantly less frequently than floor disruption. The cockpit was the segment most often experiencing loss of volume. Ditchings without thrust experienced more frequent fuselage breaks than landing short.

Fuselage breaks occurred more often on either end of the forward cabin than on either end of the rear cabin. The ditchings with thrust averaged only one-third of the rate of fuselage breaks as the ditchings without thrust. The kinematic values for ditching without thrust mishaps are in the direction expected to lead to more damage compared to the ditchings with thrust. In particular, the vertical velocity at impact for those without thrust is nearly double the value for those with thrust. The flight-path angle must be higher because the median vertical velocities are very different between the two scenarios, whereas the airspeeds are more similar.

The ditching-without-thrust and the landing-short mishaps both showed general increases in damage with either increasing airspeed or increasing vertical velocity.

The number of escape routes actually employed was generally less than the number known to be usable and was far less than the total number installed. The fraction of all escape routes identified as usable (i.e., functional, accessible, and safe) was less than half those installed.

Identifying cumulative percentile velocities was accomplished but did not reveal any strong insights. Creating a two-velocity plot (i.e., airspeed and vertical velocity as principle axes) provided a visualization for the relative velocities of the mishaps. Identifying these plotted mishaps as survivable and partially survivable did not reveal a clear pattern with regard to velocity; certainly, there was no clear cutoff. Likewise, identifying the mishaps by their severe-injury fractions did not map onto the velocity plot as predictably as would be expected. Therefore, there is no clear correlation between the resultant velocity and the fraction of severe injuries.

The fraction of severe injuries generally increases with increasing damage metrics. However, in scenarios A–C, there is a trend for more fatalities in the rear, but that is inconsistent with the trend for higher damage metrics toward the forward end. In as much as these three scenarios may end up in deep water, the bias toward increased fatalities toward the rear may be associated with difficulty in escaping from the rear.

The trend for high-wing mishaps to have greater median damage metric values than the low-wing aircraft is reflected in corresponding similar trends in the injury data.

Based on the damage-metric trend and the fatalities trend, the ditching-without-power scenario (B) appears to have more severe injury consequences than the ditching-with-power scenario (A). However, as can be seen in looking at the engine configuration and wing configuration interactions, the aircraft design characteristics would appear to also affect the outcomes.

The approach of using a binary logistic regression to model the fraction of severe injuries using single or multiple kinematic parameters as input has not been productive for the group of mishaps encompassing landing on the water from the air (scenarios A–C). Some models even failed to predict the anticipated trend.

The multi-parameter model for scenario B is potentially useful. The multi-parameter models for the other single scenario datasets (scenarios C and E) are not.

4. TASK 2 – RJ IMPACT STUDY

4.1 SELECTING MISHAPS FOR THE STUDY – RJ

The overall mishap-selection and data-extraction processes were described previously in section 2 of this report. The criteria for inclusion in the RJ study are different than the criteria for the water impact. The intent was to study a particular class of aircraft rather than a particular type of mishap. The term “regional jet” has no formal definition in the regulatory environment and, in fact, has been evolving over time. For the purposes of this study, an RJ is a turbojet-powered (includes turbofan) aircraft used for commercial purposes with a capacity of up to 100 passengers. Historically, this class of aircraft grew in size from business jets and expanded into commercially viable transport aircraft, and, therefore, to purpose-built commercial transports in the seating capacity range of 50–100. At 100, the seating capacity encroaches on the low end of narrow-body commercial airliners as exemplified by the B737-100/200 or the Airbus 318. One general structural difference between the regional jet class and short-/medium-range narrow-body class is the diameter of the fuselage and its influence on the underfloor space usage. RJs generally do not use the underfloor space for baggage stowage.

The mishap search criteria included:

- Weight class = B (12,500–100,000 lb)
- Operation = Passenger
- Impact related = Y
- Engine type = Turbojet
- Contains official report = Not ticked

The output from this query was 242 mishaps. Not requiring a formal report was key to receiving a large population of candidate mishaps. Quite a few of the mishaps were such events as turbulence leading to a passenger or attendant injury, and these were eliminated from consideration. The list of 242 mishaps was reviewed by reading the summary description and verifying that a report was available. When available, reports were downloaded from the Internet. Nineteen of the identified

mishaps had reports that were not readily available. Sixteen of these mishaps were reported in ICAO documents. This list was emailed to the same people contacted about obtaining water-mishap reports. As in the case of the water impacts, there were no documents forthcoming, and these mishaps could not be used. Three additional mishaps were identified as having reports, but these reports were not found through the Internet, and paper copies could not be located.

The only limitation placed on the nature of the mishap was that enough information existed to determine the nature of the damage and injuries caused by the impact. This criterion tends to eliminate crashes with severe post-crash fire because knowledge of the post-impact damage is lost in the fire. One of the mishaps in this study is also in the water study, and one mishap rejected from the water study due to prior impact with terrain is included in the RJ study. The list of mishaps used in the study is provided in appendix D.

4.2 ANALYSIS – AIRCRAFT POPULATION – RJ

Although a diverse population of aircraft was sought, the population available ultimately consists of those airplanes that have crashed in mishaps with sufficiently documented investigations. The aircraft in the dataset are characterized by such design features as number of engines, location of engines, wing position, weight class, and seats per row. The database contained dozens of crashes by YAK-40 aircraft, but none of these had a complete report. Table 47–51 characterize the aircraft in the dataset in terms of these parameters. All aircraft in this study were powered by non-prop turbine engines, because turbojet power was a database selection criterion for this task. The database differentiates between turboprop and turbojet, but it does not differentiate turbofans from turbojets. All aircraft in this study were in weight class B (12,500–100,000 lb) because that weight class was used as a selection criterion. A list of the aircraft involved in the mishaps is provided (see table 52). The decision was made to include charter aircraft in the dataset to increase the sample size. It was believed that these aircraft would behave in a similar fashion to RJs in a crash. In fact, the inclusion of these aircraft into the dataset benefitted the kinematics and damage data, but it did not benefit the injury data. Some of these aircraft were so small that they did not exhibit five distinct fuselage segments (see sections 3.2.6 and 3.2.7). The other difference with the charter aircraft is that they have far fewer seats than a commercial transport of similar size, and the fraction of seats occupied is also lower. Consequently, they contributed little to injury sample size.

Table 47. Number of engines—RJ dataset

Number of Engines	Number of Aircraft in the Dataset
2	21
4	3

Table 48. Engine configurations—RJ

Engine Configuration	Number of Aircraft With Configuration
Engines on wing	4
Engines on tail	20

Table 49. Wing configuration—RJ

Wing Configuration	Number of Aircraft With Wing Configuration
Low-wing	21
High-wing	3*

*One in the overrun scenario and two in the compromised landing scenario.

Table 50. Seats per row—RJ

Total Seats per Row (Maximum)*	Number of Aircraft*
2	2
3	3
4	8
5	7
6	1

*Differs from definition in the CSTRG database, which is the maximum number of seats without an aisle.
*Three aircraft were operated as charters and had unknown interior configurations.

Table 51. Total seats on aircraft—RJ

	Total Passenger Seats
Average Number of Seats	66.4
Median Number of Seats	50
Greatest Number of Seats	116
Least Number of Seats	6
No. Aircraft With No Information	1

Table 52. List of mishap aircraft – RJ

EMB145	CANADAIR RJ200 (2)	BAC1-11 (2)
EMB135LR	Fokker 70	Fokker 28-100
CANADAIR RJ200-LR	CANADAIR RJ100 (3)	CL600-2A12
EMB170	GULFSTREAM III	CL600-2B19
BAE 146-200A	GULFSTREAM II	Fokker 100
AVRO RJ100 (2)	GULFSTREAM IV (2)	F28-4000

The mishaps included in the study covered a range of scenarios and severity. These mishaps covered most phases of flight except cruise (see table 53). The study mishaps are predominately from the low-altitude phases of flight. Ten of the mishaps resulted in substantial damage, whereas 14 destroyed the aircraft. Injuries occurred in 13 of the 24 mishaps, with 10 resulting in fatalities. As would be expected in a more narrowly defined population of aircraft, the number of occupants

covered a narrower range. The median number of occupants was 41 (average = 44), with the minimum being 4 and the maximum 97. An emergency evacuation was conducted in 14 of the 24 mishaps. Two of the mishaps ended with the aircraft in water.

Table 53. Phase of flight – RJ

Phase of Flight	Number of Mishaps
Aborted takeoff	2
Takeoff	4
CLIMB	1
APPROACH	3
GO-AROUND	1
LANDING	13
Characterized as "overrun," including both takeoff and landing (included above)	6

For the purpose of this study, injuries caused by the impact are the primary interest (see table 54). Those injuries, which were clearly identified in the report as unrelated to the impact, are excluded from the injury count. Lap infants are excluded from the passenger counts and injury counts in this study. In many investigation reports, minor injury counts are combined with no-injury counts; consequently, these two counts are combined throughout the analysis for consistency. The median value being lower than the average value in some categories indicates that the average was raised by one or two mishaps with large numbers. The distribution of injuries is discussed in section 4.2.6.

Table 54. Severity of injuries – RJ

	Total Fatalities	Total Severe Injuries	Total Minor/No Injury
Median	0	0	32.5
Average	8	2	32
Maximum	83	13	93
Minimum	0	0	0

4.2.1 Mishap Scenarios—RJ

The RJ mishaps cover a diverse range of circumstances, and for this study, grouping the mishaps into scenarios for analysis proved to be useful. The 24 mishaps were classified into five scenarios (see table 55). The first and most common (seven mishaps) scenario includes runway overruns both on landing and takeoff. These mishaps are characterized by relatively low velocities and low, idle level thrust from the engines. The scenario includes both aborted takeoffs and poor, but controlled, landings in which the aircraft exceeded the boundaries of the airfield. A scenario characterized as "compromised landing with mild impact" includes landings in which a failure of some type occurred, which damaged the aircraft, but the impact was not severe. These three mishaps include a gear-up landing, a main gear collapse, and a tail strike. All ended with the aircraft on the airfield. A third scenario (four mishaps) consists of impacting terrain short of the

runway during an attempted approach or landing; these impacts are characterized by low descent rates and moderate airspeeds. The fourth scenario consists of hard landings that result in loss of control of the aircraft (four mishaps). The fifth and second most common scenario is loss of control on takeoff, most commonly due to wing ice/snow contamination (six mishaps). This scenario also includes a takeoff from an incorrect (too short) runway. The reason for including the wrong runway mishap in this particular scenario is that it shares the characteristics of crashing under takeoff power and loss of control by the pilots.

Briefly, the scenarios are designated as:

- Scenario F – Runway overrun (landing or takeoff)
- Scenario G – Compromised landing (mild impact)
- Scenario H – Impacted terrain short of runway (generally on approach)
- Scenario J – Hard landing with loss of control post-impact
- Scenario K – Loss of control on, during, or following takeoff (includes wing contamination)

Table 55. Mishap scenarios—RJ

CSTRG ID	Short Name	Aircraft Type	Scenario
20100616A	OTTAWA EMB145	EMB145	F
20091207A	GEORGE EMB135	EMB135LR	F
20070412C	TRAVERSE CITY CRJ200	CANADAIR RJ200-LR	F
20070218A	CLEVELAND EMB170	EMB170	F
20061010A	STORD 146 CLIFF & FIRE	BAE 146-200A	F
20041201B	TETERBORO G-IV	GULFSTREAM IV	F
19780709A	ROCHESTER BAC1-11	BAC1-11	F
19720719A	CORFU BAC1-11	BAC1-11	F
20090213A	LONDON CITY NOSE GEAR COLLAPSE	AVRO RJ100	G
20070818A	LONDON CITY TAIL STRIKE	AVRO RJ100	G
20070124A	BARCELONA RJ200 gear up	CANADAIR RJ200	G
20040105A	MUNICH F70	F70	H
20030622A	BREST CANADAIR RJ100	CANADAIR RJ100	H
20010329A	ASPEN GULFSTREAM III	GULFSTREAM III	H
19760926A	HOT SPRINGS GII	GULFSTREAM II	H
20071216B	PROVIDENCE, OFF RUNWAY	CANADAIR RJ200	J
20070520B	TORONTO CROSSWIND	CANADAIR RJ100	J
19971216A	NEW BRUNSWICK CL600	CL600-2B19	J
20070125A	PAU F28 (IN FRENCH)	F28-100	K
20060827C	BLUE GRASS CANADAIR	CANADAIR RJ100	K
20041128B	MONTROSE CO, CL600	CL600-2A12	K
19961030A	PEEWAUKEE IL	GULFSTREAM IV	K
19930305A	SKOPJE F100	F100	K
19920322A	LA GUARDIA F28	F28-4000	K

To determine how representative the study sample of the RJs mishaps is with regard to the frequency of each scenario, the larger population of mishaps returned by the original query (242) was reviewed. The summary descriptions were read, and if applicable, the mishaps were assigned to one of the scenarios. Of the 242 mishaps returned, 131 were assignable, including the 24 in the study population. The remaining mishaps either had insufficient information (23 mishaps) or were not applicable to this study (81 mishaps). Reasons for non-applicability mainly centered on little to no expectation for survivable outcome. The study sample tracks the larger population (see table 56) reasonably well. It under-represents the compromised landings and impacts short of the runway each by 4 percentage points (approximately 20%–25% by the number of impacts) and over-represents the loss of control on takeoff by 7 percentage points (almost 40% by the number of impacts). It is ideal to add mishaps to the two scenarios that are underrepresented, but all mishaps that had sufficient information are already included in the interest of improving the statistics. Columns may not add to 100% because of round-off error.

Table 56. Scenario frequency—RJ

	24 Mishaps Studied in Detail (percent)	131 Mishaps From Query With Assignable Scenario (percent)
Runway Overrun Takeoff or Landing (F)	33	33
Compromised Landing Without Severe Impact (G)	13	17
Impacted Short of Runway (H)	17	21
Hard Landing, Lost Control (J)	13	12
Loss of Control During Takeoff Roll or Early Climb (K)	25	18

4.2.2 Kinematics of Mishaps – RJ

A larger dataset will be reviewed first, and then this larger dataset will be broken down into scenarios. For the purpose of setting design guidelines and test conditions, knowledge of the larger set of data may be more beneficial. In this analysis, the data for scenarios G–K are grouped together. These scenarios have the common attribute that the impact occurs from the air or in the attempt to become airborne. Being airborne causes at least two factors to be different compared to the overrun scenario (F): The velocity is higher, and the attitude has an additional degree of freedom. The overrun scenario is analyzed in the subsequent section in which each scenario is reviewed separately.

The limited number of mishaps and diverse nature of these mishaps result in statistical analysis results with large uncertainties. Therefore, the data will be presented in several graphical ways to facilitate the reader's interpretation of where critical transitions may be occurring. In the following section, the kinematic data are presented as both histogram frequency charts and as cumulative percentile charts. The histograms are created to show the number of mishaps that occurred within ranges or "bins" of each parameter. In the percentile distribution curves, the value for each mishap is ranked in ascending order and then assigned a percentile value. The percentile value for a

particular mishap means that *N* percent of the events occurred at a lower value of the parameter than the value for a particular mishap. Therefore, the plot can be used to determine either what percentile a given value corresponds to or the corresponding parameter value for a particular percentile.

The first parameter analysis is for the absolute value of the vertical velocity (see figure 36)[4]. Vertical velocity is normally negative, but in one RJ case, the aircraft crash inverted and, therefore, had a positive vertical velocity, as expressed in the aircraft reference frame (vertical velocity is plotted as positive on the histogram for clarity). The histogram reveals that most mishaps occurred within the range 0–20 ft/s. For the vertical velocity, the median value of -16.0 ft/s is similar to the average value of -16.6 ft/s. The red curve presents the cumulative percentile of crashes; therefore, 62.5% of the mishaps in the dataset occurred with a vertical velocity less than or equal to 20 ft/s. One occurred at a velocity greater than 50 ft/s.

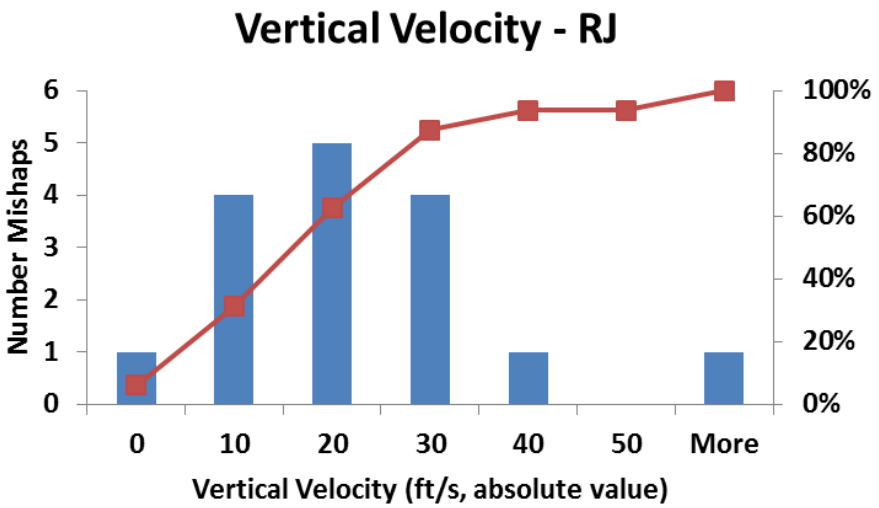

Figure 36. Vertical velocity distribution—RJ

The airspeed is the velocity along the flight path; the data for scenarios G–K are widely divergent (see figure 37). One mishap occurred at 50 ft/s and one between 100 and 150 ft/s; these were both poorly executed landings, resulting in stall conditions above the runway. The median value of 200 ft/s is similar to the average of 203 ft/s. In this case, the fact that the two are approximately equal is a confirmation that they represent the center tendency of the sample set. However, the two low-speed events make it a wide and non-symmetric distribution. The cumulative percentile curve, as does the median value, indicates that roughly half of the mishaps in the dataset had airspeeds of 200 ft/s or less.

[4] These histogram charts created in Excel are read using the number under the column as the upper limit for that bin. The width of the bin is the difference between two adjacent labels. In the diagram, there was one mishap with a velocity between -10 and 0, four mishaps in the range 0-10 ft/s and five mishaps between 10 and 20.

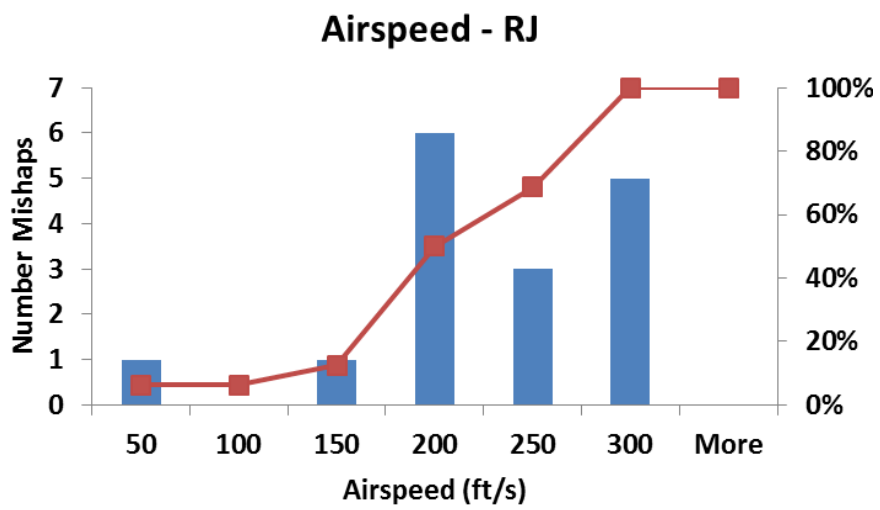

Figure 37. Airspeed velocity distribution (G–K)—RJ

The flight-path angle is the angle between the path of the aircraft center of gravity and the horizon (see figure 3); descent is a negative angle. The flight-path angle isolates the direction of the impact from the velocity, and is a ratio between the airspeed and the vertical velocity. In the RJ dataset, all the flight-path angles were zero or negative (plotted as positive values) with 80% of the mishaps occurring with flight paths of 8º or less (see figure 38).

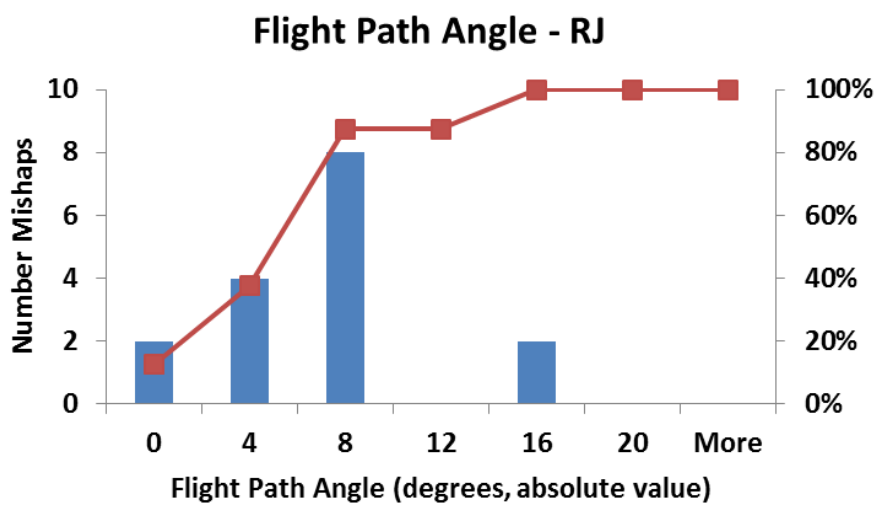

Figure 38. Flight-path angle distribution (G–K)—RJ

The pitch angle is the angle between the longitudinal axis of the aircraft and the horizon; nose-up is positive pitch angle. The pitch angle chart (see figure 39) reveals that, of the 16 mishaps, one impacted with the nose down (negative pitch) more than 5º. Three occurred with the nose less than 5º down. The common attitude was in the range 0º–10º nose up.

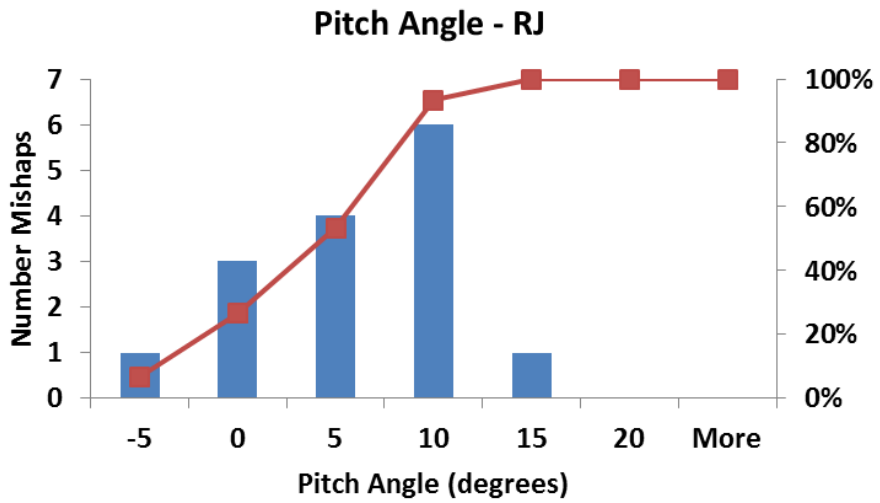

Figure 39. Pitch angle distribution (G–K)—RJ

The roll (see figure 40) and yaw angles (see figure 41) at impact in many of these mishaps are very near neutral values because the aircraft impacts from controlled flight. However, in scenario K, in which control of the aircraft is lost, more extreme values of these two angles are recorded. It is readily apparent that approximately half of these events occurred with the roll and yaw angles at the normal near-zero value. The absolute values are plotted considering the symmetry of the airplane. The important quantity is the magnitude of deviation from nominal attitude; the effect on the airframe presumably will be equal, regardless of which side is affected. The extreme values generally indicate a scenario K event.

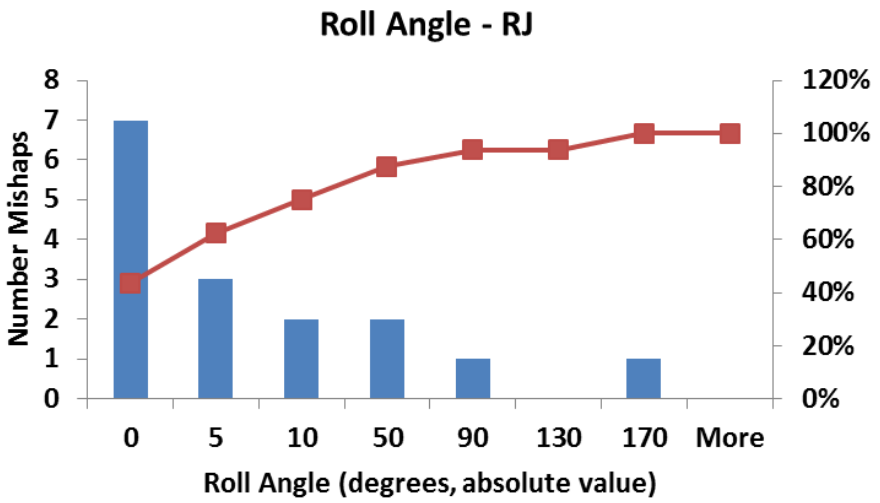

Figure 40. Roll angle distribution (G–K)—RJ

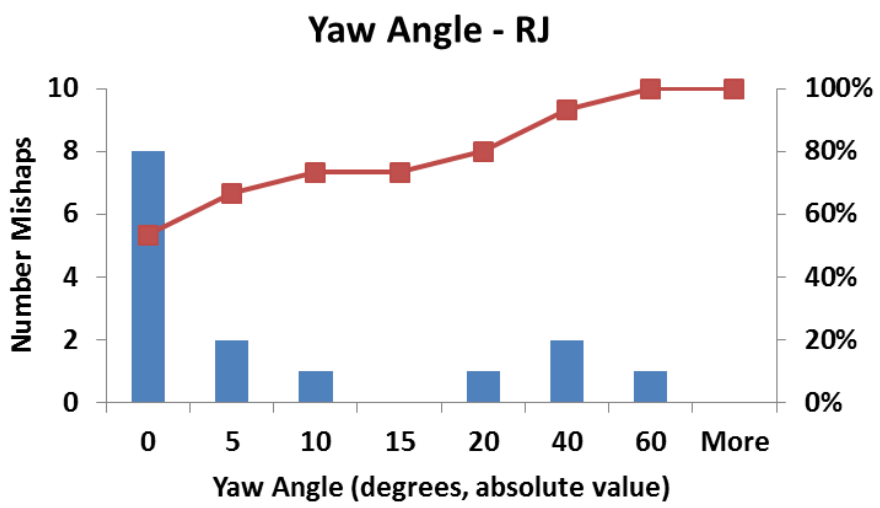

Figure 41. Yaw angle distribution (G–K)—RJ

Most of the acceleration force values used in this study are estimated by impact reconstructions. The vertical acceleration (also referred to as "normal acceleration" in several reports) was recorded in a few aircraft; none of the aircraft were equipped to record longitudinal or lateral acceleration. Note that to capture the shape of the deceleration pulse in the actual impact, the recording frequency for the acceleration in each axis must be much higher than the recording frequency normally used to capture flight data. As can be seen in the vertical deceleration histogram (see figure 42), the vertical deceleration was less than 10 G in most of the mishaps but with several extreme cases. The high vertical decelerations and the one inverted crash (-31.9 G) were associated with mishaps involving ice-/snow-contaminated wings at takeoff.

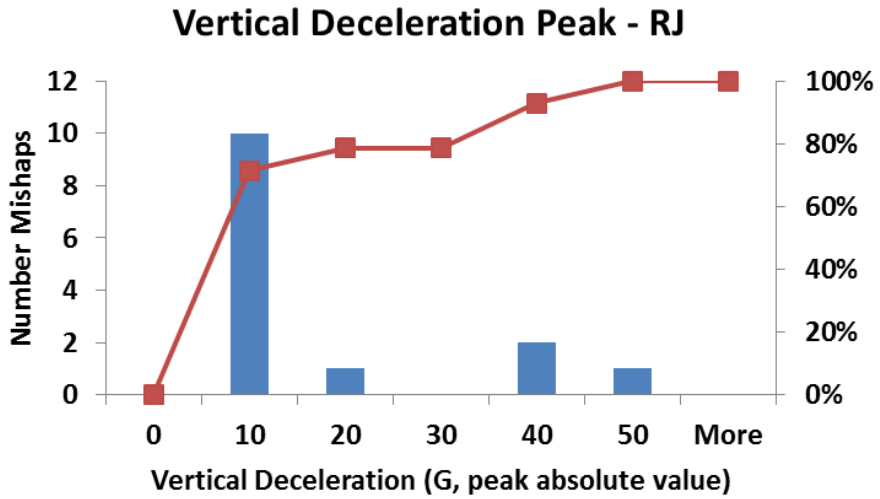

Figure 42. Vertical deceleration – RJ

The longitudinal deceleration histogram (see figure 43) reveals a very wide distribution of events. Twelve of the events experienced relatively modest decelerations, as would be expected for fixed-wing landing mishaps. The single event above 40 G was actually 155 G and was a Gulfstream

impacting the side wall of a ravine short of the runway. The other two high values of longitudinal deceleration are associated with contaminated-wing takeoffs.

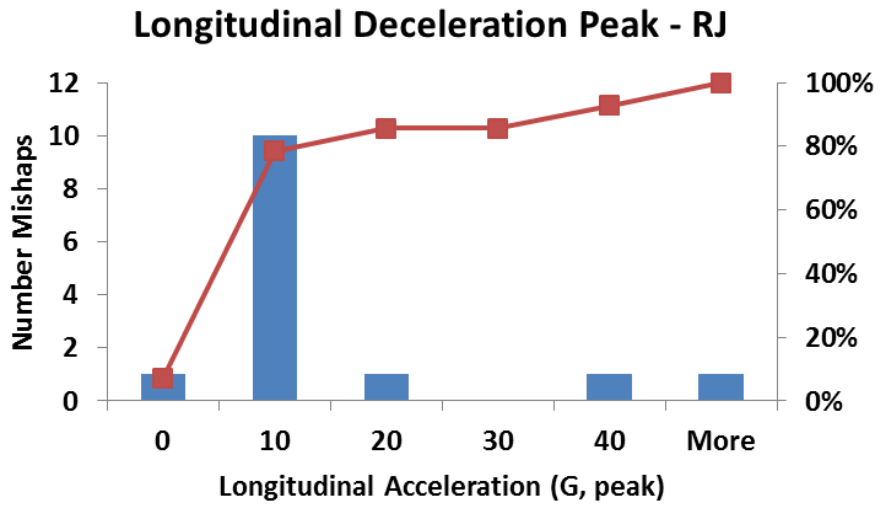

Figure 43. Longitudinal deceleration—RJ

The lateral deceleration is generally non-zero only when the roll or yaw angles have deviated from 0º. As was seen previously in the angle charts, relatively few of the mishaps occur at extreme angles, and that fact is reflected in lateral deceleration values (see figure 44). Two-thirds of the mishaps have lateral decelerations of 10 G or less.

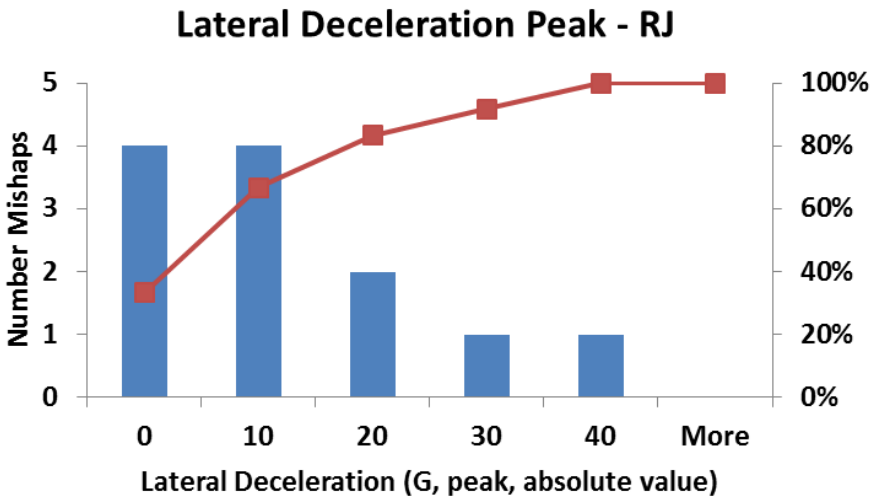

Figure 44. Lateral deceleration—RJ

4.2.2.1 Kinematics of each mishap scenario—RJ

The kinematic characteristics of the different scenarios are generally consistent with the nature of the scenario. The runway overruns (scenario F) have a lower airspeed (longitudinal velocity) than the other scenarios (see table 57). A few of these events had a vertical velocity component in the impact due to the terrain dropping off ditches or ravines. The median longitudinal peak deceleration is higher than some of the other scenarios because the aircraft impacted an obstacle of some type.

Table 57. Kinematics by scenario—RJ

Scenario {# of events in scenario}	Med./Avg. Vert. Vel. (ft/s)	Med./Avg. Airspd. Vel. (ft/s)	Med./Avg. Flight-Path Angle (deg.)	Med./Avg. Pitch Angle (deg.)	Med./Avg. Vert. Accel. (G)	Med./ Avg. Long. Accel. (G)
F Runway overrun {8}	0/ -3.9	68.0/ 70.8	0/ -4.8	0/ -2.2	0.7/ 2.0	-7.1/ -4.7
G Problem landing, no impact {3}	-4.0/ -7.7	190/ 219	-1.0/ -1.9	6.0/ 5.1	1.3/ 1.3	-0.1/ -0.1
H Impact terrain, short{4}	-19.4/ -18.6	200/ 213	-5.5/ -4.8	4.0/ 3.0	2.6/ 17.7	-6.3/ -54
J Hard landing, lose control {3}	-11.0/ -13.9	114/ 128	-5.1/ -6.8	4.5/ 4.7	3.3/ 3.7	-0.6/ -3.3
K Loss-of-control takeoff {6}	-19.8/ -21.4	243/ 236	-5.9/ -6.5	5.5/ 5.8	8.1/ 5.4	-5.0/ -10.5

The problem-landing, no-impact scenario is characterized by landings that were well executed up to the point of touchdown. Consequently, the kinematics (see table 57) are consistent with the kinematics of normal landing. In one event, the airspeed was high because of a failure in the flap-deployment mechanism. Although the pilots flew a well-executed, no-flaps landing, they neglected to lower the landing gear. The other two events were a main gear failure and a tail strike.

The impacted-terrain short scenario (scenario H) is the aircraft impacting the terrain short of the runway. Although airspeeds (see table 57) in this scenario are similar to the problem-landing category, the vertical velocity at impact is significantly higher, and because of the terrain being other than a runway, the outcomes are far less favorable in terms of damage and injury.

The hard-landings, lose-control scenario (scenario J) is notable for low airspeeds and high vertical velocities (see table 57). Upon looking into the individual mishaps within this scenario, the hard landings with loss of control were all found to be poorly executed landings, which effectively led to stall situations over the runway. In one case, the aircraft bounced severely, but because of the throttle setting, the anti-bounce response did not activate. When the pilots realized the omission and pulled back the throttle, the anti-bounce response activated as the aircraft was well above the runway, effectively stalling the aircraft and dropping it onto the runway. As a consequence of these

stall-like events, the longitudinal velocities are lower than might be expected, and the vertical impact velocities are higher compared to normal landings. In more than one, the vertical velocity was apparently beyond the capability of the landing gear.

Four of the loss of control on takeoff mishaps were related to contaminated wings. These crashes demonstrated the most extreme impact attitudes often involving extreme pitch, roll, and yaw angles. The aircraft becomes airborne and then one wing stalls, causing a severe roll and associated yaw; in some cases, this deviation is caught and recovered, but over-correction leads to impact at extreme attitude in the opposite direction. Another mishap in this scenario was literally loss of directional control of the aircraft during acceleration on the ground, and the resulting destruction of the aircraft after it veered off the runway. The remaining event was an attempted takeoff from the wrong runway, which was insufficient in length for the aircraft to become airborne. This mishap was assigned to takeoff scenario because of similarities with the loss-of-control mishaps; the impact was at high velocity, high power, and off the prepared airport surfaces.

4.2.3 Quantifying Damage—RJ

The same definition for the damage metric is used for the RJ study as is used for the water impact study. The calculation of this metric was described previously in section 2 of this report. The damage modes reported in the database are underside fuselage damage, floor disruption, seat failure, fuselage breaks, and loss of occupied volume. The information in the database was supplemented by photographs. To record frequency and severity of occurrence for each mode of damage in each segment of the aircraft, a cell for each segment/damage mode was populated with: “none,” “widespread,” or “local,” and these values are accumulated to form the damage metric for each segment (see table 58). In general, the damage for the RJ mishaps was thoroughly reported; only five mishaps had any missing information. The worst of these was missing five of 24 cells. The effect of any missing cell is to reduce the value of the damage metric because NI is assigned a zero value. Several means for working around this missing data were considered, but none were deemed satisfactory. Table 58 lists the number of cells containing NI; the total damage factor for these mishaps may be lower than would have been recorded had all of the information been available. Each fuselage break (see table 59) that occurred was entered as damage to the rearward segment relative to the break. This decision was based on the observation that the injuries related to a break tend to occur in the seats behind the break rather than ahead of the break.

In every case, the underside of the nose experienced some damage. There is a weak trend of more damage occurring at the front of the aircraft (see table 58). It is unexpected that loss of occupant volume occurs as frequently, or more frequently, than seat failure. However, seat failure is tied closely to floor failure and was assumed to occur when the floor was severely compromised. Loss of occupant volume could occur not only from floor upheaval, and crushing in of sides or top of the fuselage, but it was taken to have occurred locally at fuselage breaks. That seat failures and loss of occupant volume occurred in 25%–40% of each segment in the 24 mishaps is indicative of the potential for serious injuries and loss of life in these accidents.

Table 58. Mishap damage metrics—RJ

Reference # ID	Scenario (F-K)	Cockpit Damage Metric	Fwd Cabin Damage Metric	OW Cabin Damage Metric	Rr Cabin Damage Metric	Tail Damage Metric	Total Damage Metric	# of NI
20100616A	F	1	0	0	0	0	1	0
20091207A	F	10	0	0	0	1	11	0
20070412C	F	2	0	0	0	0	2	0
20070218A	F	1	1	1	1	1	5	0
20061010A	F	4	8	4	8	2	26	0
20041201B	F	5	0	0	0	0	5	0
19780709A	F	2	2	2	2	2	10	0
19720719A	F	1	0	0	0	0	1	0
20090213A	G	2	2	2	2	1	9	0
20070818A	G	0	0	0	1	1	2	1
20070124A	G	2	2	2	2	2	10	0
20040105A	H	2	2	2	2	2	10	0
20030622A	H	14	5	2	2	2	25	1
20010329A	H	20	23	23	23	23	112	0
19760926A	H	20	23	23	23	5	94	0
20071216B	J	0	0	0	0	0	0	5
20070520B	J	1	2	2	2	1	8	0
19971216A	J	13	11	2	2	2	30	0
20070125A	K	4	2	2	2	2	12	0
20060827C	K	20	23	20	15	11	89	0
20041128B	K	20	11	10	8	12	61	3
19961030A	K	17	20	23	20	5	85	0
19930305A	K	20	23	23	20	23	109	0
19920322A	K	17	17	23	17	13	87	1

Table 59. Damage occurrence in each segment—RJ

All Mishaps (24)	Cockpit (# of Mishaps)	Forward Cabin (# of Mishaps)	Over-wing Cabin (# of Mishaps)	Rear Cabin (# of Mishaps)	Tail (# of Mishaps)
Underside Skin Damage	22	16	17	17	18
Floor Disruption	12	8	7	7	4
Seat Failure	8	7	6	6	3
Loss of Occupant Volume	11	9	7	8	5
Breaks	NA	7	5	3	5

Two mishaps have very high damage metrics (109 and 112); one of these mishaps is a landing-short event in which the aircraft impacts the wall of a ravine. The other mishap is a loss-of-control on takeoff due to icing; in this event, the aircraft develops extreme attitude angles and crashes beyond the boundary of the airport. The two scenarios, short-of-runway (scenario G) and lost control during takeoff (scenario K), accounted for all of the fuselage breaks and averaged roughly two breaks per mishap (see table 60).

Table 60. Fuselage breaks by scenario—RJ

	Number of Fuselage Breaks	Fuselage Breaks/Mishap
Scenario F, Overruns (8 events)	0	0
Scenario G, Compromised Landing (3 events)	0	0
Scenario H, Short of Runway (4 events)	9	2.25
Scenario J, Hard Landing, Lost Control (3 events)	0	0
Scenario K, Lost Control During Takeoff (6 events)	11	1.83
Scenarios G–K (16 events)	20	1.25

Fuselage breaks are associated with injury to occupants in the immediate area of the break. There is a weak trend indicating that more breaks occur toward the front than the rear.

Following is the number of breaks in all of the RJ mishaps and working through the joints: the cockpit-to-forward-cabin joint experienced 7 breaks in the 24 mishaps, the forward-fuselage-to-wing joint experienced 5 breaks, the wing-to-rear-cabin joint had 3 breaks, and the rear-cabin-to-tail joint experienced 5 breaks. If the breaks are assigned to the three high-density segments, the trend remains: forward cabin, 12 breaks; overwing cabin, 8 breaks; and rear cabin, 8 breaks. Scenarios H and K are the most severe as measured by number of fuselage breaks/mishap.

4.2.3.1 Damage related to kinematics—RJ

The damage plotted against the various kinematics parameters reveal general trends. In the case of velocity cases (see figure 45), one can see the expected trends in some scenarios. For example, in the loss-of-control on takeoff scenario (scenario K), the damage metric increases as the magnitude of the airspeed increases, although two points do not follow the trend. Likewise, in the other violent scenario, impact-short-of-the-runway (scenario H), the damage metric increases steeply as both the airspeed and the vertical velocity increase (see figures 45–46). For the two scenarios G (compromised landing) and F (runway overrun)—characterized by less extreme attitudes—the damage metric depends less strongly on the velocity. The relatively modest damage associated with the accidents involving hard landings with loss-of-control (scenario H) indicates that these aircraft are robust enough to withstand very poorly executed landings. It should be noted that in selecting the events for inclusion into the study, some mishaps with severe post-crash fire were excluded because the damage prior to the outbreak of the fire could not be determined.

The trends are less evident in the flight-angle data. The two violent scenarios, impact-short-of-the-runway (scenario H) and loss-of-control on takeoff (scenario K), show strong increases in damage metric as the flight-path angle increases (see figure 47). However, there is no correlation between the damage metric and the pitch angle (see figure 48).

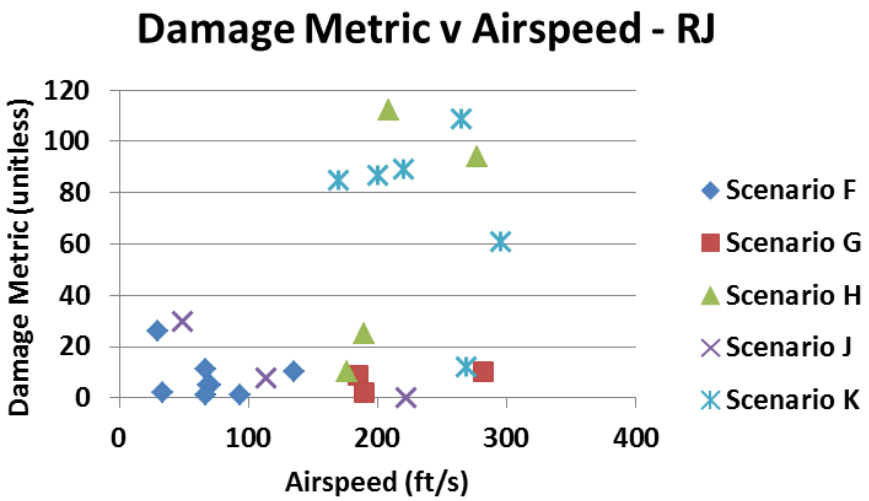

Figure 45. Damage metric vs. airspeed—RJ

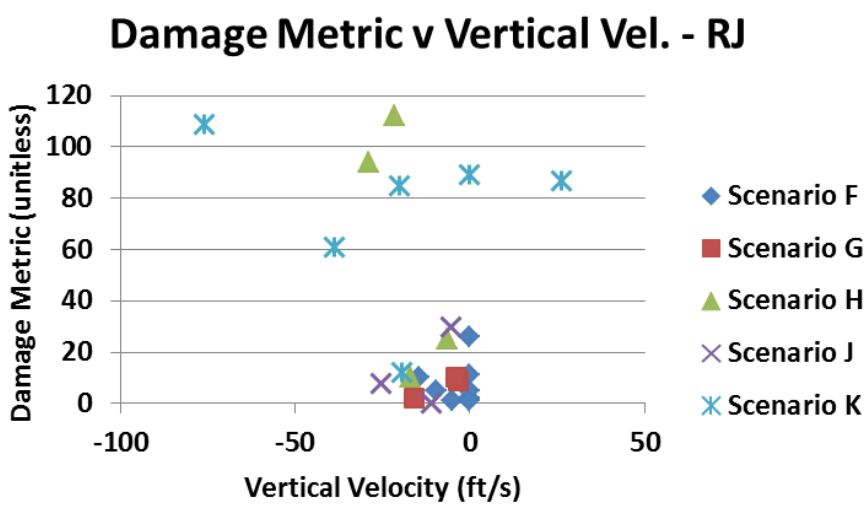

Figure 46. Damage metric vs. vertical velocity—RJ

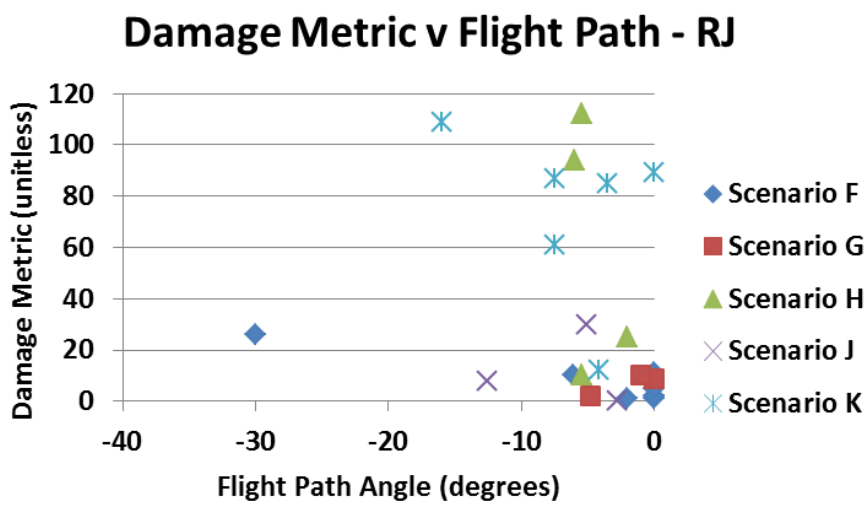

Figure 47. Damage metric vs. flight path—RJ

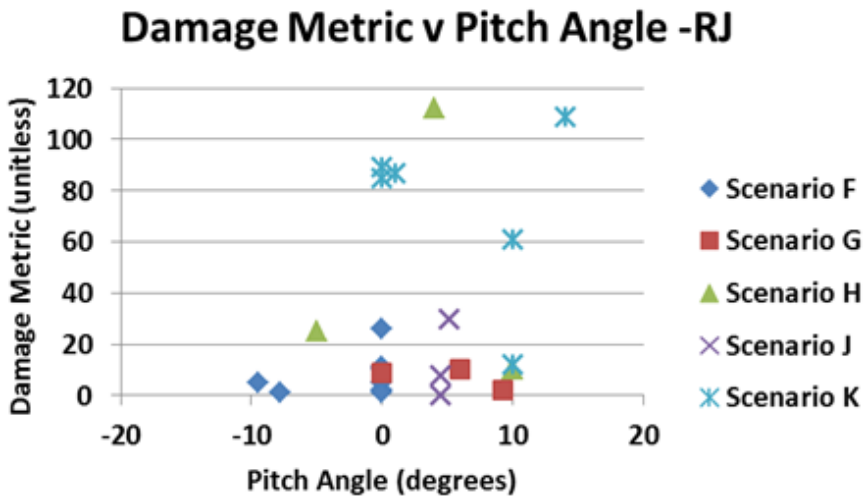

Figure 48. Damage metric vs. pitch angle—RJ

4.2.3.2 Segment damage by scenario—RJ

The damage metric is built up segment by segment. Consequently, the trends between segments within a scenario and between scenarios within a segment can be viewed in table 61. The low severity of scenarios F and G is reflected in correspondingly low damage metrics for these scenarios; there is also minimal difference in the damage metric between segments. The relatively low damage associated with scenario J, even though it involves loss-of-control of the aircraft, may be because these mishaps occur on the prepared surfaces of the airport property. Scenarios H and K occur at flight speeds and on unprepared terrain; these considerations are reflected as generally higher damage metrics throughout the aircraft, along with a slight elevation of the damage metric at the front of the aircraft.

Table 61. Segment damage metrics—RJ

	Cockpit[1] (Total Damage Metric/# of Mishaps)	Fwd. Cabin (Total Damage Metric/# of Mishaps)	OW Cabin (Total Damage Metric/# of Mishaps)	Rear Cabin (Total Damage Metric/# of Mishaps)	Tail (total Damage Metric/# of Mishaps)
Scenario F	3.3	1.4	0.9	1.4	0.8
Scenario G	1.3	1.3	1.3	1.7	1.3
Scenario H	14.0	13.3	12.5	12.5	8.0
Scenario J	4.7	4.3	1.3	1.3	1.0
Scenario K	16.3	16.0	16.8	13.7	11.0
Scenario H–K	12.9	12.5	11.9	10.5	7.8

[1]The maximum damage metric value for the cockpit is 20; the maximum for all the remaining segments is 23. The damage score of 3 due to a fuselage break is assigned to the aft segment.

4.2.3.3 Damage dependence on design characteristics—RJ

The two design factors considered are wing configuration (high, low) and engine configuration. The aircraft in the study were predominately of the low-wing design; only 3 of 24 RJ mishaps were high-wing aircraft (all of these have wing-mounted engines). Of these three, one was in the overrun scenario (F), and two were in the compromised-landing scenario (G), both low-severity scenarios. Even limiting the comparison to just mishaps within these two scenarios, one finds that the median damage metric for the eight low-wing aircraft is 5 compared with a median damage metric of 9 for the three high-wing aircraft. Both of these are very low levels of damage (112 maximum) and do not represent potentially injurious crashes.

In a similar fashion with the engine configuration, the RJ dataset is dominated by tail-mounted engines. Only four of the aircraft in the RJ dataset had wing-mounted engines, and all four of these aircraft were involved in one of the two more benign scenarios (F and G). Two of the wing-mounted engine aircraft were involved in overruns (one of these was the only low-wing aircraft with wing-mounted engines), and two of the three compromised landings involved wing-mounted-engine aircraft. Comparing the median damage metric just within the two scenarios again reveals little difference due to the engine configuration. The 4 aircraft with wing-mounted-engines had a median damage metric equal to 7, whereas the 7 aircraft with tail-mounted engines had a median damage metric equal to 5. These values are low on the damage scale (112 maximum). All the aircraft in the more violent scenarios had tail-mounted engines.

The two design factors are not distributed homogeneously through the scenarios; therefore, general conclusions regarding the dependence of the damage outcome on the design factors cannot be drawn.

4.2.4 Evacuation Routes—RJ

All aircraft in the study were equipped with doors and most had supplementary exits. Any portal intended for occupants that is less than a floor-to-standing-height opening is considered an exit. The accident database contained information on the functionality and usability of the doors and exits. A door or exit is deemed functional if it is mechanically operational post-crash. A door or an exit is deemed usable if it is both functional and able to be used for egress. Therefore, a door that had fire beyond it or was blocked by terrain may have been functional, but was not usable for escape. Functionality or usability of all doors and exits was not reported (see table 62). In less-severe mishaps in which the evacuation was not an emergency, only one door may have been used and the others left unreported. The numbers provided are for the reported doors (see table 63) and exits (see table 64).

Table 62. Overall door and exit availability—RJ

(24 Aircraft)	Doors (#)	Exits (#)
Installed on mishap aircraft	51	52
Condition reported	31	16
Reported as functional	25	14
Reported as useable	25	13

Table 63. Post-crash door availability – RJ

Doors	Doors on Aircraft (average # / minimum #)	Functional Doors (average # / minimum #)	Usable Doors (average # / minimum #)
Scenario F	2.38 / 1.00	1.57 / 0.00	1.57 / 0.00
Scenario G	3.33 / 2.00	3.00 / 2.00	3.00 / 2.00
Scenario H	1.50 / 1.00	0.33 / 0.00	0.33 / 0.00
Scenario J	2.00 / 2.00	0.67 / 0.00	0.67 / 0.00
Scenario K	1.67 / 1.00	0.40 / 0.00	0.33 / 0.00
Scenario G–K	2.00 / 1.00	1.00 / 0.00	0.93 / 0.00

Table 64. Post-crash exit availability – RJ

Exits	Exits on Aircraft (Average #/ Minimum #)	Functional Exits (Average #/ Minimum #)	Usable Exits (Average #/ Minimum #)
Scenario F	1.75 / 0.00	1.33 / 0.00	1.13 / 0.00
Scenario G	3.00 / 2.00	2.00 / 2.00	2.00 / 2.00
Scenario H	1.50 / 1.00	0.33 / 0.00	0.33 / 0.00
Scenario J	2.00 / 2.00	2.00 / 2.00	2.00 / 2.00
Scenario K	2.67 / 2.00	0.25 / 0.00	0.25 / 0.00
Scenario G–K	2.27 / 1.00	0.67 / 0.00	0.67 / 0.00

At least two of the RJ events had post-crash fires, and consequently, the availability of escape routes is important. At Stord, Norway (20061010A), the aircraft went off the end of the runway, down a rocky slope, and caught fire. The impact of the cockpit with a boulder left only the rear door functional. Surviving occupants had to climb uphill over a severely disrupted floor (rolled slightly toward the port side), and they needed to use the twisted seats as hand-holds to reach the rear door; 10 of the 16 occupants were severely injured or killed. The four fatalities were the forward cabin attendant and three passengers seated forward along the right side of the plane. The pilots escaped through a cockpit hatch. Two of the passenger fatalities were reported to have been moving about during the evacuation. A queue was reported to get out of the one available exit. The last survivors out were more severely burned than the earlier ones. The accident at Brest (20030622A) also had a post-crash fire, but the only fatality was a pilot who died of trauma. All of the 21 passengers and the flight attendant exited through a hole left by the right service door being torn away. The last few passengers to escape were hampered by smoke. The hole left by the torn-away service door was the only usable exit. The boarding door was not functional, and the over-wing exits were blocked by fire. All of the remaining crashes caused fatalities by trauma; evacuation was not a factor.

Although several scenarios in both tables show zero as a minimum for available doors or exits, there were five mishaps with both zero doors and zero exits available: three of six in scenario K, and two of four in scenario H. In all these cases, the aircraft were destroyed. Only the Skopje

mishap (19930305A) had survivors (14/97). The report does not describe how the survivors escaped, but it does state that the only survivable volume was the left rear fuselage and that the remainder of the aircraft was torn apart, and much of it destroyed in post-crash fire. In as much as the right side of the fuselage was torn away, it can be inferred that the survivors were able to escape by stepping out of the wreckage. The few photographs in the report did not reproduce well.

4.2.5 Survivable Crashes—RJ

The rationale for identifying the crashes as survivable, partially survivable, or non-survivable was discussed previously in section 2 of this report. The method for determining survivability is the same for both the water mishaps and the RJ mishaps. The runway overrun crashes (scenario E) are excluded from this analysis, as there is generally just the longitudinal velocity, and the nature of the impacts are different from the impacts when the aircraft has been airborne.

The dataset includes ten mishaps: two mishaps were partially survivable, and eight mishaps were survivable. Two of four mishaps within scenario H were identified as non-survivable, and four of eight within scenario K were identified as non-survivable. Looking only at the vertical velocity (see figure 49), one of the partially survivable crashes occurred at the highest vertical velocity of the dataset, and the aircraft was inverted. The other was a very severe landing during which the aircraft was stalled above the runway and incurred a great deal of damage despite a low vertical velocity and airspeed. Therefore, on the airspeed plot (see figure 50), one of the partially survivable crashes was actually that with the lowest airspeed, and the other was a mid-value for airspeed but occurred with the aircraft inverted and at a high vertical velocity. The 90th percentile is marked for reference on each plot.

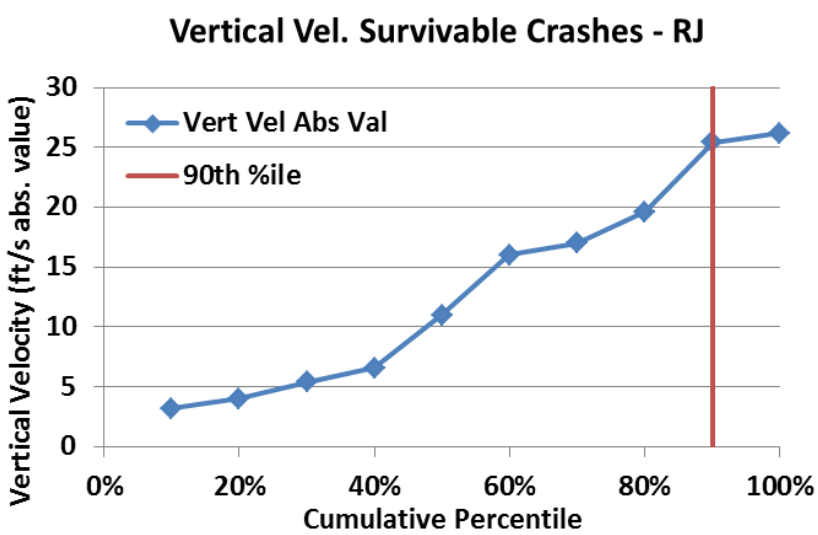

Figure 49. Cumulative vertical velocity survivable crashes—RJ

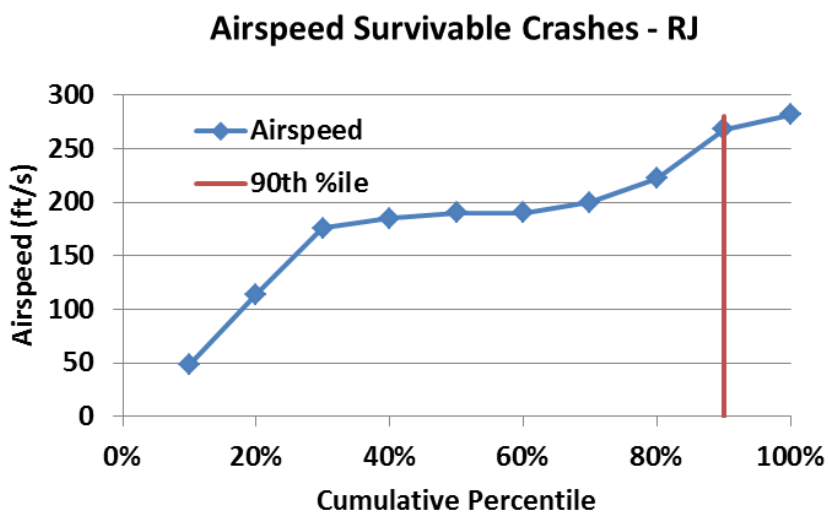

Figure 50. Cumulative airspeed survivable crashes—RJ

Using the 90th percentile as a reference for the two primary velocity directions, an estimate can be made of the 90th percentile survivable impact velocity. The 90th percentile velocities on each axis are used as the intercepts for the equation of an ellipse, which corresponds to the vector resultant for any combination of two velocities falling within the 90th percentile limits (see figure 51). All of the mishaps, which occurred from the air (scenarios G–K), are plotted as point pairs of the two velocities and labeled for their survivability rating. All but one of the non-survivable crashes falls outside the 90th percentile ellipse.

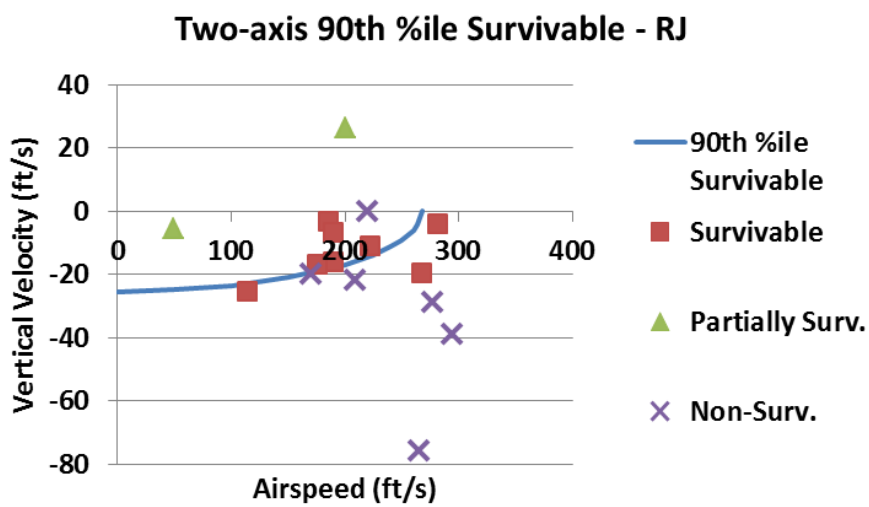

Figure 51. Two-axis velocity plot—RJ

4.2.6 Injury Analysis

In analyzing the injuries resulting from the mishaps in this study, the distribution of injuries among the different types of mishaps will be viewed. The injuries will be correlated with the kinematics and aircraft characteristics. The injuries for the entire aircraft will be viewed first, and then the injury fraction will be looked at by aircraft segment.

In many of the reports, minor injuries are treated in one category with non-injuries. In other reports, two separate counts are provided for minor and non-injury. Because numbers from the combined reports cannot be separated again, minor injuries and non-injuries are reported together for all mishaps. Less than 20% of all occupants were fatally injured (see table 65). Only 4% were seriously injured. The remaining 77% had either minor or no injuries.

Table 65. Number and severity of injuries—RJ

	Number of Occupants	Percent of Occupants
Fatally Injured	201	19
Severely Injured	46	4
Minor or Not Injured	810	77
Total Occupants	1,057	100

The overview for injuries in the RJ mishaps included in this study reveals that fatalities and serious injuries were confined to those mishaps occurring at extreme attitudes or on terrain away from the prepared surfaces around the airport. The fraction of fatalities and serious injuries in the overrun accidents (scenario F) was very low (see table 66). The fact that the median values for fatal and serious injuries are both 0 indicates that more than half of these accidents had no fatal or serious injuries. The 100% median value for minor/no injuries confirms this observation. The mishaps occurring from the air have higher injury rates, with most of the injuries concentrated in the most severe scenario, K. These injuries in scenario K raise the average values compared to near-zero median values for this subset of mishaps. Once again, the average values should add up to near 100%, but the median values need not.

Table 66. Injury rates—RJ

	Scenarios G–K Impact From Air (Median / Average)	Scenario F Overrun Impacts (Median / Average)
Fatal Injury (percent of all occupants)	2/37	0/3
Serious Injury (percent of all occupants)	0/8	0/5
Minor/No injury (percent of all occupants)	79/56	100/92
Total Occupants (#)	41/42	44/48
Number of Mishaps (#)	16	8

4.2.6.1 Injury dependence on velocity

The two-axis velocity plot can also be used to visualize the dependence of injuries on impact speeds (see figure 52). The plot displays all the mishaps in scenarios G–K. The fractions of serious plus fatal injuries for these mishaps fell in three clusters, as indicated in the figure legend. This plot shows no clear correlation between the two velocities and the injury fraction. Of seven mishaps with zero fraction of severe injuries, three occurred outside the 90th percentile ellipse and three more just inside it. Both of the mishaps with a 0–0.25 severe-injury fraction fell within the ellipse. Two accidents with high fractions were extreme cases, and one of these was inverted, so

at least these are consistent with expectation. Four of five mishaps with the severe fraction equal to 1 fell on or outside the ellipse, as would be expected.

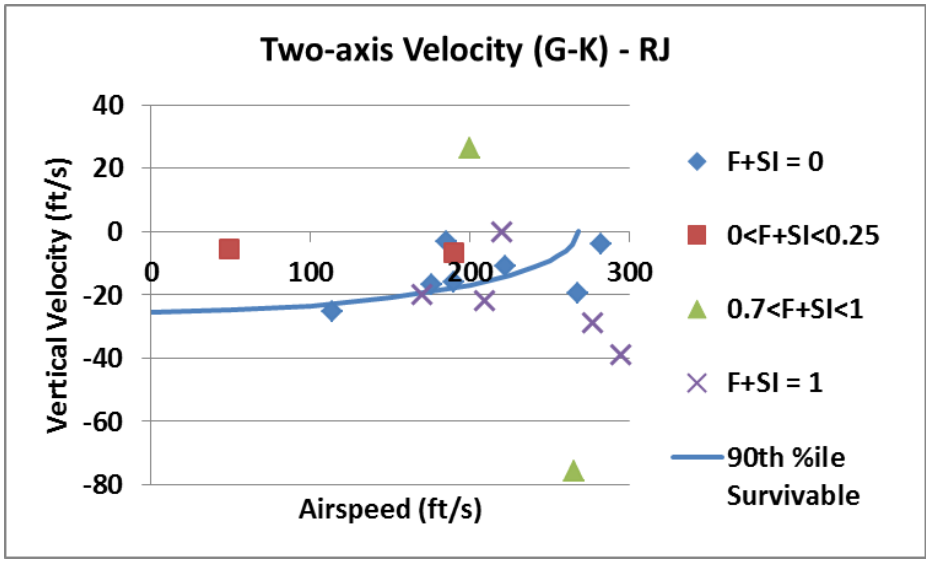

Figure 52. Flight mishap velocity—RJ

4.2.6.2 Injuries in each scenario and segment

Transport aircraft fuselages and cabins are not dimensionally isotropic. They have one long dimension (length) and two approximately equal dimensions (width and height). As a consequence of this dimensional difference, it is reasonable to expect that the impact conditions and, consequently, the injury outcomes may not be uniform throughout the aircraft. It is readily imagined that if an aircraft impacts nose downward, then the longitudinal deceleration forces experienced in the forward areas will be higher than those experienced in the rear, especially if there is crushing in the forward areas. Alternatively, if the aircraft impacts nose-high and then pivots downward about the tail, the vertical impact felt in the forward area may be significantly higher than experienced in the tail or even over-wing. The data have been grouped by segment and scenario to see what effect this anisotropy has on the injury distributions in aircraft (see table 67). For the purpose of this analysis, fatalities and serious injuries have been grouped together, and the percentage of all occupants that were either fatally or seriously injured is determined. From the values in table 67, the cockpit has a higher incidence of injuries. This effect is to be expected in scenario F (overruns), in which the velocities are low, and there may only be enough energy to damage the cockpit area. In scenario K, the loss of control on takeoff and the most violent scenario, the injuries are more uniformly distributed. The injury fractions for the tail segment represent a small sample of people, only 13 occupants in total. It should also be noted that 6 of the 24 mishaps had no information on the distribution of passengers, and 3 of these 6 mishaps with no information were in scenario H.

Table 67. Injuries by scenario and aircraft segment—RJ

	Cockpit (% of Occupants Fatal or Serious Injury)	Forward Cabin (% of Occupants Fatal or Serious Injury)	Over-wing Cabin (% of Occupants Fatal or Serious Injury)	Rear-cabin (% of Occupants Fatal or Serious Injury)	Tail (% of Occupants Fatal or Serious Injury)
Scenario F	14	2	2	2	25
Scenario G	0	0	0	0	0
Scenario H*	64	0	0	0	No occupants
Scenario J	13	28	0	0	No occupants
Scenario K	78	59	80	97	86
Scenarios G–K	51	35	33	33	67

*The locations for only 7 of the 34 injured occupants were known in scenario H. The 4 mishaps had a total of 85 occupants, resulting in a total injury fraction of 40%. Therefore, the injury fractions for the three cabins are likely understated. All injured persons were located in the other scenarios. The values in the table for scenario H are for just one mishap.

The group of mishaps identified as loss of control on takeoff (scenario K) contains most of the fatalities and serious injuries (see table 68). By comparing the number of fatalities occurring in each segment for the scenario K mishaps to those occurring in all mishaps, it is evident that virtually all of the fatalities occurred in the scenario K mishaps. Only the cockpit segment has several fatalities and serious injuries in mishaps outside of scenario K. The difference in serious injuries between scenario K and the rest of the mishaps in the forward cabin is all attributed to one scenario J mishap, which had a tree penetrate the forward cabin. Not all the fatalities are accounted for in the analysis by segment (see table 68). By looking at the total numbers of these severe injuries (see table 68), it can be determined that the locations for 26 fatalities and 2 serious injuries are not known. Consequently, the severe injuries in scenario H are distinctly undercounted in the segment-by-segment distribution.

Table 68. Severe injury by segment—RJ

	Cockpit	Forward Cabin	Overwing Cabin	Rear Cabin	Tail	Total {Total in Dataset}
Fatalities All Mishaps (#)	18	66	68	22	1	175 {201}
Fatalities Scenario K (#)	11	64	67	22	1	165 {166}
Serious Injuries All Mishaps (#)	7	11	8	12	6	44 {46}
Serious Injuries Scenario K (#)	3	2	7	10	4	26 {26}

4.2.6.3 Injuries related to kinematics

The first approach to looking for the relationships between injuries and the kinematic parameters is to plot the injuries versus parameters for each mishap. Because these mishaps have a wide range of occupant capacity and a wide range of load factors, it is necessary to use the fraction of individuals injured in each mishap, rather than the numbers. The data point for each mishap is coded through the legend to reveal with which scenario the mishap is associated (see figure 53). The reader can view the group of mishaps as a whole by simply looking at all the data points and ignoring the marker type. The injuries show no trend when plotted against the airspeed. The benign scenarios, overrun (scenario F)[5] and compromised landing (scenario G), have very few injuries, and these do not depend on airspeed. In fact, the only injury to occur in this group occurs in the lowest speed mishap. The most severe scenario, the loss of control on takeoff, contains four mishaps in which all were injured, one in which approximately 70% were injured, and one in which none were injured. The non-injury mishap is the second highest airspeed. In scenario H (landing short), there is a very rapid rise from no one injured to all injured. However, the circumstances of the mishap with no injuries are very different from those in which all were lost. The results are similar for the vertical velocity (see figure 54). In the benign scenarios, there are few injuries and, consequently, no trend. In the severe scenarios H and K, there is no uniform increase in the injury fraction as the velocity increases, although all perished in the highest velocity cases. The one positive vertical velocity was a case in which the plane impacted inverted. Even if one plots this point to the corresponding negative vertical velocity, it occurred at a slightly greater vertical velocity than a crash in which all passengers were lost.

[5] Scenario F includes the Skopje mishap, in which the aircraft went down a hillside and impacted a large rock outcrop after overrunning. The crash was followed by fire. Injuries were in the cabin; both pilots survived.

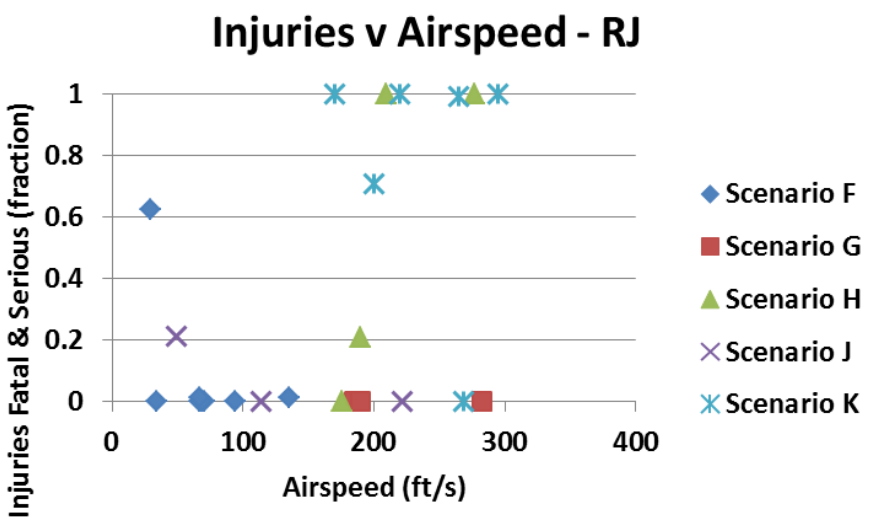

Figure 53. Injury fraction vs. airspeed—RJ

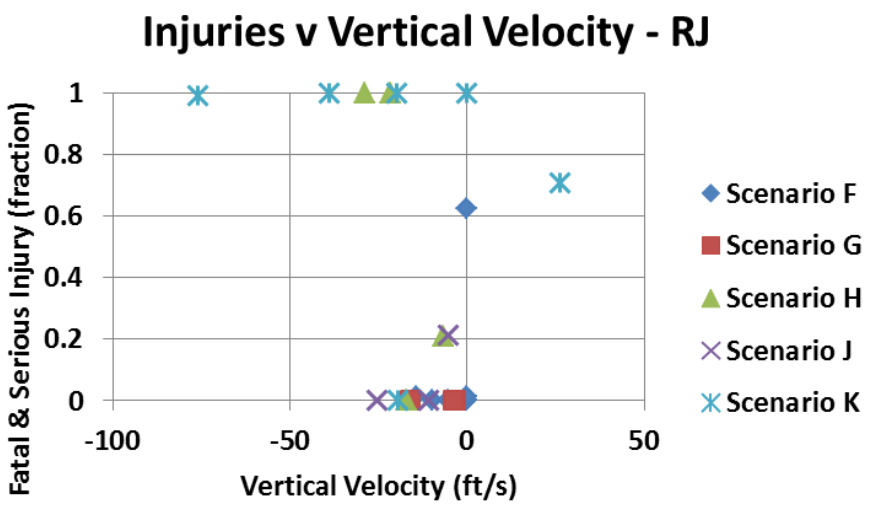

Figure 54. Injury fraction vs. vertical velocity—RJ

The injury fraction plotted against the flight-path angle (see figure 55) and pitch angle (see figure 56) parameters also reveal much scatter from any trend. One expects the injury fraction to increase as the flight path becomes steeper; however, the data include a totally fatal event at a very low flight-path angle. Even excluding the runway overruns (i.e., all zero flight-path angles), there is no clear trend to the data. For the pitch angle, one might expect that 0º pitch would represent a minimum in the injury fraction with injury rate increase, with nose pitched either more upward or more downward at impact.

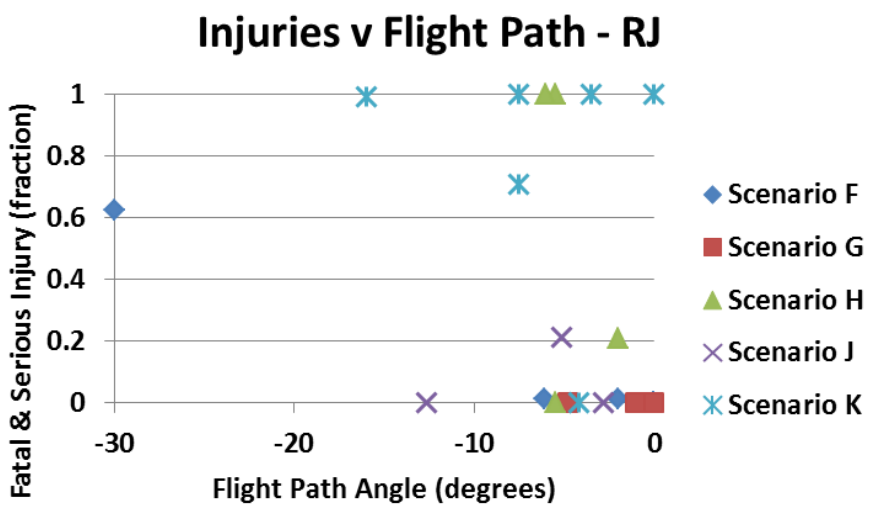

Figure 55. Injury fraction vs. flight path—RJ

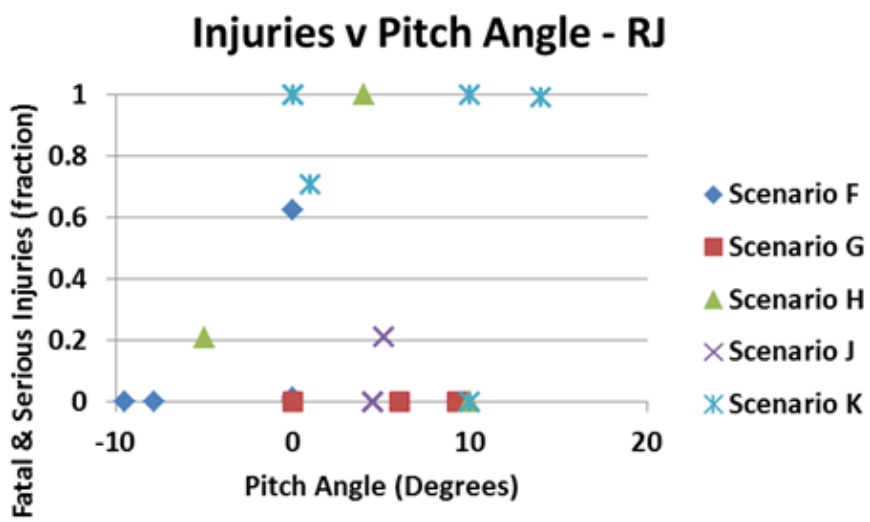

Figure 56. Injury fraction vs. pitch angle—RJ

4.2.6.4 Injuries related to design characteristics

The study of RJ mishaps by its nature comprises a set of aircraft with more homogeneous design features than the water study. The aircraft in this study include only two engine configurations and a far narrower range of weights and fuselage diameters. The design diversity represented in the data is very limited, consisting of just three high-wing aircraft with engines on the wings, and one low-wing aircraft with engines on the wing. The balance of the aircraft is low-wing with tail-mounted engines. The one low-wing aircraft with engines on the wing was involved in the Stord mishap, which was a singular event among the overruns in that the aircraft went down an embankment, and many of the injuries resulted from post-crash fire, compounded by evacuation difficulties. Because both the aircraft and the event are singular, it is risky to draw any conclusions. One of the other engine-on-wing aircraft was also involved in an overrun leaving only two engine-on-wing aircraft, both of which were in the relatively benign scenario G (compromised landing).

The injury data for the wing configurations are presented below (see table 69), as are the injury data for engine configuration (see table 70).

Table 69. Injuries related to wing configuration—RJ

Scenarios G–J	High-Wing Fatalities	Low-Wing Fatalities	High-Wing Serious Injuries	Low-Wing Serious Injuries
Median % occupants injured	0	0	0	0
Average % occupants injured	0	26	0	5
# of aircraft configuration in scenario (#G / #H / #J)	2/0/0	1/4 /3	2/0/0	1/4/3
Scenario K				
Median % occupants injured	No mishaps	69	No mishaps	6
Average % occupants injured	No mishaps	64	No mishaps	14
# of aircraft configuration in Scenario K	0	6	0	6

Table 70. Injuries related to engine configuration—RJ

Scenarios G–J	Engine on Wing Fatalities	Engine on Tail Fatalities	Engine on Wing Serious Injuries	Engine on Tail Serious Injuries
Median % occupants injured	0	0	0	0
Average % occupants injured	0	26	0	5
# of aircraft configuration in Scenario (#A / #B / #C)	2/0/0	1/4/3	2/0/0	1/4/3
Scenario K				
Median % occupants injured	No mishaps	69	No mishaps	8
Average % occupants injured	No mishaps	64	No mishaps	14
# of aircraft configuration in Scenario K (#)	0	6	0	6

4.2.6.5 Injury related to damage

The general trend is that as the aircraft damage metric increases, the fraction of the occupants experiencing severe injury (fatal or serious) also increases (see figure 57). The overrun scenario F has just one mishap with a non-zero injury fraction, and this same mishap has the highest damage metric in the group of mishaps. The injury fraction looks higher than the trend, but this mishap is the Stord mishap in which the aircraft went down an embankment and had a post-crash fire. The number of severe injuries was increased by the consequences of the fire. The impacting short of landing (scenario H) is the second most severe, and likewise, follows the trend. The loss of control on takeoff (scenario K) is the most severe, and the injury fraction follows the general trend. A trend line has been fitted to the scenario K data to illustrate the trend. It is evident that the slope for this line would be close to one fitted to the scenario H data.

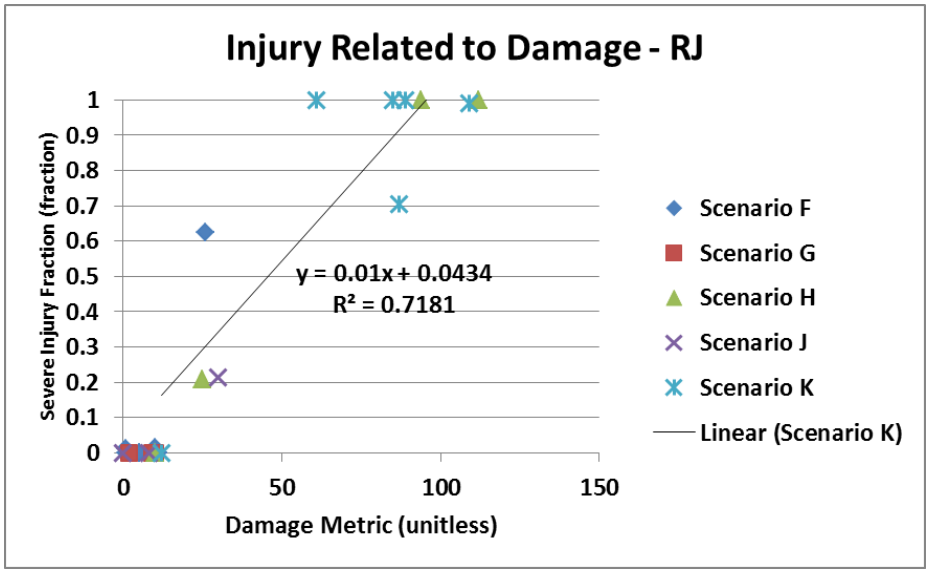

Figure 57. Injury related to damage—RJ

4.2.6.6 Injury binary logistic regression analysis—RJ

The binary logistic approach interprets the injury data as having just one of two outcomes for each occupant: severe injury (fatal or serious) or no injury (including minor injury). In this view, the expectation is that for each parameter the fraction of severe injuries will be low (near zero) for low values of the parameter, and the severe-injury fraction will increase to the limit value of one as the value of the parameter increases. For example, it is expected that the fraction of severe injuries will increase as the impact velocity increases. For details of the analysis, see section 2 of this report. The equation that the logistic regression fits assumes that the dependence on the parameter is linear. Therefore, the equation being fitted is an exponential with a linear form to the exponent. The output variable *p* is the estimated probability that an occupant in a similar crash scenario will be severely injured. For an *n*-parameter model, the equation contains one constant and *n* coefficients (see equation 7). The linear form of the equation is:

$$p = \frac{1}{1 + e^{-(\beta_0 + \beta_1 x)}} \tag{7}$$

In the following discussion, one evaluation of the BLM is purely qualitative. This subjective evaluation by the author is in regard to the direction of the trend predicted by the model. The model predicted trend is either intuitive (i.e., the trend expected by the author) or counterintuitive (i.e., opposite the trend expected by the author).

For the RJ study, single-parameter models were generated for the set of mishaps in the group of scenarios G–K (see table 71), all the scenarios that were not runway overruns. For the most part, these events occurred with the aircraft coming from the air to land or having just become airborne. The *p*-value of the coefficient (see columns 2 and 3 of table 71) indicates whether the coefficient is likely to have a non-zero value. If the *p*-value is less than or equal to 0.100, then the coefficient's value is likely a meaningful number. Only two of the single-parameter models have strong

predictive capability—lateral and longitudinal peak deceleration (see table 71, last two rows). Within the range of input data, the model can be used to predict the severe-injury fraction for future mishaps using the coefficients listed (see table 72). However, the reader must be cautious in so doing, because the goodness-of-fit statistics indicate a general lack of fit for these models.

Table 71. Binary regression on scenarios G–K—RJ

Parameter (Mishaps/ Occupants)	Constant Coefficient (*p*-value & coeff. Value)	Regressor Coefficient (*p*-value & coeff. Value)	Goodness-of-Fit (*p*-value)	Summary Measures of Assoc.	Trend: Intuitive or Counter	Predictive Capability
Airspeed (16/672)	$p \leq 0.000$ -3.567	$p \leq 0.000$ 0.014	0.000 0.000 0.000	0.41 0.42 0.19	Intuitive	Low – moderate
Vertical velocity (16/672)	$p \leq 0.000$ -1.224.	$p \leq 0.000$ -0.030	0.000 0.000 0.000	0.19 0.19 0.09	Intuitive	Low
Flight path (16/672)	$p \leq 0.000$ -1.772	$p \leq 0.000$ -0.184	0.000 0.000 0.000	0.46 0.49 0.21	Intuitive	Moderate
Pitch (15/661)	$p \leq 0.000$ -0.973	$p = 0.002$ +0.0491	0.000 0.000 0.000	0.11 0.12 0.05	Intuitive	Low
Roll (16/672)	$p \leq 0.000$ -1.495	$p \leq 0.000$ +0.0339	0.000 0.000 0.000	0.42 0.48 0.19	Intuitive	Moderate
Yaw (15/618)	$p \leq 0.000$ -0.989	$p \leq 0.000$ +0.0722	0.000 0.000 0.000	0.23 0.31 0.11	Intuitive	Low-Moderate
Vertical peak deceleration (14/611)	$p \leq 0.000$ -1.460	$p \leq 0.000$ +0.0633	0.000 0.000 0.000	0.47 0.48 0.19	Intuitive*	Moderate
Lateral peak deceleration (12/525)	$p \leq 0.000$ -4.982	$p \leq 0.000$ +0.664	0.000 0.000 0.000	0.93 0.96 0.41	Intuitive	Strong
Longitudinal peak deceleration (14/611)	$p \leq 0.000$ -3.209	$p \leq 0.000$ -0.366	0.000 0.000 0.000	0.93 0.94 0.38	Intuitive	Strong

*One crash was inverted with a high value of the opposite sign. The injury rate would be expected to increase with greater values of peak deceleration on either side of zero.

Table 72. Scenarios G–K predictive single-parameter models—RJ

Input Parameter	Range (G)	Constant Coefficient	Regressor Coefficient
Peak lateral deceleration	0 to 35.7 (absolute value)	-4.98	+0.664
Peak longitudinal deceleration	0 to -155	-3.21	-0.366

The plot of the airspeed BLM (see figure 58) is representative of most of the single kinematic models that have weak predictive capability. The trend is correct, but the data scatter is severe. The plots for the two models that show strong predictive capability (see figures 59–60) exhibit far less variation of the observations from the model.

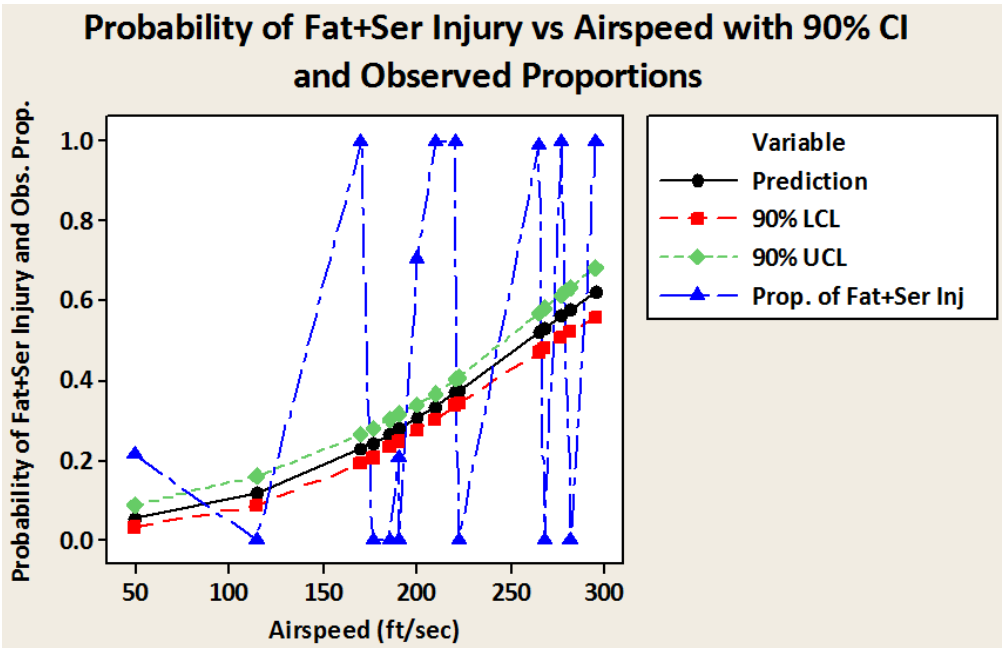

Prop. = Proportions

Figure 58. Airspeed BLM for scenarios G–K—RJ

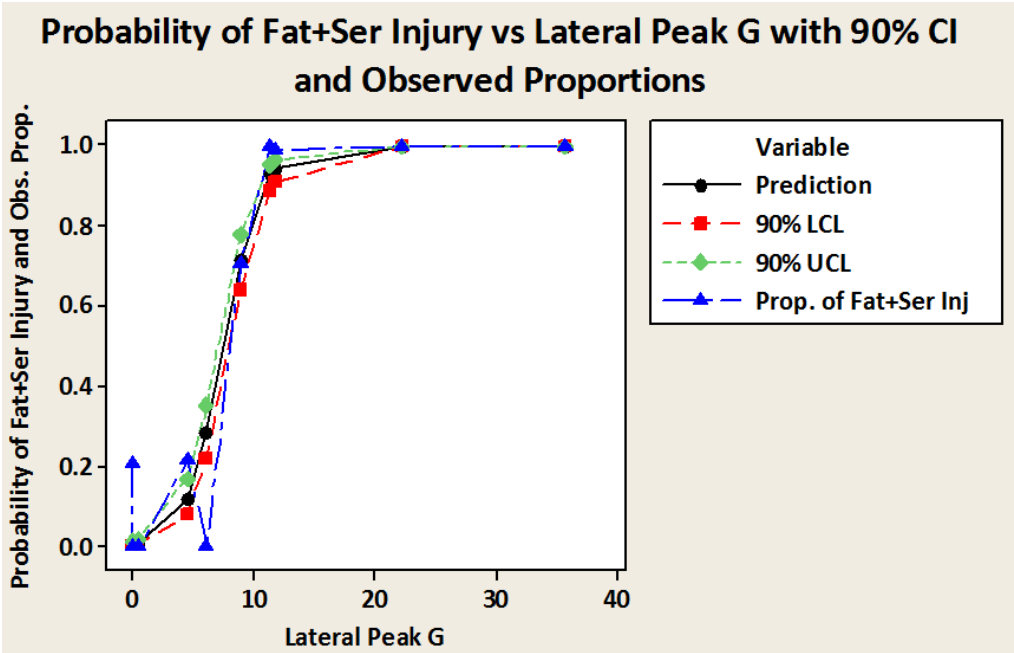

Figure 59. Lateral deceleration BLM for scenarios G–K—RJ

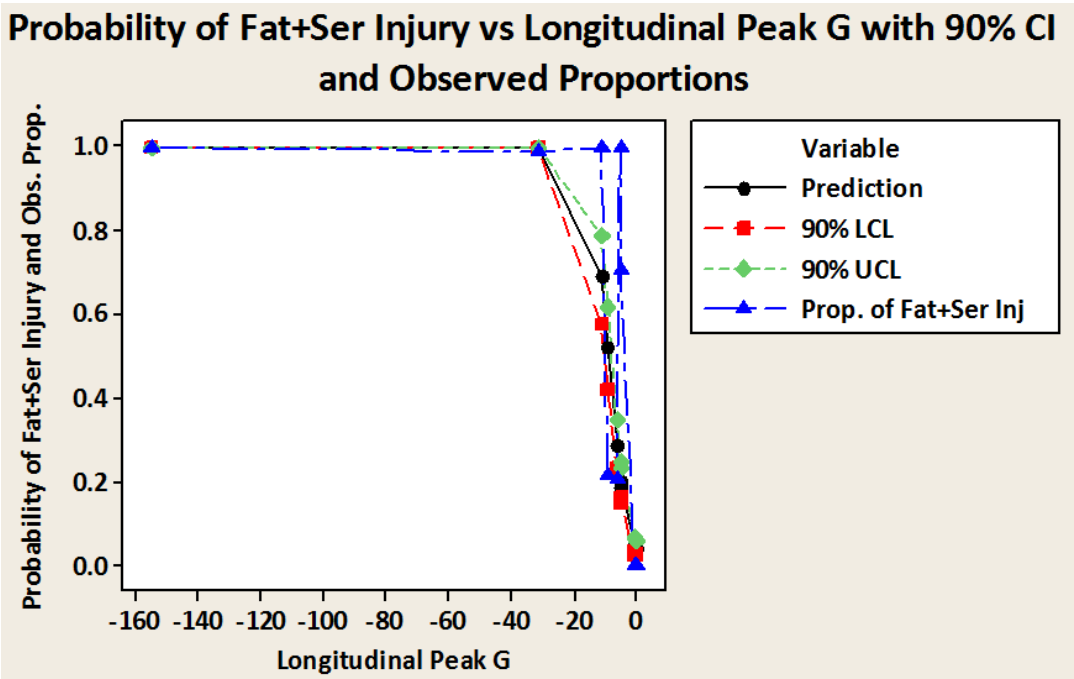

Figure 60. Longitudinal deceleration BLM for scenarios G–K—RJ

A multi-parameter model was also created using this dataset. The software indicated that the parameter airspeed, vertical velocity, flight path, pitch angle, roll angle, and yaw angle would have non-zero coefficients. The goodness-of-fit metrics had all low *p*-values (0.000, 0.000, and 0.040).

However, the summary measures of association were all strong or moderate (0.98, 0.99, 0.46), which indicates a strong predictive capability. The equation for this model is given by:

$$\hat{p} = \frac{1}{1+e^{-(-44.6812+0.212378x_1-0.965525x_2+7.79568x_3-2.47599x_4+0.620787x_5+3.00973x_6)}} \qquad (8)$$

The model's predictive capability is limited to the range of each input parameter. These limits together with the parameter coefficients are described below (see table 73). Because the multi-parameter BLM has six input parameters, a seven-dimensional plot would be required to demonstrate its output. Lacking the ability to present a seven-dimensional plot on this two-dimensional interface, an alternate presentation is offered (see figure 61). The observed value of the severe-injury fraction is plotted along the *x*-axis, and the model predicted value is plotted along the *y*-axis; perfect predictions will fall on a line connecting (0,0) to (1,1). In several cases, the model makes good predictions, but in two cases, it predicts no severe injuries, when, in fact, each is a highly injurious event.

Table 73. G–K multi-parameter model—RJ

Parameter	Coefficient	Valid Input Range	Units
Constant	-44.7	All	
Airspeed	+0.212	49 to 295	ft/s
Vertical velocity	-0.966	+26.2 to -75.9	ft/s
Flight-path angle	+7.80	0 to-16.0	Degrees
Pitch angle	-2.48	-5 to +14	Degrees
Roll angle (absolute value)	+0.62	0 to 144	Degrees
Yaw angle (absolute value)	+3.01	0 to 60	Degrees

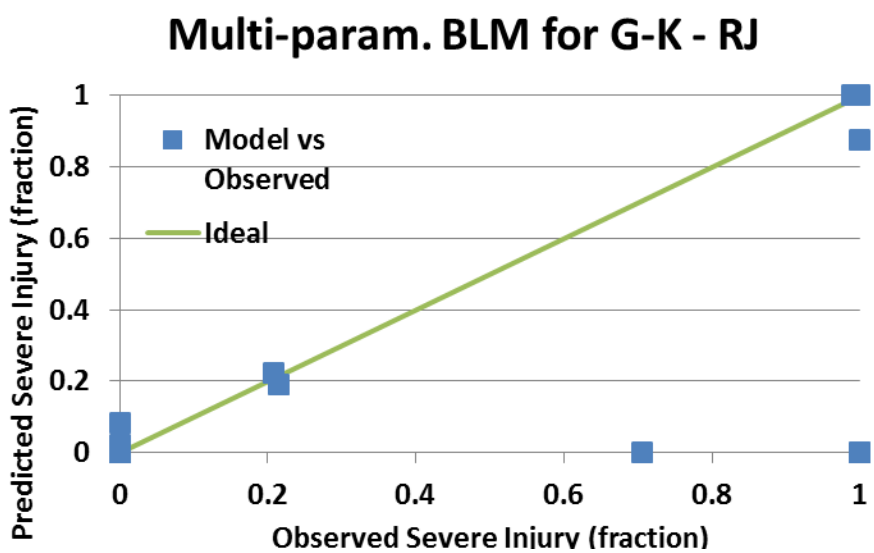

Figure 61. Multi-parameter BLM scenarios G–K—RJ

Scenario K (loss of control during takeoff) has a wide range in values for the parameters and high values for the severe injury probability. Consequently, single-parameter models (see table 74) were attempted for this scenario and a multi-parameter model. The details for the two models with high predictive capability are provided in table 75. This model uses data from six mishaps and includes the outcomes for 262 occupants.

Table 74. Single-parameter BLMs for scenario K—RJ

Parameter	Constant Coefficient (*p*-value & coeff. value)	Regressor Coefficient (*p*-value & coeff. value)	Goodness-of-Fit (*p*-value)	Summary Measures of Assoc.	Trend: Intuitive or Counter	Predictive Capability
Airspeed	$p \leq 0.000$ +5.001	$p=0.002$ -0.0161	0.000 0.000 0.000	0.56 0.59 0.22	Counter Intuitive	Moderate
Vertical velocity	$p \leq 0.000$ +0.646	$p \leq 0.000$ -0.0163	0.000 0.000 0.000	0.23 0.25 0.09	Intuitive	Low to moderate
Vertical peak deceleration	$p \leq 0.000$ +0.550	$p \leq 0.000$ +0.0298	0.000 0.000 0.000	0.54 0.57 0.24	Intuitive	Moderate
Lateral peak deceleration	$p=0.001$ -10.70	$p \leq 0.000$ +1.301	0.949 0.905 0.989	0.68 0.95 0.13	Intuitive	High
Longitudinal peak deceleration	$p \leq 0.000$ -2.302	$p \leq 0.000$ -0.571	0.000 0.000 0.004	0.93 0.99 0.41	Intuitive	Moderate to good

Table 75. Scenario K, predictive single-parameter BLMs—RJ

Input Parameter	Range (G)	Constant Coefficient	Regressor Coefficient
Peak lateral deceleration	8.9 to 35.7 (absolute value)	-10.7	+1.30
Peak longitudinal deceleration	-0.25 to -31.2	-2.30	-0.571

Two reduced multi-parameter models were also attempted with the scenario K data. In the first model, only two parameters are used: the airspeed and the vertical velocity. This first reduced model uses all six mishaps in scenario K and includes the 262 occupants. The statistical metrics (see table 76) and the model coefficients and usable parameter ranges are also provided (see table 77). In the other model, the statistical metrics (see table 78) and the model coefficients and usable parameter ranges are also provided (see table 79). In table 78, the vertical peak deceleration parameter is added to make 3 input parameters, but this model necessitated dropping 1 mishap because of a missing datum; dropping the 1 mishap means the remaining 5 mishaps cover 212 occupants.

Table 76. Scenario K, 2-parameter BLM metrics—RJ

Parameter	Constant Coefficient (*p*-value & coeff. value)	Regressor Coefficient (*p*-value & coeff. value)	Goodness-of-Fit (*p*-value)	Summary Measures of Assoc.	Predictive Capability
Airspeed	$p \leq 0.000$ +37.567	$p \leq 0.000$ -0.160	0.000 0.000 0.000	0.88 0.92 0.34	Moderate to Good
Vertical velocity		$p \leq 0.000$ -0.179	NA	NA	NA

Table 77. Scenario K, 2-parameter BLM coefficients—RJ

Parameter	Coefficient	Valid Input Range	Units
Constant	37.6	All	Unitless
Airspeed	-0.160	170 to 295	Ft/s
Vertical Velocity	-0.179	-75.9 to +26.2	Ft/s

Table 78. Scenario K, 3-parameter BLM metrics—RJ

Parameter	Constant Coefficient (*p*-value & coeff. value)	Regressor Coefficient (*p*-value & coeff. value)	Goodness-of-Fit (*p*-value)	Summary Measures of Assoc.	Predictive Capability
Airspeed	$p \leq 0.000$ +21.499	$p \leq 0.000$ -0.124	0.000 0.000 0.061	0.91 0.97 0.40	Moderate to Good
Vertical velocity		$p \leq 0.000$ -0.508	NA	NA	NA
Peak vertical deceleration		$p \leq 0.000$ -0.550	NA	NA	NA

Table 79. Scenario K, 3-parameter BLM coefficients—RJ

Parameter	Coefficient	Valid Input Range	Units
Constant	+21.5	All	Unitless
Airspeed	-0.124	170 to 295	Ft/s
Vertical velocity	-0.508	-75.9 to 26.2	Ft/s
Peak vertical deceleration	-0.550	-31.9 to +32.3	G

4.2.7 Summary of Binary Logistic Regression Analysis

The experiment to fit binary regression models to the RJ mishap data has produced only a few strongly predictive relationships. Ideally, the transition from mishaps with low-injury fractions to mishaps with high-injury fractions would occur over a narrow range in values for some if not all kinematic parameters. When a narrow transition occurs, one is justified in selecting a value near that range for design guidance. The expectation in creating these models was to understand the dependence of severe injury on the various kinematic parameters and, therefore, be able to use these models to assist in selecting test conditions for crashworthiness testing or to select values for design guidance.

For the group of mishaps (scenarios G–K), excluding the runway overruns, only two parameters were strongly predictive: lateral and longitudinal peak decelerations. These two parameters showed the desired narrow transition from low to high severe-injury fraction and, therefore, may be useful for defining design guidelines. Although the single-parameter velocity models were not predictive, the multi-parameter model may add value because it includes both velocities. The multi-parameter model includes airspeed, vertical velocity, flight-path angle, pitch angle, roll angle, and yaw angle as inputs. Although it under-predicts the injury probability in two of the five severe input cases, the model is capable of predicting across the entire spectrum of output fractions. The multi-parameter model used in conjunction with the two single-parameter models may be useful for setting either test conditions or design guidelines. An additional positive aspect is that the input variables generally have wide usable ranges.

Because the most severe accidents were those in loss-of-control scenario K, this group of mishaps was considered as a separate dataset. The same two parameters—peak lateral and peak longitudinal deceleration—produced predictive single-parameter models. The multi-parameter model for the scenario K dataset alone was less successful than the one for scenarios G–K. Two models were actually created. In the first model, only the airspeed and the vertical velocity were included. This model produced only moderate-to-good prediction capability, but the model does include arguably the most important parameters for defining a drop test, with flight-path angle fixed by the ratio of the two velocities. By dropping one mishap, this first model could be expanded to include peak vertical deceleration as a third parameter. These three parameters combined can be used to set a target test condition that includes the peak deceleration, at least in the vertical direction.

4.3 TASK 2 – SUMMARY CONCLUSIONS

The relative frequency of event types, as described by the scenarios in this study, closely reflects the frequency with which the mishap types occur in a much larger population of accidents.

Two scenarios, landing short (scenario J) and loss of control on takeoff (scenario K), accounted for all of the fuselage breaks and averaged more than one break per aircraft. The mishaps in these same two scenarios accounted for 98% of the fatalities in the study and 65% of the serious injuries.

Little could be concluded about the influence of design characteristics on injury outcome. The study was dominated by the low-wing, tail-mounted engine configuration. Further, the exceptional aircraft were involved in the non-injurious mishap scenarios.

In two cases of post-crash fire, egress was critical. In one mishap, the service door was torn away by impact, and everyone on board, except the pilots, exited through the resulting hole. In the other escape-critical mishap, only one door was available at the rear, and it was difficult to use for multiple reasons. The limited ability to use this escape route directly affected the number and severity of injuries.

The identification of survivable crashes and the plotting of their cumulative velocities had limited use. A 90th percentile limit was established for airspeed and vertical velocity; however, when the mishaps were plotted using their velocities and coded to show their severe-injury fraction, the result was not the expected uniform increase in severe-injury fraction with increasing velocity that was expected.

Only the multi-parameter binary logistic regression models were practically predictive and potentially useful. The model using scenario K data, which takes into account most of the fatalities and more than half of the serious injuries, is likely to be of the greatest benefit.

5. REFERENCES

1. Cress, J., Vortechs Helicopter Analytics, Prunedale, CA.

2. Etkin, B., Reid, L. D. (1995). Chapter 4, General equations of unsteady motion. In *Dynamics of flight* (93–128), Hoboken, NJ; John Wiley & Sons.

3. Turnbow, J. W., *Summary of equations of motion for several pulse shapes*, International Center for Safety Education, Chapter 14: Appendix, 19–42.

4. Aviation Safety Network (February 10, 2017). Retrieved from http://aviation-safety.net/database.

5. Ditching, 14 CFR 25.801 (1990).

APPENDIX A—LIST OF DATA FIELDS FOR WATER MISHAP STUDY

Following is a list of the fields of data extracted from the Cabin Safety Technical Research Group (CSTRG) database for the water mishap study. The data were extracted using a feature of the database known as Export Wizard, which allows data from a list of mishaps to be exported in various formats. A list of mishap identification numbers was prepared that included the IDs for all of the mishaps that had been selected for the study. The Export Wizard presents a list of fields, each with a selectable box. By ticking the boxes, data for those fields would be extracted and exported in a Microsoft® Excel® format with the data fields becoming column headers and the mishap IDs labeling the rows. Each exported dataset went to a new Excel worksheet. The data were divided into four work sheets: Mishap Data, Kinematics, Damage, and Injury. In the initial export, the mishaps were in the datasheet in reverse chronological order (most recent first). After the analysis began and the mishaps were divided into scenarios, each worksheet was copied and sorted by scenario. As the analysis began, various computations were made, and logical operations were applied, new columns were added to contain the results of the analysis.

List of Database Fields for Export from CSTRG used to generate the data for the water mishap study.

"Column" refers to the column in the worksheet as queried, and "Field Name" is the field name as it appears on the Export Wizard page. Other columns were inserted during the analysis.

Task 1 Mishap Data Query Fields:

Col.	Field Name	Explanation
A	REF	Identification date: YEARMOnthDAyL (L=sequence letter)
B	NICKNAME	Typically place & plane type
C	AC_TYPE	Aircraft type
D	NO_ENGS	Number of engines
E	ENG_CONFIG	Position of engines: wings, tail, fin
F	ENG_TYPE	Turbojet, turboprop, reciprocating
G	WT_CAT	Weight category A, B, C
H	HW_LW	Wing configuration, high or low
I	IMAX_SPR	Maximum number seats between aisles; modified in study to be maximum number of seats across the airplane
J	NUM_SEATS	Total number of passenger seats
K	DATE	Date of mishap
L	ACC_REPORT	Accident report published, Y/N
M	IMPACT_REL	Impact related, Y/N
N	FUSE_RUPT	Fuselage ruptured, Y/N
O	RWAY_VICTY	Mishap occurred near airport, Y/N
P	OVERRUN	Aircraft overran the runway, Y/N
Q	AC_DAMAGE	Severity of damage: destroyed, substantial, minor, none
R	OCC_INJS	Occupants injured, Y/N
S	FAT_CREW	Fatalities in crew, number
T	FAT_TOTAL	Total fatalities on board, number
U	SER_TOT	Total serious injuries on board, number

V	MN_CREW	Crew with minor or no injury, number
W	MN_TOT	Total on board with minor or no injury, number
X	EVACUATION	Was the evacuation an emergency? Y/N
Y	AC_WATER	Did aircraft come to rest in water? Y/N
Z	PRE_DITCH	Was the ditching Premeditated? Y/N
AA	DAM_WATER	Was the pressure hull penetrated by water impact? Y/N
AB	DAM_GROUND	Was the pressure hull penetrated by ground impact? Y/N
AC	DIST_SHORE	Approximate distance from aircraft to shore. Miles
AD	STOW_DET	Overhead stowage detached Y/N.

Task 1 Kinematics Query Fields:

Col.	Field Name	Explanation
A	REF	Identification date: YEARMODA (sequence letter)
B	NICKNAME	Typically place & plane type
C	AC_TYPE	Aircraft type
D	DATE	Date of the mishap
E	G_VERT	Peak ‘G’ level vertical, # of G’s.
F	G_LAT	Peak ‘G’ level lateral, # of G’s.
G	G_LONG	Peak ‘G’ level longitudinal, # of G’s.

Task 1 Damage Data Query Fields:

Col.	Field Name	Explanation
A	REF	Identification date: YEARMODA (sequence letter)
B	NICKNAME	Typically place & plane type
C	AC_TYPE	Aircraft type
D	DATE	Date of the mishap
E	FUSE_RUPT	Fuselage ruptured, Y/N
F	DAM_WATER	Was the pressure hull penetrated by water impact? Y/N
G	DAM_GROUND	Was the pressure hull penetrated by ground impact? Y/N
H	STOW_DET	Percent of overhead stowage detached
I	STOW_NRET	Percent of cabin baggage not retained
J	STOW	D uncontained, Retained, No overhead stowage fitted
K	BULKHEADS	Disrupted, Retained, No bulkhead fitted
L	FLOOR_F	Floor disrupted, Y/N
M	SEAT_F	Seat disrupted, Y/N

Task 1 Injury Data Query Fields:

Col.	Field Name	Explanation
A	REF	Identification date: YEARMODA (sequence letter)
B	NICKNAME	Typically place & plane type
C	AC_TYPE	Aircraft type
D	DATE	
E	TOT_ABORD	Total people aboard, number
F	FAT_CREW	Fatally injured crew, number
G	FAT_PAX	Fatally injured passengers, number
H	FAT_TOT	Fatally injured total, number
I	SER_CREW	Seriously injured crew, number

J	SER_PAX	Seriously injured passengers, number
K	SER_TOT	Seriously injured total, number
L	MN_CREW	Minor/no injury crew, number
M	MN_PAX	Minor/no injury passengers, number
N	MN_TOT	Minor/no injury total, number
O	PAX_TOT	Passengers, number
P	CREW_TOT	Crew, number

APPENDIX B—LIST OF DATA FIELDS FOR REGIONAL JET MISHAP STUDY

List of Column Headers and Meanings by worksheet. This appendix includes the fields of data exported from the Cabin Safety Technical Research Group database and fields added during the Task 2 analysis. Not all of the added fields are listed here, as some were created simply to arrange data conveniently for plotting or for preparing tables. As with the Task 1 analysis, each worksheet had two versions: one with the mishaps ordered chronologically, and the second created after each mishap had been assigned to a scenario. The columns listed below may not be the same for both versions of the worksheet.

Task 2 Mishap Data Fields for Mishap Data worksheet.

Col.	Header	Explanation
A	REF	Identification date: YEARMOnthDAyL (L=sequence letter)
B	NICKNAME	Typically place & plane type
C	AC_TYPE	Aircraft type
D	Scenario	A-E mishap assignment to one of five types
E	NO_ENGS	Number of engines
F	ENG_CONFIG	Position of engines: wings, tail, fin
G	ENG_TYPE	Turbojet, turboprop, reciprocating
H	WT_CAT	Weight category A, B, C
I	HW_LW	Wing configuration, high or low
J	MAX_SPR	Maximum number seats between aisles; modified in study to be maximum number of seats across the airplane
K	NUM_SEATS	Total number of passenger seats
L	DATE	Date of mishap
M	ACC_REPORT	Accident report published, Y/N.
N	IMPACT_REL	Impact related, Y/N
O	FUSE_RUPT	Fuselage ruptured, Y/N
P	PHASE_FLT	Phase of flight during which mishap initiated
Q	OVERRUN	Mishap involved runway overrun Y/N
R	AC_DAMAGE	Severity of damage: destroyed, substantial, minor, none
S	OCC_INJS	Occupants injured, Y/N
T	FAT_CREW	Fatalities in crew, number
U	FAT_TOT	Total fatalities on board, number
V	SER_TOT	Total serious injuries on board, number
W	MN_CREW	Crew with minor or no injury, number
X	MN_TOT	Total on board with minor or no injury, number
Y	EVACUATION	Was the evacuation an emergency, Y/N
Z	AC_WATER	Did aircraft come to rest in water, Y/N
AA	PRE_DITCH	Was the ditching premeditated? Y/N
AB	DAM_WATER	Was the pressure hull penetrated by water impact? Y/N
AC	DAM_GROUND	Was the pressure hull penetrated by ground impact? Y/N
AD	DIST_SHORE	Approximate distance from aircraft to shore; miles
AE	STOW_DET	Overhead stowage clarify.
AF	Recon Compl?	Reconstruction of kinematics completed? Y/N

Task 2 Kinematics Data Fields for Kinematics Data worksheet

Col.	Header	Explanation
A	Reference #	Identification date: YEARMOnthDAyL (L=sequence letter)
B	Nickname	Typically place & plane type
C	Aircraft Type	Aircraft type
D	Date	Date of mishap
E	Scenario	A-E mishap assignment to one of five types
F	Pk G Vert	Peak vertical deceleration aircraft ref. frame (G)
G	Pk G Lat	Peak lateral deceleration aircraft ref. frame (G)
H	Pk G Long	Peak longitudinal deceleration aircraft ref. frame (G)
I	Vert Vel	Vertical velocity in earth reference frame
J	Airspeed	Airspeed speed along the flight path
K	Flt Path	Angle between horizon and velocity vector of c.g.
L	Pitch	Aircraft pitch angle
M	Roll	Aircraft roll angle to horizon
N	Yaw	Aircraft yaw angle to flight path
O	Thrust	At least one engine operating at water impact Y/N
P	P-FP	Pitch angle—flight-path angle
Q	HW_LW	Wing configuration high or low
r	lw vert vel.	Vertical velocity for each low-wing aircraft
S	HW Vert Vel	Vertical velocity for each high-wing aircraft

Task 2 Damage Data Fields for Damage Data Worksheet

Col.	Header	Explanation
A	Reference #	Identification date: YEARMOnthDAyL (L=sequence letter)
B	Nickname	Typically place & plane type
C	Aircraft Type	Aircraft type
D	Date	Date of mishap
E	Scenario	A-E mishap assignment to one of five types
F	FUSE_RUPT	Fuselage ruptured, Y/N
G	DAM_WATER	Was the pressure hull penetrated by water impact? Y/N
H	DAM_GROUND	Was the pressure hull penetrated by ground impact? Y/N
I	STOW_DET	Overhead stowage detached Y/N
J	STOW_NRET	Percent of cabin baggage not retained
K	STOW	D uncontained, retained, no overhead stowage fitted.
L	BULKHEADS	Disrupted, retained, no bulkhead fitted
M	FLOOR_Failure	Floor disrupted, Y/N associated with loss of occupied volume
N	SEAT_Failure	Seat disrupted, Y/N associated with restraint chain failure
O	C-LofV	Cockpit Loss of Volume Widespread /Local /None
P	FC-LofV	Forward cabin loss of volume W/L/N
Q	OW-LofV	Overwing cabin loss of volume W/L/N
R	RC-LofV	Rear cabin loss of volume W/L/N
S	T-LofV	Tail loss of volume W/L/N
T	C-Fl Dis	Cockpit floor disruption W/L/N
U	FC-Fl Dis	Forward cabin floor disruption W/L/N
V	OW-Fl Dis	Overwing cabin floor disruption W/L/N
W	RC-Fl Dis	Rear cabin floor disruption W/L/N
X	T-Fl Dis	Tail floor disruption W/L/N

Y	C-Seat Fail	Cockpit segment seat failure W-L-N
Z	FC-Seat F	Forward cabin seat failure W-L-N
AA	OW-Seat Fail	Overwing cabin seat failure W-L-N
AB	RC-Seat Fail	Rear cabin seat failure W-L-N
AC	T-Seat Fail	Tail seat failure W-L-N
AD	C-Skin Dmg Wtr	Cockpit segment underside skin damage by water impact W-L-N
AE	FC-Skin Dmg Wtr	Forward cabin underside skin damage by water impact W-L-N
AF	OW-Skin Dmg Wtr	Overwing cabin underside skin damage by water impact W-L-N
AG	RC-Skin Dmg Wtr	Rear cabin underside skin damage by water impact W-L-N
AH	T-Skin Dmg Wtr	Tail underside skin damage by water impact W-L-N
AI	Doors-Frac of Reprtd	Fraction of doors whose functionality is reported
AJ	Exits- Frac of Reprtd	Fraction of exits whose functionality is reported
AK	Doors- Frac of All Usab	Fraction of all doors usable after impact
AL	Exits- Frac of All Usab	Fraction of all exits usable after impact
AM	Doors-Frac of All Func	Doors fraction of all usable as escape path
AN	Exits-Frac of All Func	Exits fraction of all usable as escape path
AO	Fuse Brk C-FC	Fuselage break between cockpit & forward cabin Y/N
AP	Fuse Brk FC-OW	Fuselage break between forward cabin & overwing Y/N
AQ	Fuse Brk OW-RC	Fuselage break between overwing & rear cabin Y/N
AR	Fuse Brk RC-T	Fuselage break between rear cabin & tail Y/N
AS	Gear	Landing gear Up or Down
AT		*unused column*
AU	# of brks	Number of breaks in aircraft fuselage
AV	Pk G Vert	Peak ‘G’ level vertical, # of G’s.
AW	Pk G Lat	Peak ‘G’ level lateral, # of G’s.
AX	Pk G Long	Peak ‘G’ level longitudinal, # of G’s.
AY	Vert Vel	Vertical velocity (ft/s)
AZ	Airspeed	Airspeed (ft/s)
BA	Flt Path	Aircraft flight-path angle
BB	Pitch	Aircraft pitch angle
BC	Pitch - Flt Path	Pitch angle—flight-path angle, an indicative of impact severity
BD		*unused column*
BE	Cockpit Damage Factor	Damage factor for cockpit = {skin damage (2-1-0)*1 + floor disruption (2-1-0) *2 + seat failure (2-1-0)*3 + loss of volume (2-1-0)*4}.
BF	Fwd Cab Damage Factor	Damage factor for forward cabin
BG	OW Cab Damage Factor	Damage factor for overwing cabin
BH	Rr Cab Damage Factor	Damage factor for rear cabin
BI	Tail Damage Factor	Damage factor for tail segment
BJ	Total Damage Factor	Sum of damage factors from each segment
BK	Avg & Med. DF for Scen	Average and median damage factor each scenario
BL	Avg Airspd for Scen	Average airspeed for each scenario
BM	Avg Vert. Vel. For Scen	Average vertical velocity for each scenario
BN	Avg P-FP for Scen.	Average P-FP value for each scenario
BO	# of NIs in damage	# of cells having ‘NI’ for No Information in each mishap
CI	HW_LW	Wing configuration high or low
CJ	LW Vert Vel	Vertical velocity for each low wing mishap

CK	HW Vert Vel	Vertical velocity for each high-wing mishap
CL	LW Airspeed	Airspeed for each low-wing mishap
CM	HW Airspeed	Airspeed for each high-wing mishap
CN	Low Wing Damage	Total damage factor for each low-wing aircraft
CO	High Wing Damage	Total damage factor for each high-wing aircraft
CQ	MAX_SPR	Number of seats in one row across entire plane
CR	Damage Factor 4 seats/row	Damage factor for mishaps with 4 seats/row
CS	Damage Factor 6 seats/row	Damage factor for mishaps with 6 seats/row
CU	ENG_CONFIG	Location for engines on mishap aircraft
CV	Damage Factor - Wing Eng.	Damage factor for mishaps with wing mounted engines
CW	Damage Factor - Other Eng.	Damage factor for mishaps with tail and tail/fin engines
CX	Vert Vel. Wing Eng.	Vertical velocity for mishaps involving wing engines
CY	Airspeed Wing Eng.	Airspeed for mishaps involving wing engines
CZ	Vert. Vel. Tail Eng.	Vertical velocity for mishaps involving tail engines
DA	Airspeed Tail Eng.	Airspeed for mishaps involving tail engines
DB	Pitch Angle Wing Eng.	Pitch angle for mishaps involving wing engines
DC	Pitch Angle Tail Eng.	Pitch angle for mishaps involving tail engines
DD	Flight Path Angle Wing Eng.	Flight-path angle for mishaps involving wing engines
DE	Flight Path Angle Tail Eng.	Flight-path angle for mishaps involving tail engines
DF	Peak Vert. Accel. Wing Eng.	Peak vertical acceleration for mishaps involving wing engines
DG	Peak Vert. Accel. Tail Eng.	Peak vertical acceleration for mishaps involving tail engines.
DH	Peak Long. Accel. Wing Eng.	Peak longitudinal acceleration for mishaps involving wing engines.
DI	Peak Long. Accel. Tail Eng.	Peak longitudinal acceleration for mishaps involving tail engines.
DK	Fwd Cab Segmt Brks	# brks adjacent to forward cabin in mishap (0-1-2)
DL	OW Cab Segmt Brks	# brks adjacent to overwing cabin in mishap (0-1-2)
DM	RC Cab Segmt Brks	# brks adjacent to rear cabin in mishap (0-1-2)

Task 2 Injury Data Fields for Injury Data worksheet

Col.	Header	Explanation
A	Reference #	Identification date: YEARMOnthDAyL (L=sequence letter)
B	Nickname	Typically place & plane type
C	Aircraft Type	Aircraft type
D	Date	Date of mishap
E	Scenario	A-E mishap assignment to one of five types
F	TOT_ABORD	Total occupants on board crew + passengers
G	FAT_CREW	Number of crew with fatal injuries
H	FAT_PAX	Number of passengers with fatal injuries
I	FAT_TOT	Total number of occupants with fatal injuries
J	SER_CREW	Number of crew with serious injuries
K	SER_PAX	Number of passengers with serious injuries
L	SER_TOT	Total number of occupants with serious injuries
M	MN_CREW	Number of crew with minor/no injuries
N	MN_PAX	Number of passengers with minor/no injuries
O	MN_TOT	Total number of occupants with minor/no injuries
P	PAX_TOT	Total number of passengers

Q	CREW_TOT	Total number of crew
R	Seat Inj Map	Was a seat & injury map provided in the report Y/N
S	C Occup	Number of occupants in the cockpit
T	FC Occup	Number of occupants in the forward cabin
U	OW Occu	Number of occupants in the overwing cabin
V	RC Occup	Number of occupants in the rear cabin
W	T Occup	Number of occupants in the tail
X	C Fatal	Number of fatalities in the cockpit
Y	FC Fatal	Number of fatalities in the forward cabin
Z	OW Fatal	Number of fatalities in the overwing segment
AA	RC Fatal	Number of fatalities in the rear cabin
AB	T Fatal	Number of fatalities in the tail
AC	C Ser Inj	Number of occupants seriously injured in the cockpit
AD	FF Ser Inj	Number of occupants seriously injured in the forward cabin
AE	OW Ser Inj	Number of occupants of seriously injured in the overwing cabin
AF	RC Ser Inj	Number of occupants of seriously injured in the rear cabin
AG	T Ser Inj	Number of occupants of seriously injured in the tail
AH	C Est SI Drowned	Number of occupants est. to have drowned as a result of serious injuries preventing evacuation from cockpit
AI	FC Est SI Drowned	Number of occupants est. to have drowned due to SI forward cabin. This field and the fields for the remaining segments proved to be impractical to populate.
AJ	OW Est SI Drowned	Number of occupants est. to have drowned due to SI overwing cabin
AK	RC Est SI Drowned	Number of occupants est. to have drowned due to SI rear cabin
AL	T Est SI Drowned	Number of occupants est. to have drowned due to SI tail
AM	C M/N Inj	Number of occupants with minor/no injuries in cockpit
AN	FF M/N Inj	Number of occupants with minor/no injuries in forward cabin
AO	OW M/N Inj	Number of occupants with minor/no injuries in overwing cabin
AP	RF M/N Inj	Number of occupants with minor/no injuries in rear cabin
AQ	T M/N Inj	Number of occupants with minor/no injuries in tail
AR	C % Fatal	Cockpit percent of occupants fatally injured
AS	FC % Fatal	Forward cabin percent of occupants fatally injured
AT	OW % Ftl	Overwing cabin percent of occupants fatally injured
AU	RC % Ftl	Rear cabin percent of occupants fatally injured
AV	T % Ftl	Tail percent of occupants fatally injured
AW	C % Ser Inj.	Cockpit percent of occupants seriously injured
AX	FC % Ser Inj	Forward cabin percent of occupants seriously injured
AY	OW % Ser Inj	Overwing cabin percent of occupants seriously injured
AZ	RC % Ser Inj	Rear cabin percent of occupants seriously injured
BA	T % Ser In	Tail percent of occupants seriously injured
BB	C % M/N Inj.	Cockpit percent of occupants minor/no injury
BC	FC % M/N Inj	Forward cabin percent of occupants minor/no injury
BD	OW % M/N Inj	Overwing percent of occupants minor/no injury

BE	RC % M/N Inj	Rear cabin percent of occupants minor/no injury
BF	T % M/N Inj	Tail percent of occupants minor/no injury
BG	All Occ. % Fatal	Percent of all occupants fatally injured in mishap
BH	All Occ. % Ser. Inj.	Percent of all occupants seriously injured in mishap
BI	All Occ. % Min.-No	Percent of all occupants with minor/no injury in mishap
BK	HW_LW	Wing configuration for mishap
BL	HW Fatalities	High-wing mishap, percent fatalities among all occupants
BM	HW Serious Injuries	High-wing mishap, percent serious injuries among occupants
BN	LW Fatalities	Low-wing mishap, percent fatalities among all occupants
BO	LW Serious Injuries	Low-wing mishap, percent serious injuries among occupants
BQ	ENG_CONFIG	Engine configuration in mishap
BR	Eng Wing Fatalities	Engines on wing, percent fatalities among all occupants
BS	Eng Wing Serious Injuries	Engines on wing, percent serious injuries all occupants
BT	Eng Tail Fatalities	Engines on tail, percent fatalities among all occupants
BU	Eng Tail Serious Injuries	Engines on tail, percent serious injuries all occupants
BW	Fwd Cab Segmt Brks	# brks adjacent to forward cabin in mishap (0-1-2)
BX	OW Cab Segmt Brks	# brks adjacent to overwing cabin in mishap (0-1-2)
BY	RC Cab Segmt Brks	# brks adjacent to rear cabin in mishap (0-1-2)
CA	Fwd Cab w 0 Br # FI	# of occ. with fatal injuries in mishaps with 0 brks in forward cabin
CB	Fwd Cab w 1 Br # FI	# of occ. with fatal injuries in mishaps with 1 brks in forward cabin
CC	Fwd Cab w 2 Br # FI	# of occ. with fatal injuries in mishaps with 2 brks in forward cabin
CD	OW Cab w 0 Br # FI	# of occ. with fatal inj. in mishaps with 0 brks in overwing cabin
CE	OW Cab w 1 Br # FI	# of occ. with fatal inj. in mishaps with 1 brks in overwing cabin
CF	OW Cab w 2 Br # FI	# of occ. with fatal inj. in mishaps with 2 brks in overwing cabin
CG	Rr Cab w 0 Br # FI	# of occ. with fatal inj. in mishaps with 0 brks in rear cabin
CH	Rr Cab w 1 Br # FI	# of occ. with fatal inj. in mishaps with 1 brks in rear cabin
CI	Rr Cab w 2 Br # FI	# of occ. with fatal inj. in mishaps with 2 brks in rear cabin

APPENDIX C—LIST OF WATER IMPACT MISHAPS INCLUDED IN THE ANALYSIS

The reference is the identification number in the Cabin Safety Technical Research Group database.

REFERENCE	SHORT NAME	AC_TYPE	SCENARIO
20091118	NORFOLK ISL. IAI 1124A	IAI 1124A	A
19940424A	BOTANY BAY DC3	DC3	A
19700502A	ST CROIX DC9	DC9-33F	A
20090115A	HUDSON RIVER A320	A320-214	B
20050806A	PALERMO ATR72	ATR72	B
20020116A	BENGAWAN SOLO RIVER B737	B737-300	B
20010227A	SCOTLAND SD360 DITCH	SD360	B
20000113A	LIBYA SD360	SD360	B
19910418A	NUKU HIVA DO228	DORNIER 228	B
19790310A	MARINA DEL REY N262	NORD 262	B
20130413A	NGURAH RAI B737	B737-8GP	C
19790217A	NEW ZEALAND F27	F27-500C	C
19780508A	PENSACOLA B727	B727-235	C
19690113A	SANTA MONICA BAY DC8	DC8-62	C
19670630A	CARAVELLE HONG KONG	CARAVELLE III	C
20000130A	ABIDJAN A310	A310	D
19931104A	HONG KONG B747-400	B747-409B	E
19840228A	JFK DC10	DC10-30	E
19820123A	BOSTON DC10	DC10-30CF	E
19790731A	SHETLAND 748	HS748-1 -105	E
19720719A	CORFU BAC1-11	BAC1-11	E
19671105A	HONG KONG, CV880M	CV880M	E

APPENDIX D—LIST OF REGIONAL JET MISHAPS INCLUDED IN THE ANALYSIS

The reference is the identification number in the Cabin Safety Technical Research Group database.

REFERENCE	SHORT NAME	AC_TYPE	SCENARIO
20100616A	OTTAWA EMB145	EMB145	F
20091207A	GEORGE EMB135	EMB135LR	F
20070412C	TRAVERSE CITY CRJ200	CANADAIR RJ200-LR	F
20070218A	CLEVELAND EMB170	EMB170	F
20061010A	STORD 146	BAE 146-200A	F
20041201B	TETERBORO G-IV	GULFSTREAM IV	F
19780709A	ROCHESTER BAC1-11	BAC1-11	F
19720719A	CORFU BAC1-11	BAC1-11	F
20090213A	LONDON CITY NOSE GEAR	AVRO RJ100	G
20070818A	LONDON CITY TAIL STRIKE	AVRO RJ100	G
20070124A	BARCELONA, RJ200	CANADAIR RJ200	G
20040105A	MUNICH F70	F70	H
20030622A	BREST CANADAIR RJ100	CANADAIR RJ100	H
20010329A	ASPEN GULFSTREAM III	GULFSTREAM III	H
19760926A	HOT SPRINGS GII	GULFSTREAM II	H
20071216B	PROVIDENCE, OFF RNWY	CANADAIR RJ200	J
20070520B	TORONTO CROSSWIND	CANADAIR RJ100	J
19971216A	NEW BRUNSWICK CL600	CL600-2B19	J
20070125A	PAU F28 (IN FRENCH)	F28-100	K
20060827C	BLUE GRASS CANADAIR	CANADAIR RJ100	K
20041128B	MONTROSE CL600	CL600-2A12	K
19961030A	PEEWAUKEE	GULFSTREAM IV	K
19930305A	SKOPJE F100	F100	K
19920322A	LA GUARDIA F28	F28-4000 a	K